General Disclaimer

One or more of the Following Statements may affect this Document

- This document has been reproduced from the best copy furnished by the organizational source. It is being released in the interest of making available as much information as possible.

- This document may contain data, which exceeds the sheet parameters. It was furnished in this condition by the organizational source and is the best copy available.

- This document may contain tone-on-tone or color graphs, charts and/or pictures, which have been reproduced in black and white.

- This document is paginated as submitted by the original source.

- Portions of this document are not fully legible due to the historical nature of some of the material. However, it is the best reproduction available from the original submission.

Technical Memorandum No. 33-311

Structural Analysis and Matrix Interpretive System (SAMIS) Program:
Technical Report

Robert J. Melosh and Henry N. Christiansen

Philco Corporation, A Subsidiary of the Ford Motor Company
Western Development Laboratories
Palo Alto, California

N 67-22063

(ACCESSION NUMBER)

/40

(PAGES)

CR-83269

(NASA CR OR TMX OR AD NUMBER)

(THRU)

(CODE)

33

(CATEGORY)

FACILITY FORM 602

jpl
JET PROPULSION LABORATORY
CALIFORNIA INSTITUTE OF TECHNOLOGY
PASADENA, CALIFORNIA

November 1, 1966

Technical Memorandum No. 33-311

Structural Analysis and Matrix Interpretive System (SAMIS) Program Technical Report

Robert J. Melosh and Henry N. Christiansen

Philco Corporation, A Subsidiary of Ford Motor Company
Western Development Laboratories
Palo Alto, California

Approved by:

M. E. Alper

M. E. Alper, Manager
Applied Mechanics Section
Jet Propulsion Laboratory

NATIONAL AERONAUTICS AND SPACE ADMINISTRATION

JPL - TM -

Technical Memorandum No. 33-311 AND

Structural Analysis and Matrix Interpretive System (SAMIS) Program: Technical Report

Robert J. Melosh and Henry N. Christiansen

Philco Corporation, A Subsidiary of Ford Motor Company
Western Development Laboratories
Palo Alto, California

Approved by:

M. E. Alper

M. E. Alper, Manager
Applied Mechanics Section
Jet Propulsion Laboratory

JET PROPULSION LABORATORY
CALIFORNIA INSTITUTE OF TECHNOLOGY
PASADENA. CALIFORNIA
November 1, 1966

FOREWORD

The work reflected in this report was performed by the Philco Corporation Western Development Laboratories, Palo Alto, California, for the Jet Propulsion Laboratory, California Institute of Technology, Pasadena, California under Contract No. 950321. This work is part of a continuing effort to develop automated capability to solve problems in engineering mechanics. Ted Lang, Senol Utku, Virgil Smith, and Robert Reed, of the Jet Propulsion Laboratory were the Project Engineers. The research was conducted from February through August 1965 by the Engineering Mechanics Section of WDL.

Phil R. Cobb, Manager, Electro-Mechanical Department, Philco, was Project Manager for the contractor. Robert J. Melosh, Manager, Engineering Mechanics, was Project Engineer.

The principal engineers for the contractor were Henry Christiansen and Philip Diether. Mary Brennan was the senior programmer.

JPL Technical Memorandum No. 33-311

TABLE OF CONTENTS

TABLES

FIGURES

ABSTRACT

This report describes the technical basis for programs contained in the Structural Analysis and Matrix Interpretive System. It includes development of the stiffness, stress, loading, and transformation relations for representation of a structure by a collection of flat triangular shell facets, rods, beams, and tubes. It defines the basis for special and complex program links and discusses use of these programs for structural analysis. It presents a discourse on analysis error in formulating the mathematical model of a structure and in analyzing it.

Details of the associated computer program are contained in a companion report entitled, "Structural Analysis and Matrix Interpretive System (SAMIS) Program Report," JPL Technical Memorandum No. 33-307.

SECTION 1

INTRODUCTION

The Structural Analysis and Matrix Interpretive System is designed to provide precise and low cost analyses of structures of general geometry and loading. Continued implementation of the program development plan will automate a broad spectrum of the studies in engineering mechanics. The principal areas of interest contemplated include: response prediction - static and dynamic; solution of characteristic value problems - prediction of small deflection buckling loads and vibration resonances; treatment of nonlinearities - analysis of both geometric and material nonlinearities; and evaluation of structures of special materials - prediction of behavior of systems composed of anisotropic elastic, viscoelastic, and plastic materials.

The scope of the first contract includes prediction of static response and vibration resonances limited by small deflections and monotropic materials with a linear stress-strain relationship. Geometries are restricted to those represented as composed of a number of flat triangular Facets joined along their edges and line elements joined to the rest of the structure at its ends. All elements are capable of resisting stretching, shearing, bending and twisting stresses. Folded structures are included, thus permitting analysis of semimonocoque shells in two or three dimensional space. Loadings automatically generated include those caused by heating, acceleration, and pressure. Additional loads may be introduced as energy-equivalent concentrated loads at points on the structure. Structural behavior is defined by stresses, deflections,

flexibilities, and stiffnesses. Both natural frequencies and mode shapes
are produced.

The basis used to define the mathematical model of the structure is
referred to in the literature as the Stiffness Method, the Direct Stiff-
ness Method, or a Finite Element Method. The method involves two essen-
tial ideas. The first is to replace the continuous structure by an
assemblage of elements. The continuous structural system is cut into
pieces by fictitious cuts. Intersections of cutting lines are called grid-
points or nodes.

The second idea is to formulate the problem from the stiffness viewpoint.
From this viewpoint load-deflection relations can be defined independently
for each element of the structure. The coefficients defining the rela-
tions form the stiffness matrix. A given column of the matrix consists of
a list of forces at each gridpoint of the element for unit displacement
in a given direction. Forming the load-deformation relations for the
system involves summing the stiffness matrices of the pieces. Where two
or more members have a common gridpoint, forces are simply added and
arranged in a stiffness matrix for the complete structural system.

Similarly boundary conditions can be formulated in matrix notation. Grid-
point displacements are found by solving a system of simultaneous equations.
A linear transformation of displacements provides estimates of element
stresses.

The simplicity of the approach is a principal advantage for automation.
The procedure for assembling the simultaneous equations is a clerical one.
The process is independent of the geometric or topological complexity of

the structure, the material characteristics, the boundary conditions, the choice of coordinates, or the identity or number of the redundants of the system.

These basic ideas were introduced by Levy.[1] Additional developments and applications have demonstrated the usefulness of the approach. Turner, et al.[2] developed and applied relations for a triangular slice replacing the coarse torque box and beam model used by Levy and demonstrating refinement of the approach. Other authors[3-16] have provided relations for line elements, rectangular plates, segments of shells of revolution, and elements of solids. The method has been successfully applied to predicting small deflection static and dynamic behavior and buckling loads.[3,5,8, 10,13,17-22] Orthotropic materials and nonlinear stress-strain relations have been successfully treated.[3,23]

Turner, et al.[24] and Weikel, et al.[25] have developed and applied the method for predicting large deflection behavior of heated structures. The basic ideas of this analysis are representation of the element including initial prestress or prestrain and prediction of behavior by permitting a series of steps of linear deformations until the full loading is imposed. Indications are that an order of magnitude increase in computer ti e is involved in the large deflection analysis.

---

[1] Superscripts are numbers of references appearing in the list of References. When superscripts take the form 2.3, the integer specifies the section number containing the reference and the decimal part, the reference number. Integer and decimal points are omitted when the section number of the reference is the same as the section in which the reference is made.

Recent papers have stressed the importance of being selective in stiffness matrices used in an analysis.[13,26] The method has been reformulated on the basis of the variational approach and a criterion presented insuring monotonic convergence. Applications have demonstrated the desirability of conforming with the convergence criterion. This selectivity can provide the capability to bound stresses and displacements at gridpoints[27,28,29] under static loads (See Appendix B).

This document defines the theoretical basis and analysis error associated with calculations performed by the present computer program. The next section of the document contains the development of the equations used in the program. The basis for stiffness, stress, loading, and transformation relations for the Facet and line element representations are presented. The third section defines the mathematical basis and use of the matrix operation links. The final section of the document presents a general discussion of the errors involved in formulating the mathematical model and analyzing it. This part considers the causes of the errors, their relative importance and how they can be measured. Some discussion of how analysis errors may be reduced is also given.

SECTION 2

DEVELOPMENT OF STRUCTURAL EQUATIONS*

The general form of the mathematical equations of the structure are:

$$[K]\{d\} - \lambda[K_i]\{d\} + [C]\{\dot{d}\} = \{P(t)\} - [M_s]\{\ddot{d}\}$$

$$\{\sigma\} = [R]\{d\} \tag{2-1}$$

where
- d is the vector of gridpoint displacements: dots indicate time derivatives.
- σ is the vector of element stresses.
- K is the small deflection stiffness matrix.
- C is the small deflection damping matrix.
- K_i is the initial stress stiffness matrix and λ a scalar defining the magnitude of the initial stress distribution.
- M_s is the mass loading matrix.
- P is the force loading matrix.
- R is the matrix of stress coefficients.

and sufficient boundary conditions on d and σ are defined to make the equations solvable. The signs of the elements are selected to correspond with conventional formulation of the equations. The first equation is used to determine the static and dynamic displacement response of the structure. The second equation defines the "stress" associated with a given set of displacements.

When loading matrices are omitted, λ is assigned, and homogeneous boundary conditions considered, (1) yields an eigenvalue equation whose roots define the damped frequencies of a prestressed structure. When the mass and damping matrices are also omitted and unassigned, the eigenvalues define load magnitudes at which small deflection buckling

---

* This section is co-authored by Dr. Senol Utku of the Jet Propulsion Laboratory and the Document authors.

occurs. If nonhomogeneous boundary conditions are considered, (1) can define a boundary value problem for a structure with initial stresses. Repeated application of equations (1) can be used to perform a large deflection or large strain analysis.

In this chapter, the stiffness, loading and stress matrices are developed for use in structural analyses. Necessary coordinate transformations are also given.

2.1 DEVELOPMENT OF FACET EQUATIONS

This section contains development of the mathematical model representing the structural behavior of the thin flat shell element, triangular in plan form and of uniform thickness. (Hereafter this element will be referred to as Facet). This section includes development of the stiffness, loading, stress coefficients and necessary coordinate transformations.

The stiffness coefficients are developed, using a potential energy approach, from an assumed displacement function which is continuous over the Facet and preserves continuity across its edges. Equations are developed in a rectangular cartesian coordinate system. Love's hypothesis is imposed. Monotropic stress-strain relations are used. The resulting stiffness matrix provides an inadequate representation of the out-of-plane shear stiffnesses. These terms are replaced by an analog.

The resulting coefficients define forces and moments at the apexes of the triangle which satisfy macroscopic force and moment equilibrium conditions. The matrix of stiffness coefficients is a positive semi-definite matrix of rank nine when the material coefficient matrix in the stress-strain equations has a rank of six.

The loading coefficients are developed using the minimum potential energy approach and the displacements assumed for derivation of stiffness coefficients. Stress boundary conditions corresponding to a temperature varying linearly throught the facet, uniform pressure over the area of the triangle, and constant acceleration in the overall x, y, and z directions are considered. Coefficients of the resulting vectors satisfy macroscopic force and moment equilibrium conditions.

The stress coefficients are developed using the stress-strain and strain deformation relations and the assumed displacement functions. Since displacements imply constant stresses, these are interpreted as mean stress at the Facet centroid. The resulting coefficients lead to zero stresses for rigid body displacements.

The theoretical basis for the derivations are included in Appendix A. In this Appendix the matrix formulation of the minimum potential approach appears.

Transformations are required relating the two rectangular cartesian coordinate systems of interest. These are the overall system and the local system. The overall coordinate system is a system common to all

Facets. Its function is to provide a system in which quantities with the same interpretation can be identified and manipulated. For example, components of forces at a gridpoint can be added when forces are transformed to the common system.

Each local coordinate system has its x-y plane coincident with the midplane of the facet. These coordinate systems are used to define monotropy coordinates, to simplify defining Facet geometry and simplify imposing boundary conditions. If adjacent Facets are in the same plane, a local system can serve as an overall system, and conversely.

2.1.1 Facet Stiffness Coefficients

2.1.1.1 Assumed Displacements

Figure 2.1-1 shows a Facet of thickness t and its associated coordinate system. The x-y plane is coincident with the midplane of the Facet. The z axis is normal to the midplane. The apexes of the Facet (called joints or gridpoints) are labelled proceeding in the counterclockwise direction for an observer on the +z axis.

The displacements of point "j" on the middle surface are defined by the components of the d vector as follows:

$$\{d_j\} = \begin{Bmatrix} u_{xj} \\ u_{yj} \\ u_{zj} \\ \theta_{xj} \\ \theta_{yj} \end{Bmatrix} \tag{2.1-1}$$

where u_{xj}, u_{yj}, and u_{zj} are translations of joint j in the x, y, and z directions, respectively, and θ_{xj}, θ_{yj} are rotations about these axes.

Each component of deflection is assumed to vary linearly over the middle surface. Then, a deflection component at any point can be expressed as

$$d_i = q_i x + b_i y + c_i \tag{2.1-2}$$

where a_i, b_i, and c_i are constants and x, y the coordinates of any point. The constants can be defined in terms of joint deflections by substituting joint coordinates in (2) and solving the equations.
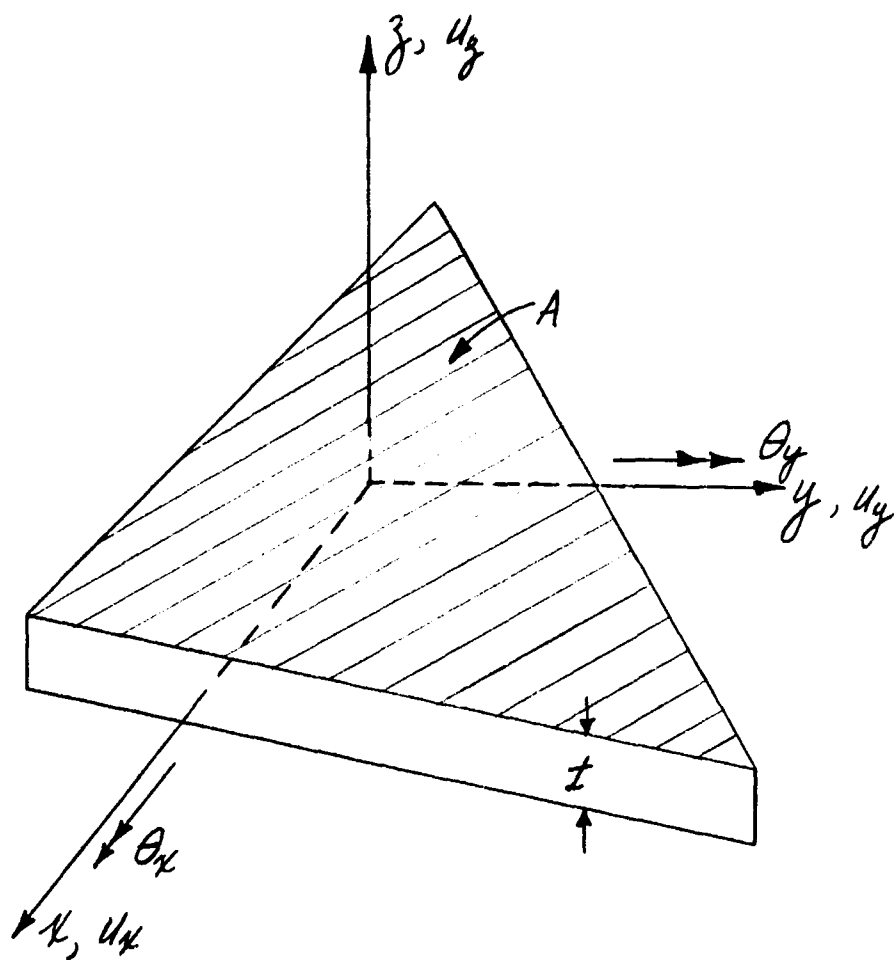
FACET COORDINATES AND GEOMETRY

Figure 2-1

This yields

$$\lfloor d_i \rfloor = \frac{1}{2A} \lfloor x \quad y \quad 1 \rfloor \begin{bmatrix} y_{23} & y_{31} & y_{12} \\ x_{32} & x_{13} & x_{21} \\ \lambda_1 & \lambda_2 & \lambda_3 \end{bmatrix} \begin{bmatrix} u_{x1} & u_{y1} & u_{z1} & \theta_{x1} & \theta_{y1} \\ u_{x2} & u_{y2} & u_{z2} & \theta_{x2} & \theta_{y2} \\ u_{x3} & u_{y3} & u_{z3} & \theta_{x3} & \theta_{y3} \end{bmatrix} \qquad (2.1\text{-}3)$$

where
$$A = \frac{1}{2}\left(x_{21} y_{31} - x_{31} y_{21} \right)$$
$$\lambda_1 = x_2 y_3 - x_3 y_2$$
$$\lambda_2 = x_3 y_1 - x_1 y_3$$
$$\lambda_3 = x_1 y_2 - x_2 y_1$$
$$x_{k\ell} = x_k - x_\ell$$
$$y_{k\ell} = y_k - y_\ell \qquad (2.1\text{-}4)$$

Note that A is the planform area of the Facet. Thus, (3) defines the deflection vector for any point x, y in the middle surface.

2.1.1.2 Stress-Strain Relations

The thermoelastic stress-strain relationship is expressed by

$$\begin{Bmatrix} \sigma_{xx} \\ \sigma_{yy} \\ \sigma_{xy} \\ \sigma_{zz} \\ \sigma_{xz} \\ \sigma_{yz} \end{Bmatrix} = \begin{bmatrix} D_{11} & D_{12} & D_{13} & D_{14} & 0 & 0 \\ & D_{22} & D_{23} & D_{24} & 0 & 0 \\ & & D_{33} & D_{34} & 0 & 0 \\ & & & D_{44} & 0 & 0 \\ Sym. & & & & D_{55} & D_{56} \\ & & & & & D_{66} \end{bmatrix} \begin{Bmatrix} \varepsilon_{xx} \\ \varepsilon_{yy} \\ \varepsilon_{xy} \\ \varepsilon_{zz} \\ \varepsilon_{xz} \\ \varepsilon_{yz} \end{Bmatrix} - \begin{Bmatrix} \alpha T \\ \alpha T \\ 0 \\ \alpha T \\ 0 \\ 0 \end{Bmatrix} \qquad (2.1\text{-}5)$$

where $\sigma_{k\ell}$ are components of stress

$\epsilon_{k\ell}$ are components of strain

α is the __isotropic__ volumetric coefficient of thermal expansion

T is the temperature rise

$D_{k\ell}$ are elastic coefficients for a material with one plane of symmetry (in this case, the midplane of the element). Materials of this nature will be referred to as "monotropic".

In order that a real material be represented, the matrix of elastic coefficients in (5) must be positive semi-definite or positive definite.

It is customary in thin shell analysis to adopt Love's hypothesis (which is also the first Kirchhoff assumption), i.e., assume $\sigma_{33} \equiv 0$. This implies that the thickness/radius ratio for the shell is small compared to one. This hypothesis is consistent with the hypothesis that normals to the middle surface remain normal.[4]

Imposing this condition on (5), eliminating ϵ_{33}, and partitioning gives

$$\{\bar{\sigma}\} = [\bar{D}]\{\bar{\xi} - \bar{\xi}_T\}$$

$$\{\bar{T}\} = [\bar{\bar{D}}]\{\bar{\gamma}\}$$

(2.1-6)

where $\{\bar{\sigma}\} = \begin{Bmatrix} \sigma_{xx} \\ \sigma_{yy} \\ \sigma_{xy} \end{Bmatrix}$ $\{\bar{\xi}\} = \begin{Bmatrix} \epsilon_{xx} \\ \epsilon_{yy} \\ \epsilon_{xy} \end{Bmatrix}$ $\{\bar{\xi}_T\} = \begin{Bmatrix} \alpha T \\ \alpha T \\ 0 \end{Bmatrix}$

$$\{\bar{\mathcal{T}}\} = \left\{\begin{matrix} \sigma_{x3} \\ \sigma_{43} \end{matrix}\right\}; \quad \{\bar{\gamma}\} = \left\{\begin{matrix} \gamma_{x3} \\ \gamma_{43} \end{matrix}\right\}$$

$$[\bar{D}] = \begin{bmatrix} D_{11} - \dfrac{D_{41}^2}{D_{44}} & D_{12} - \dfrac{D_{41} D_{42}}{D_{44}} & D_{13} - \dfrac{D_{41} D_{43}}{D_{44}} \\[2mm] & D_{22} - \dfrac{D_{42}^2}{D_{44}} & D_{23} - \dfrac{D_{42} D_{43}}{D_{44}} \\[2mm] SYM. & & D_{33} - \dfrac{D_{43}^2}{D_{44}} \end{bmatrix} \tag{2.1-7}$$

$$[\bar{\bar{D}}] = \begin{bmatrix} D_{55} & D_{56} \\ SYM & D_{66} \end{bmatrix} \tag{2.1-8}$$

Note that each of $\bar{D}$ and $\bar{\bar{D}}$ is a symmetric positive definite matrix.

2.1.1.3 Strain-Displacement Relations

According to the second Kirchhoff assumption, the in-plane strains ($\bar{\xi}$) varies linearly across the thickness and the out-of-plane shear strains ($\bar{\gamma}$) are constant. Then,

$$\{\bar{\xi}\} = \{\xi_0\} + 3\{\mathcal{L}\}$$

$$\{\bar{\gamma}\} = \{\gamma_0\} \tag{2.1-9}$$

where ξ_0 are the middle surface strains

3 is the coordinate normal to the middle surface

$\mathcal{L}$ is the vector of curvature changes

Note that since transverse shears are not assumed zero, normals to the middle surface are no longer normal after deformation.

In small deflection theory, the components of the strain are given by terms of deflections by

$$
\{\xi_o\} = \left\{ \begin{array}{c} \dfrac{\partial u_x}{\partial x} \\ \dfrac{\partial u_y}{\partial y} \\ \dfrac{\partial u_x}{\partial y} + \dfrac{\partial u_y}{\partial x} \end{array} \right\}
\tag{2.1-10}
$$

$$
\{\kappa\} = \left\{ \begin{array}{c} -\dfrac{\partial \theta_y}{\partial x} \\ \dfrac{\partial \theta_x}{\partial y} \\ \dfrac{\partial \theta_x}{\partial x} - \dfrac{\partial \theta_y}{\partial y} \end{array} \right\} \approx - \left\{ \begin{array}{c} \dfrac{\partial^2 u_3}{\partial x^2} \\ \dfrac{\partial^2 u_3}{\partial y^2} \\ 2\dfrac{\partial^2 u_3}{\partial x \partial y} \end{array} \right\}
$$

$$
\{\gamma_o\} = \left\{ \begin{array}{c} \dfrac{\partial u_3}{\partial x} \\ \dfrac{\partial u_3}{\partial y} \end{array} \right\} + \left\{ \begin{array}{c} \theta_y \\ -\theta_x \end{array} \right\}
\tag{2.1-11}
$$

Substituting derivatives of (3) in (10), gives the strains in terms of the gridpoint displacements, i.e.,

$$
\{\xi_o\} = \frac{1}{2A} \left[M \,\vdots\, N \right] \left\{ \begin{array}{c} \bar{u}_x \\ \bar{u}_y \end{array} \right\}
$$

$$
\{\kappa\} = \frac{1}{2A} \left[-N \,\vdots\, M \right] \left\{ \begin{array}{c} \bar{\theta}_x \\ \bar{\theta}_y \end{array} \right\}
\tag{2.1-12}
$$

$$
\{\gamma_o\} = \frac{1}{2A} \left[L \right] \{\bar{u}_3\} + \left\{ \begin{array}{c} \theta_y \\ -\theta_x \end{array} \right\}
$$

where

$$[M] = \begin{bmatrix} \psi_{23} & \psi_{31} & \psi_{12} \\ 0 & 0 & 0 \\ \psi_{32} & \psi_{13} & \psi_{21} \end{bmatrix}$$

(2.1-13)

$$[N] = \begin{bmatrix} 0 & 0 & 0 \\ \psi_{32} & \psi_{13} & \psi_{21} \\ \psi_{23} & \psi_{31} & \psi_{12} \end{bmatrix}$$

(2.1-14)

$$[L] = \begin{bmatrix} \psi_{23} & \psi_{31} & \psi_{12} \\ \psi_{32} & \psi_{13} & \psi_{21} \end{bmatrix}$$

(2.1-15)

$$\{\bar{u}_x\} = \begin{Bmatrix} u_{x1} \\ u_{x2} \\ u_{x3} \end{Bmatrix}; \quad \{\bar{u}_y\} = \begin{Bmatrix} u_{y1} \\ u_{y2} \\ u_{y3} \end{Bmatrix}; \quad \{\bar{u}_z\} = \begin{Bmatrix} u_{z1} \\ u_{z2} \\ u_{z3} \end{Bmatrix};$$

$$\{\bar{\theta}_x\} = \begin{Bmatrix} \theta_{x1} \\ \theta_{x2} \\ \theta_{x3} \end{Bmatrix}; \quad \{\bar{\theta}_y\} = \begin{Bmatrix} \theta_{y1} \\ \theta_{y2} \\ \theta_{y3} \end{Bmatrix}$$

(2.1-16)

Similarly, the transfer shear strains can be defined in terms of displacements by substituting derivatives of (3) into (11). This leads to

an unsatisfactory representation. This difficulty and alternate approach is described in Section 2.1.1.7.

Equations (12) through (16) define the strains in terms of the generalized displacements, the joint deflections, and rotations.

2.1.1.4 Strain-Energy

The general expression for internal strain-energy is given by

$$U = \int_{V_o} \int_0^\epsilon \lfloor \sigma \rfloor \{d\epsilon\} \, dV_o \tag{2.1-17}$$

where V_o is the volume of the element and initial strains and stresses are zero.

Substituting (9) in (17), the strain energy can be written for the Facet as

$$U = U_M + U_\beta + U_s \tag{2.1-18}$$

where

$$U_M = \frac{t}{2} \int_A \lfloor \xi_o \rfloor [\bar{D}] \{\xi_o\} \, dA \tag{2.1-19}$$

$$U_B = \frac{t^3}{48} \int_A \lfloor \mathcal{H} \rfloor [\bar{D}] \{ \mathcal{H} \} \, dA \tag{2.1-20}$$

$$U_S = \frac{t}{2} \int_A \lfloor \gamma_o \rfloor [\bar{\bar{D}}] \{ \gamma_o \} \, dA \tag{2.1-21}$$

t is the Facet thickness

U_M, U_B, and U_S are, respectively, the membrane, bending, and shear strain energies.

The second derivative of the strain energy of the element, with respect to joint deflections, yields the stiffness coefficients (See Appendix A). These are developed for the Facet in the next four sections.

2.1.1.5 **Membrane Stiffness Coefficients**

Substituting (12) in (19) and differentiating yields the membrane contribution to the Facet stiffness matrix. With displacement unknowns ordered by (1), this is given by,

$$[K_M] = \frac{t}{4A} \begin{bmatrix} P & R & 0 & 0 & 0 \\ & Q & 0 & 0 & 0 \\ & & 0 & 0 & 0 \\ & & & 0 & 0 \\ Sym. & & & & 0 \end{bmatrix} \tag{2.1-22}$$

where

$$\left[P \right] = \left[M^T \right]\left[\overline{D} \right]\left[M \right]$$

$$\left[Q \right] = \left[N^T \right]\left[\overline{D} \right]\left[N \right]$$

$$\left[R \right] = \left[M^T \right]\left[\overline{D} \right]\left[N \right]$$

(2.1-23)

Equation (22) defines a matrix of order 15 and rank 3. This matrix is identical to that given by Turner, et al[1,2]. No joint forces are involved with rigid body motions of the Facet using this matrix.

2.1.1.6 Bending Stiffness Coefficients

Substituting (12) in (20) and differentiating yields the bending contribution to the Facet stiffness matrix. With displacement unknowns ordered by (1), this is given by

$$\left[K_B \right] = \frac{\ell^3}{48A}\begin{bmatrix} 0 & 0 & 0 & 0 & 0 \\ & 0 & 0 & 0 & 0 \\ & & 0 & 0 & 0 \\ & & & Q & R^T \\ & & & & P \end{bmatrix}$$

(2.1-24)

where P, Q, and R are defined by (23).

Equation (24) defines a matrix of order 15 and rank 3. No joint moments are involved with rigid body motions of the Facet using the matrix.

2.1.1.7 Shear Deformation Stiffness Coefficients

The assumed displacements (1) through (4) imply a linear variation of shear strain if used in (11). As indicated in reference 1.3, this generality is not required to lead to exact analyses of bending behavior. Moreover, including the linear terms will lead to an excessively rigid representation unless the planform area of the Facet is small compared with the Facet thickness.

On the other hand, omission of the shear stiffness is inadmissible. In particular, if only the membrane and bending stiffnesses are considered, forces acting normal to the Facet cannot be treated.

This difficulty is resolved by considering only constant shears. The shear deformation stiffness matrix is written formally as,

$$[K_s] = \frac{t}{4A} \begin{bmatrix} 0 & 0 & 0 & 0 & 0 \\ & 0 & 0 & 0 & 0 \\ & & S_{11} & S_{12} & S_{13} \\ & & & S_{22} & S_{23} \\ & & & & S_{33} \end{bmatrix}$$

(2.1-25)

If only the constant portion of the shear strains, (11), are retained, S_{11} is found to be

$$[S_{11}] = [L^T][\bar{\bar{D}}][L]$$

(2.1-26)

Use of this matrix alone would imply that rigid body motions of the Facet generate elastic energy. This unacceptable condition is removed by constructing the remaining partitions of K_S such that macroscopic equilibrium is satisfied. Reference 1 develops the required relation using a beam analogy. Reference 2 obtains the same coefficients considering the extension of beam equilibrium requirement from one to two dimensions.

The coefficients in S_{21} and S_{31} can be written in terms of the coefficients of S_{11}. Similarly, the coefficients of S_{22} and S_{32} can be written in terms of those of $S_{12} = S_{21}^T$, and S_{23} and S_{33} in terms of $S_{13} = S_{31}^T$. For each of these sets, the same relations are involved. Let f_i, $m_{x_{ij}}$ and $m_{y_{ij}}$ where $i = 1,2,3$, $j = 1,2,3$ be the coefficients of the first (e.g. S_{11}), second (e.g. S_{21}), and third (e.g. S_{31}) partitions in a column partition of K_S. Then,

$$m_{x_{ij}} = -\frac{1}{2}\left[(1-\delta_{ij})f_{ij}\,y_{ij} + \delta_{ij}\left(f_{i+1,j}\,y_{i+1,j} + f_{i+2,j}\,y_{i+1,j}\right)\right] \quad (2.1\text{-}27)$$

$$m_{y_{ij}} = \frac{1}{2}\left[(1-\delta_{ij})f_{ij}\,x_{ij} + \delta_{ij}\left(f_{i+1,j}\,x_{i+1,j} + f_{i+2,j}\,x_{i+2,j}\right)\right]$$

where subscripts are modulo 3. e.g., when $i = 3$, $i + 1 = 1$, and δ_{ij} is the Kronecker delta ($\delta_{ij} = 1$ $i = j$; $\delta_{ij} = 0$ $i \neq j$)

The shear deformation stiffness matrix is of order 15 and generally of rank 3[8]. In the special case when an angle of the triangle is 90°, the matrix is of rank 2. The matrix is positive semi-definite for all triangles whose largest angle is less than 90°. When an obtuse angle

exists in the Facet, the matrix is indefinite and thus unsatisfactory. Therefore, the analyst should avoid selection of joint locations which result in triangles with obtuse angles. Most accurate solutions can be anticipated when the triangle is equilateral.

To eliminate existence of indefinite stiffness matrices for triangles with an obtuse angle, the definition of (S_{11}) (26) is modified for this case. The modification consists of nullifying the positive off-diagonal elements in (S_{11}) and changing the remaining elements so that S_{11} is the same as before. Numerical experimentation has demonstrated the adequacy of this approach.[8]

2.1.1.8 Total Facet Stiffnesses

The Facet stiffness matrix is composed of the sum of the membrane, bending, and shear stiffness matrices, in accordance with (18). Thus,

$$\left[K\right] \quad \left[K_M\right] + \left[K_B\right] + \left[K_S\right]$$

(2.1-28)

where K is the total stiffness matrix.

The total stiffness matrix is of order 15 and rank 9. If an angle is 90°, the matrix is of rank 8. This degeneracy will only require special treatment if the structure consists of a single triangle on determinate supports.

2.1.2 Facet Loading Vectors

For any given loading condition, gridpoint forces are defined from the integral A-11. In this section, gridpoint forces for the Facet are obtained for discrete loading and loadings induced by temperature change, acceleration, and pressure.

Figure 2-2 shows the notation used for distributed loadings. Uniform upper and lower surface temperatures are imposed,   and   . The mass of the Facet is uniformly distributed.

2.1.2.1 Discrete Joint Loads

If the loading consists of discrete loads acting on the gridpoints, it is defined by

$$\{P_o\} = \left\{ \begin{array}{c} F_{xj} \\ F_{yj} \\ F_{zj} \\ M_{xj} \\ M_{yj} \end{array} \right\}$$

(2.1-29)

where P_D is the vector of discrete loads, F_{xj}, F_{yj}, F_{zj} are the forces at joint "j" in the x, y, and z directions, respectively, and M_{xj}, M_{yj} are moments about the x and y axes at joint "j".

Equation (29) does not contain a moment about the z axis, M_{zj}. If such a torque acts, it must be treated by considering a couple composed of F_x and F_y forces.
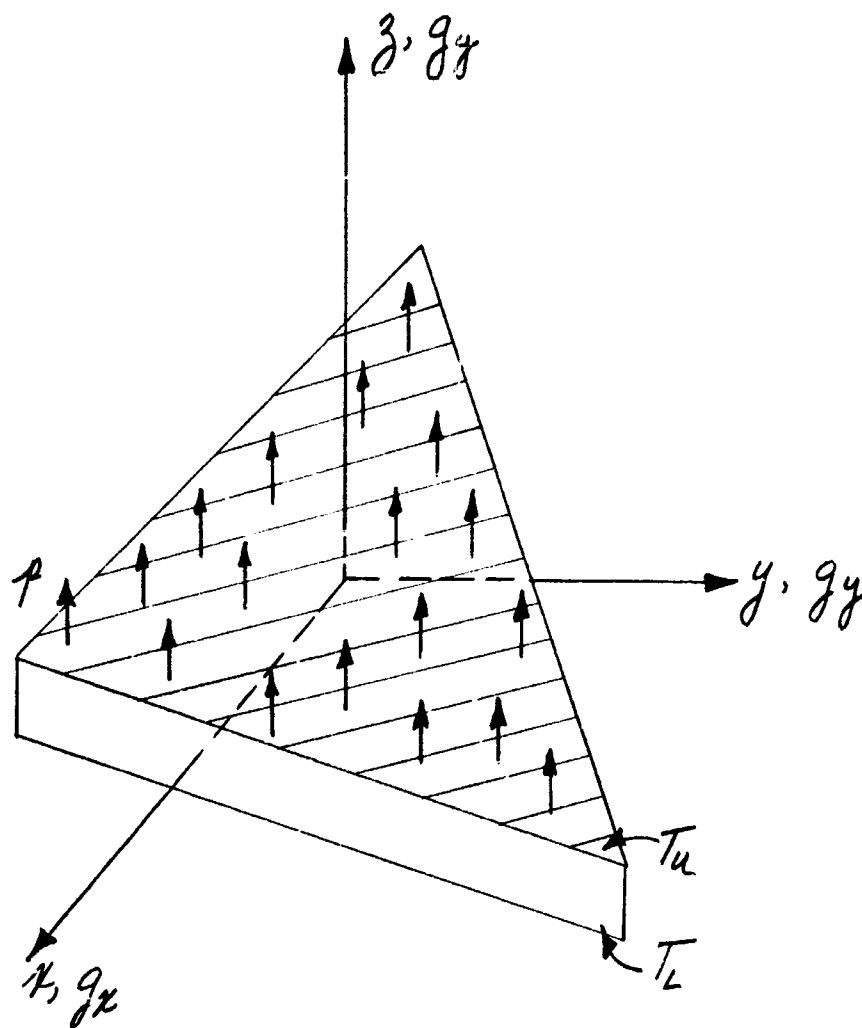
FACET LOADING NOTATION

Figure 2-2

2.1.2.2 Thermal Loading Vector

Let the temperature be constant over the Facet surface but vary linearly through the thickness. Then, the temperature distribution can be expressed as,

$$T = \frac{1}{2}(T_u + T_l) + \frac{z}{t}(T_u - T_l) \qquad (2.1\text{-}30)$$

where T_u is the temperature change between the upper (+z) surface temperature and the temperature of fabrication.

T_l is the temperature change for the lower (-z) surface.

The stress loads developed by temperature are defined by (6), i.e.,

$$\{\sigma_T\} = -[D]\{\xi_T\} \qquad (2.1\text{-}31)$$

where σ_T is the vector of temperature stresses and ξ_T is defined by equation (6). Using (31) in the work integral for body forces, the last member of equation A-8 , gives

$$V_T = \int_{v_o} \lfloor \xi_T \rfloor [D]\{\bar{\xi}\}\, dv_o$$

where $\bar{\xi}$ is defined (9), as before.

Making the indicated substitutions and integrating over the volume of the

element gives

$$V_T = \frac{\alpha t}{4}(T_u + T_L)\lfloor 1 \mid 0 \rfloor [D][M \mid N]\begin{Bmatrix} \bar{u}_x \\ \bar{u}_y \end{Bmatrix}$$
$$+ \frac{\alpha t^2}{24}(T_u - T_L)\lfloor 1 \mid 0 \rfloor [D][-N \mid M]\begin{Bmatrix} \bar{\theta}_x \\ \bar{\theta}_y \end{Bmatrix} \qquad (2.1\text{-}32)$$

The energy equivalent joint forces are obtained by differentiating (32) with respect to joint displacements. This gives,

$$\{P_T\} = \begin{bmatrix} c_1 M^T D \\ c_1 N^T D \\ 0 \\ -c_2 N^T D \\ c_2 M^T D \end{bmatrix}\begin{Bmatrix} 1 \\ 1 \\ 0 \end{Bmatrix} \qquad (2.1\text{-}33)$$

where P_T indicates the thermal loading vector and

$$c_1 = \frac{\alpha T}{4}(T_u + T_L); \qquad c_2 = \frac{\alpha t^2}{24}(T_u - T_L)$$

The forces given by (33) represent joint forces induced by the temperature change when the joints are not permitted to move. Thus, stresses obtained using these forces and releasing the joints must be superimposed with the implied prestress in accordance with (5). Stress-displacement equations are discussed in more detail in section 2.1.3.

2.1.2.2 Acceleration and Pressure Loading Vectors

The body forces induced by constant accelerations is taken as

$$\lfloor G_g \rfloor = \rho \lfloor \bar{g}_x \mid \bar{g}_y \mid \bar{g}_z \mid 0 \mid 0 \rfloor \qquad (2.1\text{-}34)$$
$$\lfloor \bar{g}_n \rfloor = \lfloor g_n \quad g_n \quad g_n \rfloor$$

where ρ is the material density and $\ddot{q}_x$, $\ddot{q}_y$, and $\ddot{q}_z$ are the linear accelerations in the local x, y, and z directions.

Using (34) and (3) in the work integral for body forces, the last member of equation A-8, and differentiating with respect to joint dis‑placements and integrating over the element volume will give the loading vector for accelerations.

$$\left\{ \begin{matrix} \rho_q \end{matrix} \right\} = \frac{M_F}{3} \begin{bmatrix} I & 0 & 0 \\ 0 & I & 0 \\ 0 & 0 & I \\ 0 & 0 & 0 \\ 0 & 0 & 0 \end{bmatrix} \left\{ \begin{matrix} \ddot{q}_x \\ \ddot{q}_y \\ \ddot{q}_z \end{matrix} \right\} \tag{2.1-35}$$

where $M_F = At\rho$, the total mass of the element.

The astute reader will observe that (35) is developed assuming the origin of coordinates lies at the centroid of the Facet. This choice of origin is selected so that the acceleration potential is stationary with respect to choice of origin. It is noted that this consideration was not involved in development of the stiffness matrix. This matrix was naturally invariant with the location of the origin of coordinates.

The pressure loading vector may be obtained directly from (35) by letting $\ddot{q}_x = \ddot{q}_y = 0$, $\ddot{q}_z = 1$ and $M_F = pA$ where p is the pressure intensity. p is positive if the pressure acts in the +z direction.

2.1.2.3 Inertia Matrix

For each Facet a number of different mass representations are possible. To insure that high estimates of frequency are obtained, a potential

energy formulation of the mass matrix should be used. Since, often better and always lower frequency estimates are obtained if a finite difference mass matrix is used with the potential energy stiffness, both will be presented.

In the potential energy case, the assumed modes are substituted in the expression for kinetic energy and the result introduced into Lagrange's equation. The kinetic energy, N is given by,

$$N = \frac{1}{2} \int_{\mathcal{V}_o} \rho(x, y, z)\left(\dot{u}_x^2 + \dot{u}_y^2 + \dot{u}_z^2\right) dv_o \qquad (2.1\text{-}36)$$

where the dot denotes the first time derivative and ρ the material density.

Introducing (3) into (36), assuming the mass is uniformly distributed over the Facet and lies on the neutral plane, and using Lagrange's equation leads to the potential energy mass matrix,

$$[M_s] = \begin{bmatrix} M_{II} & 0 & 0 & 0 & 0 \\ & M_{II} & 0 & 0 & 0 \\ & & M_{II} & 0 & 0 \\ & & & 0 & 0 \\ Sym. & & & & 0 \end{bmatrix} \qquad (2.1\text{-}37)$$

where

$$[M_{II}] = \frac{\rho t}{4A^2} \int_A \begin{bmatrix} y_{23} & y_{31} & y_{12} \\ x_{32} & x_{13} & x_{21} \\ \lambda_1 & \lambda_2 & \lambda_3 \end{bmatrix} \begin{bmatrix} 1 & x & y \\ x & x^2 & xy \\ y & xy & y^2 \end{bmatrix} \begin{bmatrix} y_{23} & y_{31} & y_{12} \\ x_{32} & x_{13} & x_{21} \\ \lambda_1 & \lambda_2 & \lambda_3 \end{bmatrix} dA$$

Let the coordinate axes be principle axes. Then M_{11} can be written

$$[M_{11}] = \frac{\rho t}{4A^2}\int_A \begin{bmatrix} y_{13} & y_{31} & y_{12} \\ y_{32} & y_{13} & y_{21} \\ \lambda_1 & \lambda_2 & \lambda_3 \end{bmatrix} \begin{bmatrix} 1 & 0 & 0 \\ 0 & x^2 & 0 \\ 0 & 0 & y^2 \end{bmatrix} \begin{bmatrix} y_{23} & y_{31} & y_{12} \\ y_{32} & y_{13} & y_{21} \\ \lambda_1 & \lambda_2 & \lambda_3 \end{bmatrix} dA \qquad (2.1\text{-}38)$$

It can be shown that the mass matrix is invariant with rotation of the coordinate system since the transformation on M_{11} is negated by the transformation of the displacements. Furthermore, considering an arbitrary triangle, it can be shown algebraically that M_{11} can be written in the simplified form

$$[M_{11}] = \frac{M_F}{12} \begin{bmatrix} 2 & 1 & 1 \\ & 2 & 1 \\ SYM & & 2 \end{bmatrix} \qquad (2.1\text{-}39)$$

A finite-difference mass matrix can be developed and gives for the mass matrix,

$$[M_{11}'] = \frac{M_F}{3} \begin{bmatrix} 1 & 0 & 0 \\ & 1 & 0 \\ SYM. & & 1 \end{bmatrix} \qquad (2.1\text{-}40)$$

Mass matrix (40) must lead to lower estimates of frequency than (39) for all resonances and all structures. This is proved by applying Schwarz' inequality to the expressions for Kinetic energy.

2.1.3 Stress-Displacement Equations

Rather than stresses, stress resultants are of interest. These are the zeroth and first moment of the stresses obtained by integrating over

the thickness of the element. Thus, the stress resultants, excluding transverse shears, are defined by

$$
\begin{Bmatrix} N_{xx} \\ N_{yy} \\ N_{xy} \\ M_{xx} \\ M_{yy} \\ M_{xy} \end{Bmatrix} = \int_{-\frac{t}{2}}^{\frac{t}{2}} \begin{bmatrix} I \\ \hline \\ \zeta I \end{bmatrix} \{ \bar{\sigma} \} \, d\zeta
$$

(2.1-41)

where $N_{k\ell}$ are resultant forces

$M_{k\ell}$ are moment resultants

I is a 3 x 3 identity matrix

Using (6), (9), and (12) in (41) and integrating leads to the stress-displacement relation,

$$
\begin{Bmatrix} N_{xx}/t \\ N_{yy}/t \\ N_{xy}/t \\ M_{xx}/(t^3/12) \\ M_{yy}/(t^3/12) \\ M_{xy}/(t^3/12) \end{Bmatrix} = \frac{1}{2A} \begin{bmatrix} DM & DN & 0 & 0 & 0 \\ \hline 0 & 0 & 0 & -DN & DM \end{bmatrix} \begin{Bmatrix} \bar{u}_x \\ \bar{u}_y \\ \bar{u}_3 \\ \bar{\theta}_x \\ \bar{\theta}_y \end{Bmatrix}
- \begin{Bmatrix} D\bar{c}_1 \\ D\bar{c}_2 \end{Bmatrix}
$$

(2.1-42)

where $\{ \bar{c}_1 \} = \begin{Bmatrix} c_1 \\ c_1 \\ c_1 \end{Bmatrix}$, $\{ \bar{c}_2 \} = \begin{Bmatrix} c_2 \\ c_2 \\ c_2 \end{Bmatrix}$

and c_1, and c_2 are given by (33).

29

The last column of (42) can be regarded as a thermal correction vector. Similar correction vectors may be developed for the other distributed loadings; i.e., acceleration and pressure. These are omitted under the assumption that elements are sufficiently small so that these corrections are negligible for these loadings.

Transverse shear resultants may be estimated by differentiating moments,

$$Q_x = \frac{\partial M_{xx}}{\partial x} + \frac{\partial M_{xy}}{\partial y}$$

$$Q_y = \frac{\partial M_{yy}}{\partial y} + \frac{\partial M_{xy}}{\partial x}$$

(2.1-43)

where Q_x and Q_y are the shear resultants in the xz and yz planes.

Equation (42) defir es stress resultants satisfying this requirement, but other choices are possible. Utku[7] has considered a number of definitions for the stress resultants. His studies show that (42) provides satisfactory estimates of forces and moments. Transverse shears defined by (43) are often unsatisfactory.

2.1.4 Facet Transformations

Transformations are necessary to write Facet relations in different coordinate systems. Transformations are required of the Facet gridpoint coordinates, of forces and deflections, and of stresses and strains. Coordinates of the Facet may be defined in an overall or the local rectangular cartesian system. The overall coordinate system may be rotated and translated from the local system which has its x-y plane coincident

with the elastic plane of the Facet. Matrices of coefficients are developed in the local Facet coordinate system which is rectangular cartesian, whose x-y plane coincides with the Facet elastic plane, whose origin is at the centroid of the Facet planform. Transformations of coordinates are required between the overall or local coordinate systems to account for axis rotation. Translations can be disregarded.

Forces and displacements may be represented in the local or overall system at each gridpoint. To provide for this option, the transformation from the local to the appropriate final coordinate system is required. This transformation considers only axis rotations. In addition, transformations are required to impose boundary conditions and represent load-transfer at other than the elastic plane. This transformation involves both rotations and translations.

Stress and strain transformations are required to allow the principal axes of the material to have any orientation with respect to the Facet sides. Since elastic coefficients are assumed to be based on the local coordinate system, transformation is required from the material axes to the local axes for the Facet.

2.1.4.1 Coordinate Transformations

If coordinates are given in the overall coordinate system, a transformation from the local to overall system must be accomplished. This relationship, between coordinates in the local and overall systems, in-

volves the orthogonal matrix S, thus,

$$
\begin{Bmatrix} X \\ Y \\ Z \end{Bmatrix} = \begin{bmatrix} S_{Xx} & S_{Yx} & S_{Zx} \\ S_{Xy} & S_{Yy} & S_{Zy} \\ S_{Xz} & S_{Yz} & S_{Zz} \end{bmatrix} \begin{Bmatrix} x \\ y \\ z \end{Bmatrix}
$$

(2.1-44)

S_{ij} is the cosine of the angle between the overall i and local j axis, and x, y, z are coordinates in the local system whereas X, Y, Z are coordinates in the overall system.

If the local reference system uses side 1-2 of the Facet as the local x axis, the direction cosines S_{ij} are defined in the following manner:

For the local x axis

$$
S_{Xx} = \frac{X_{21}}{L_{21}}; \quad S_{Yx} = \frac{Y_{21}}{L_{21}}; \quad S_{Zx} = \frac{Z_{21}}{L_{21}}
$$

$$
L_{21} = \left(X_{21}^{2} + Y_{21}^{2} + Z_{21}^{2} \right)^{1/2}
$$

(2.1-45)

where the positive square root is selected.

The equation of the reference plane is

$$
\begin{Vmatrix} X & Y & Z & 1 \\ X_1 & Y_1 & Z_1 & 1 \\ X_2 & Y_2 & Z_2 & 1 \\ X_3 & Y_3 & Z_3 & 1 \end{Vmatrix} = aX + bY + cZ + d = 0
$$

(2.1-46)

Writing Equation (46) in normal form gives the direction cosines of a normal to the plane (i.e., local z-direction).

$$
S_{Xz} = \frac{a}{\ell}; \quad S_{Yz} = \frac{b}{\ell}; \quad S_{Zz} = \frac{c}{\ell}
$$

$$
\ell = \left(a^{2} + b^{2} + c^{2} \right)^{1/2}
$$

(2.1-47)

The sign of the square root is chosen so that the scalar triple product of the normal, the reference line (side 1-2), and a line from the local origin (gridpoint 1) to the reference point (gridpoint 3) is positive, i.e.,

$$\left\| \begin{array}{ccc} Sx_3 & Sy_3 & Sz_3 \\ Sx_4 & Sy_4 & Sz_4 \\ (X_3-X_1) & (Y_3-Y_1) & (Z_2-Z_1) \end{array} \right\| > 0 \qquad (2.1\text{-}48)$$

This computation serves to define the positive sense of the normal to the midplane, and hence, the z axis if the displacements or forces are desired in the local reference coordinate system. To assure that adjacent Facets have the same kind of positive z axis, a consistent method of listing gridpoint numbers must be used. For example, referring to Figure 2-3, a consistent set of gridpoint numbers for the two Facets would be

Gridpoint	Facet 1	Facet 2
First	9	54
Second	10	100
Third	100	10

This order is achieved by proceeding counter-clockwise around each Facet.
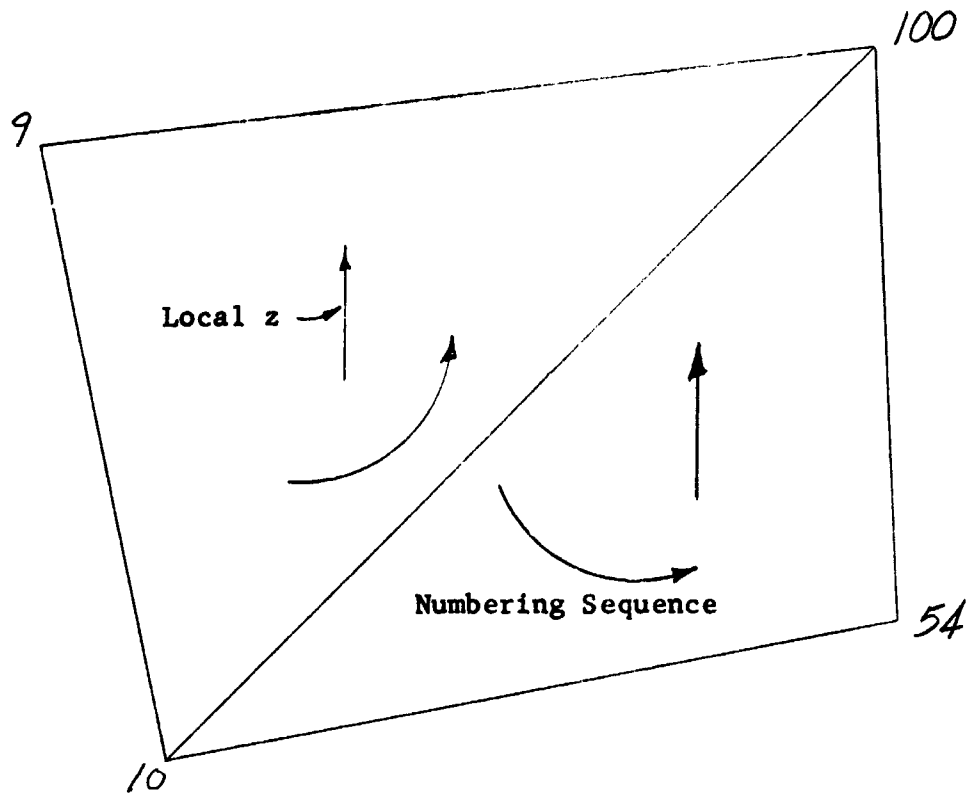
LOCAL Z AXIS SELECTION

Figure 2-3

Direction cosines for the local y axis are obtained as the components of the cross product of the normalized vector in the local x direction and the normalized vector on the local z direction. Thus

$$S_{X_y} = S_{Y_z} S_{Z_x} - S_{Y_x} S_{Z_z}$$
$$S_{Y_y} = S_{X_x} S_{Z_z} - S_{Y_z} S_{Z_x}$$
$$S_{Z_y} = S_{X_z} S_{Y_x} - S_{X_x} S_{Y_z}$$

$$(2.1-49)$$

The transformation between the coordinates in the local and overall coordinate systems will be identical since the S is an orthogonal matrix, i.e.,

$$\left\{ \begin{matrix} \mathcal{U} \\ \mathcal{V} \\ \mathcal{W} \end{matrix} \right\} = \left[S \right]^{T} \left\{ \begin{matrix} X \\ Y \\ Z \end{matrix} \right\}$$

(2.1-50)

2.1.4.2 Force and Deflection Transformations

If the original generalized displacements can be formed from a linear transformation of a new set of generalized coordinates, i.e.,

$$\left\{ d \right\} = \left[W \right] \left\{ \tilde{d} \right\}$$

(2.1-51)

where W is the transformation matrix and $\tilde{d}$ the new generalized coordinates. Then, equations (1) can be written,

$$[K][W]\{\tilde{d}\} + \lambda [K_{L}][W]\{\tilde{d}\} + [C][W]\{\dot{\tilde{d}}\} = \\ \{P\} - [M_{S}][W]\{\ddot{\tilde{d}}\}$$

(2.1-52)

$$\{\sigma\} = [R][W]\{\tilde{d}\}$$

(2.1-53)

Equations (52) are equilibrium requirements for forces written for the original basis in terms of displacements in the new basis. Transformation of forces to the new basis is accomplished by

$$\{\tilde{P}\} = [W]^{T} \{P\}$$

(2.1-54)

This is immediately evident if the invariant form (energy) is examined from whence the first equation of (52) can be obtained. (See Appendix A). Then, premultiplying (52) by W^T gives the equilibrium requirements in the new system as

$$[W]^T[K][W]\{\tilde{d}\} + \lambda[W]^T[K_i][W]\{\tilde{d}\} + [W]^T[C][W]\{\dot{\tilde{d}}\}$$
$$= \{\tilde{P}\} - [W]^T[M_s][W]\{\ddot{\tilde{d}}\} \qquad (2.1\text{-}55)$$

Therefore, a change of basis for forces and displacements requires a congruent transformation of the elastic stiffness, initial stress stiffness, damping and mass matrices, and a post multiplication of the stress matrix. Then,

$$\{\tilde{d}\} = [W]^T\{d\} \qquad (2.1\text{-}56)$$

Holonomic displacement or force boundary conditions can be written in the form (51) or (54). With thus defined, boundary conditions are imposed by putting the equations of motion in the form (55). Note that in the special case when a displacement component is fixed, transformation of forces removes from (52) the equations defining restraint forces.

Three types of continuity may be defined at each gridpoint:

(1) Forces and deflections of one element may be made to match those of the adjacent element at the gridpoint. This is the normal continuity condition.

(2) Deflections at a joint may be prevented. This is attained by setting this displacement zero in the equations of motion. The relevant equation is then of value only if the reaction is required.

(3) A displacement component of one element may not match that of the neighboring element. This is achieved by letting the displacement be an independent degree of freedom.

As an example of how these continuity conditions may be used, consider the imposition of symmetry boundary conditions. Assume that the x-z plane is a plane about which the structure and the loading is symmetrically disposed. Then, only half the structure needs to be analyzed. For points in the x-z plane, it is required that:

$$U_x \neq 0; \quad U_y = 0; \quad U_z \neq 0; \quad \theta_x = 0; \quad \theta_y \neq 0; \quad \theta_z = 0 \qquad (2.1\text{-}57)$$

This is imposed by fixing U_y, θ_x and θ_z displacements.

Alternately, assume that the x-z plane is a plane of symmetry for the structure and asymmetry for the loading. Then, for points on the x-z plane

$$U_x = 0; \quad U_y \neq 0; \quad U_z = 0; \quad \theta_x \neq 0; \quad \theta_y = 0; \quad \theta_z \neq 0 \qquad (2.1\text{-}58)$$

These conditions are imposed by fixing U_x, U_z, and θ_y.

Though the Facet is mathematically an elastic plane, it can be represented as having thickness by permitting loads to be transferred at points other than those required to define the elastic characteristics. These points are called substitute gridpoints. A typical case occurs in the sandwich crossection represented in Figure 2-4.
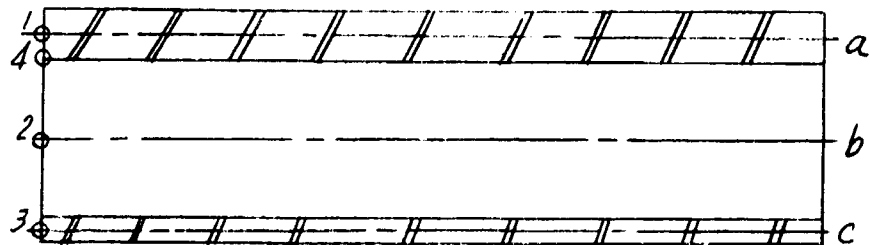
USE OF SUBSTITUTE JOINTS

Figure 2-4

The elastic planes lie along the lines a, b, and c. Elastic gridpoints are shown for one end at the left of the figure and numbered one, two, and three. Thickness of each laminae is represented by transferring the gridpoint forces at each point in the three elastic planes to the substitute point four, which may be located anywhere.

The required transformation can be written from equilibrium conditions. Assuming that gridpoint coordinates, displacements, and forces are in the same coordinate system for both the substitute and the elastic point, the relation between forces at any substitute and elastic point pair is given by

$$
\begin{Bmatrix} F_{xs} \\ F_{ys} \\ F_{zs} \\ M_{xs} \\ M_{ys} \\ M_{zs} \end{Bmatrix}
=
\begin{bmatrix}
1 & 0 & 0 & 0 & 0 & 0 \\
0 & 1 & 0 & 0 & 0 & 0 \\
0 & 0 & 1 & 0 & 0 & 0 \\
0 & (z_s - z_E) & (y_E - y_s) & 1 & 0 & 0 \\
(z_E - z_s) & 0 & (x_s - x_E) & 0 & 1 & 0 \\
(y_s - y_E) & (x_E - x_s) & 0 & 0 & 0 & 1
\end{bmatrix}
\begin{Bmatrix} F_{xE} \\ F_{yE} \\ F_{zE} \\ M_{xE} \\ M_{yE} \\ M_{zE} \end{Bmatrix}
\qquad (2.1\text{-}59)
$$

where x_E, y_E and z_E are coordinates of the elastic gridpoints and x_s, y_s, z_s, coordinates of the substitute gridpoints.

Equation (60) is of the form

$$\left\{ P_s \right\} = \left[W^T \right] \left\{ P_E \right\}$$

(2.1-60)

where W^T is the transpose of the required transformation matrix.

It is convenient to base the acceleration loading vectors on one "g" accelerations in the overall x, y, and z directions rather than in the local. This requires a special transformation to be introduced in Equation (35). The local accelerations are given in terms of the overall by

$$\left\{ \begin{matrix} g_x \\ g_y \\ g_\partial \\ g_\partial \end{matrix} \right\} = \left[S^T \right] \left\{ \begin{matrix} g_X \\ g_Y \\ g_Z \end{matrix} \right\}$$

(2.1-61)

where g_x, g_y and g_{∂}'' are in the local and g_X'', g_Y'' and g_Z'' accelerations in the overall coordinate system and S is the transpose of the orthogonal matrix defined by (45).

Using (61) in (35) gives the final form of the acceleration loading vectors

$$\left\{ P_g \right\} = \begin{bmatrix} I_c & 0_c & 0_c \\ 0_c & I_c & 0_c \\ 0_c & 0_c & I_c \\ 0_c & 0_c & 0_c \\ 0_c & 0_c & 0_c \end{bmatrix} \left[S^T \right] \left\{ \begin{matrix} g_X \\ g_Y \\ g_Z \end{matrix} \right\}$$

(2.1-62)

where $\left[I_c \right]^T = \lfloor 1 \quad 1 \rfloor$; $\lfloor 0_c \rfloor^T = \lfloor 0 \quad 0 \quad 0 \rfloor$

2.1.4.3 Stress and Strain Transformation

In the previous sections, it has been implicitly assumed that the material axes are coincident with the local coordinate axes. If this is not the case, the stress-strain relation can be transformed into the local system.

Let the stress strain relation in the material axes be given by

$$\{\hat{\sigma}\} = [\hat{D}]\{\hat{\epsilon}\}$$

(2.1-63)

where

$$\{\hat{\sigma}\} = \begin{Bmatrix} \hat{\sigma}_{xx} \\ \hat{\sigma}_{yy} \\ \hat{\sigma}_{xy} \\ \hat{\sigma}_{zz} \\ \hat{\sigma}_{yz} \\ \hat{\sigma}_{xz} \end{Bmatrix} ; \qquad \{\hat{\epsilon}\} = \begin{Bmatrix} \hat{\epsilon}_{xx} \\ \hat{\epsilon}_{yy} \\ \hat{\epsilon}_{xy} \\ \hat{\epsilon}_{zz} \\ \hat{\epsilon}_{yz} \\ \hat{\epsilon}_{xz} \end{Bmatrix}$$
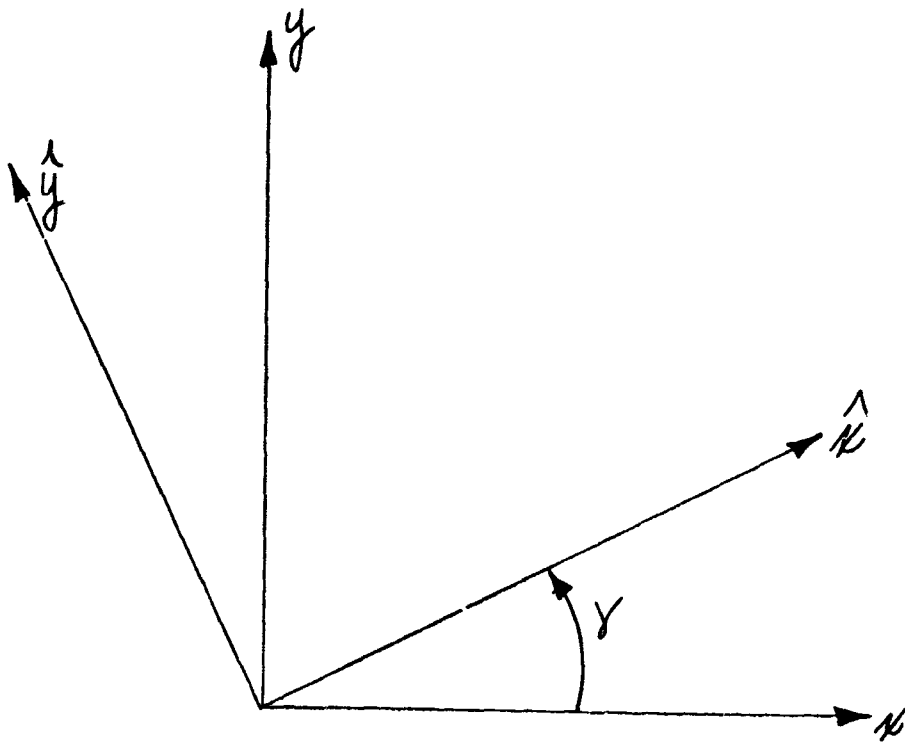
and $\hat{D}$ is of the form given in Equation (5).

Consider the equilibrium of the element shown in Figure 2-4. Here the material and Facet z axes are coincident and the material x-y axes are rotated from the local axes by an angle δ. The relation between stresses in the two systems is given by

$$\{\sigma\} = [H]\{\hat{\sigma}\}$$

(2.1-64)

where

$$[H] = \begin{bmatrix} \cos^2\delta & \sin^2\delta & 2\sin\delta\cos\delta & 0 & 0 \\ \sin^2\delta & \cos^2\delta & -2\sin\delta\cos\delta & 0 & 0 \\ -\sin\delta\cos\delta & \sin\delta\cos\delta & \cos^2\delta-\sin^2\delta & 0 & 0 \\ 0 & 0 & 1 & 0 & 0 \\ 0 & 0 & 0 & \cos\delta & \sin\delta \\ 0 & 0 & 0 & -\sin\delta & \cos\delta \end{bmatrix}$$

MATERIAL AND LOCAL AXES

Figure 2-5

The transformation between strains in the two systems involves a replace-
ment of the differentials in the material axes with those in the local
axes (See reference 4). The strains are transformed by

$$\left\{ \hat{\epsilon} \right\} = \left[H^T \right] \left\{ \epsilon \right\}$$

(2.1-65)

where H^T is the transpose of H . (Note that $H^T \neq H^{-1}$). Thus, sub-
stituting (65) in (63) and multiplying by H gives

$$\left\{ \sigma \right\} = \left[H \right] \left[\hat{D} \right] \left[H^T \right] \left\{ \epsilon \right\}$$

(2.1-66)

Equation (65) defines the transformation of the elastic coefficients so
that the stress-strain relation in the local coordinates is defined in
terms of elastic coefficients related to material axes.

2.2 DEVELOPMENT OF LINE ELEMENT EQUATIONS

This section contains development of the mathematical model representing the structural behavior of a line element with uniform properties. Included is development of stiffness, loading, and stress coefficients and necessary transformations.

The mathematical model for a line element is formed by superimposing models for axial elongation, torsional rotation, and shearing and bending. Two types of shearing and bending components are developed. The classical bending element provides for the analysis of frames and stiffened structures where the principle resistance to bending is provided by the stiffeners. The shear-bending element provides an element with deformations which are consistent with those of Facet. Use of Facet and shear-bending elements together insures bounding the strain energy (and yielding displacements which tend to be too small) for flat surfaces.

The stiffness coefficients are obtained using assumed displacement shapes a potential energy approach. In both the classical bending and shear-bending cases, the final stiffness matrix is a 12 by 12 matrix of rank 6.

Loading coefficients are developed for distributed loadings using the assumed displacement functions and the potential energy approach. Loadings corresponding to a temperature varying through the depth and width but constant over the length, uniform pressure along the length of the line, and constant accelerations in the x, y, and z directions are considered. Potential energy mass matrices are derived for uniformly

distributed mass. Coefficients of the resulting loading vectors are statically equivalent to the actual loads. Stress resultant coefficients are obtained directly from the stiffness matrix. Values of the coefficients give stresses at the end points of the line.

The line element is illustrated in Figure 2-6. The "natural coordinate system", x, y, z, has its origin at one end of the line, its x axis along the line and its x-y and x-z planes coinciding with principle planes for moments of inertia. u_{xj}, u_{yj}, u_{zj} are displacements along the coordinate axes at end j in the x, y, and z directions respectively and θ_{xj}, θ_{yj} and θ_{zj} rotation of the axes at end j. A right-handed coordinate system is used. The local coordinate system is a rectangular cartesian system with its x-y plane coincident with the natural system x-y plane. The origin need not lie on the line nor the x axis coincide with it. The overall coordinate system is a right-handed rectangular cartesian system.

2.2.1 Line Element Stiffness Coefficients

Stretching, twisting, and bending and shearing deformations of the line element are assumed to occur independently. In the next paragraphs, rod, tube, and beam stiffness coefficients are developed under this assumption.

2.2.1.2 Rod Stiffness Coefficients

The rod is assumed to be stress-free other than the direct stresses along its x axis, i.e.,

$$\sigma_{xx} \neq 0; \quad \sigma_{zz} = \sigma_{yy} = \sigma_{xy} = \sigma_{xz} = \sigma_{yz} = 0 \qquad (2.2\text{-}1)$$
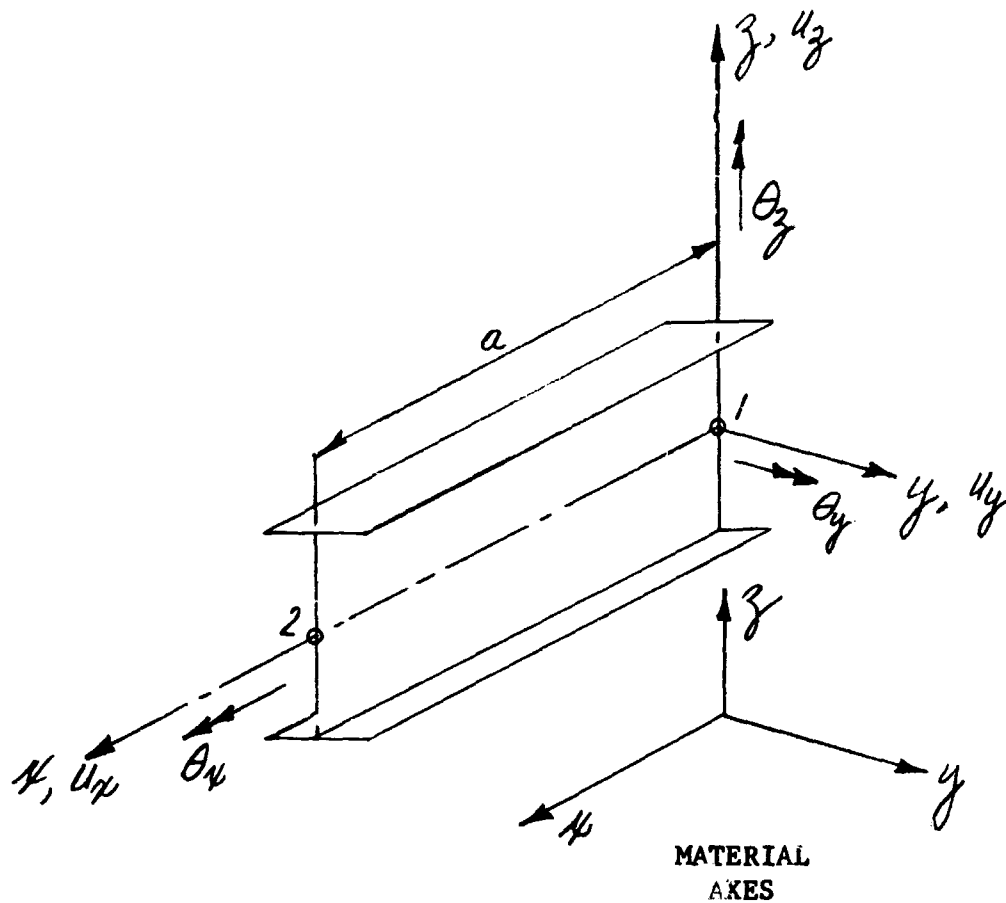
LINE ELEMENT REPRESENTATION

Figure 2-6

Imposing these constraints on the stress-strain relations, eq. (2.1-5), the σ_{yy} stress is expressed in terms of ϵ_{xx} by,

$$\sigma_{xx} = \hat{D}_{11} \, \epsilon_{xx}$$

$$\hat{D}_{11} = D_{11} - \lfloor D_{12} \; D_{13} \; D_{14} \rfloor \begin{bmatrix} D_{22} & D_{23} & D_{24} \\ & D_{33} & D_{34} \\ Sym. & & D_{44} \end{bmatrix} \begin{Bmatrix} D_{12} \\ D_{13} \\ D_{14} \end{Bmatrix} \qquad (2.2\text{-}2)$$

For an isotropic material (2) reduces to Young's modulus.

Substituting (1) and (2) in the strain energy expression (2.1-17), and using the strain-displacement relation gives

$$U_o' = \frac{1}{2} \int_{V_o'} \hat{D}_{11} \left(\frac{\partial u_{xj}}{\partial y} \, \delta - \alpha T \right) dv_o \qquad (2.2\text{-}3)$$

where u_{xj} is the displacement in the y direction and V_o the element volume. Assume displacements vary linearly with the y coordinate. Then u_{xj} can be written

$$u_y = \frac{(u_{x2} - u_{x1})}{a} y + u_{x1} \qquad (2.2\text{-}4)$$

where a is the element length.

Substituting (4) in (3), assuming the crossectional area is constant, and using Castigliano's theorem produces the load-deformation relation

$$\begin{Bmatrix} F_{x1} \\ F_{x2} \end{Bmatrix} = \frac{\hat{D}_{11} A}{a} \begin{bmatrix} 1 & -1 \\ -1 & 1 \end{bmatrix} \begin{Bmatrix} u_{x1} \\ u_{x2} \end{Bmatrix} \qquad (2.2\text{-}5)$$

where F_{x_j}' is the force at end j in the $\not{x}$ direction,

$\hat{A}$ is the crossectional area resisting axial stress,

and $\hat{D}_{11}$ is given by (2).

2.2.1.3 Tube Stiffness Coefficients

The tube is assumed to be stress-free except for shear stresses in the x-z plane. The development of the load-deflection relation parallels that for the rod. It is based on a linear variation of rotation with the $\not{x}$ coordinate and an isotropic material in shear. The equation corresponding to (5) is

$$\left\{ \begin{array}{c} M_{x_1} \\ M_{x_2} \end{array} \right\} = \frac{D_{33}\,J}{a} \left[\begin{array}{cc} 1 & -1 \\ -1 & 1 \end{array} \right] \left\{ \begin{array}{c} \theta_{x_1} \\ \theta_{x_2} \end{array} \right\}$$

(2.2-6)

where M_{x_j}' is the twist moment at end j about the $\not{x}$ axis

$D_{31} = D_{32} = D_{43} = 0$, by assumption

J is the <u>effective</u> torsional rigidity (polar moment of the crossection for cylinders)

2.2.1.4 Classical Beam Stiffness Coefficients

The classical beam deformations are obtained from the exact solution to the Timoshenko beam equations under the assumption of end loading only. This model considers the superposition of two "springs" in series --- a spring of pure bending and a spring of pure shear. The deflections of the line for bending about the $\not{y}$ axes are given by McCalley[6] as,

$$u_3 = \frac{1}{(1+12\beta_{x_3})}\left[\left(\frac{\ell^3}{a^2}-2\frac{\ell^2}{a}+\ell-6\beta_{x_3}\left[\frac{\ell^2}{a}-\ell\right]\right),\left(2\frac{\ell^3}{a^3}-3\frac{\ell^2}{a^2}+1-12\beta_{x_3}\left[\frac{\ell}{a}-1\right]\right),\right.$$
$$\left(\frac{\ell^3}{a^2}-\frac{\ell^2}{a}+6\beta_{x_3}\left[\frac{\ell^2}{a}-\ell\right]\right),\left(-2\frac{\ell^3}{a^3}+3\frac{\ell^2}{a^2}+12\beta_{x_3}\frac{\ell}{a}\right)\right]\begin{Bmatrix}-\theta_{y_1}\\u_{3_1}\\-\theta_{y_2}\\u_{3_2}\end{Bmatrix}$$

$$\beta_{x_3} = \hat{D}_{11}\,I_y/(\hat{D}_{55}\,A_{x_3}a^2)$$

$$\hat{D}_{55} = D_{55}$$

(2.2-7)

where I_y is the uniform crossectional moment of inertia and A_{x_3} the

uniform __effective__ area deforming in shear. With deformations in th's

form, integration of strain-energy over the crossection is already

implied. Therefore, (7) is introduced in the potential energy expression

integrated over the length, and differentiated with respect to the dis-

placements to define the load deformation relations. These operations

produce,

$$\begin{Bmatrix}F_{3_1}\\M_{y_1}\\F_{3_2}\\M_{y_2}\end{Bmatrix} = k_1\begin{bmatrix}2 & a & -2 & a\\ & k_2+k_3 & -a & k_2-k_3\\ & & 2 & -a\\ Sym & & & k_2+k_3\end{bmatrix}\begin{Bmatrix}u_r\\ \dot{\theta}_{y_1}\\ u_{3_2}\\ \theta_{y_2}\end{Bmatrix}$$

(2.2-8)

$$k_1 = \frac{6\hat{D}_{11}I_y}{a^3[1+\beta_{x_3}]}\ ;\quad k_2 = \frac{a^2}{2}\ ;\quad k_3 = \frac{a^2}{6}(1+\beta_{x_3})$$

These results can also be produced directly from equilibrium considerations.

A similar result can be written for bending about the z axes, combining

this result with (8) and rearranging terms provides the force-deformation

relation for the classical beam.

$$
\begin{Bmatrix} F_{y1} \\ F_{z1} \\ M_{y1} \\ M_{z1} \\ F_{y2} \\ F_{z2} \\ M_{y2} \\ M_{z2} \end{Bmatrix}
=
\begin{bmatrix}
2l_1 & 0 & 0 & al_1 & -2l_1 & 0 & 0 & al_1 \\
 & 2k_1 & ak_1 & 0 & 0 & -2k_1 & ak_1 & 0 \\
 & & l_1(k_2+k_3) & 0 & 0 & -ak_1 & l_1(k_2+k_3) & 0 \\
 & & & l_1(l_2+l_3) & al_1 & 0 & 0 & l_1(l_2+l_3) \\
 & & & & 2l_1 & 0 & 0 & -al_1 \\
 & & & & & 2k_1 & -ak_1 & 0 \\
 & & & & & & l_1(k_1+k_2) & 0 \\
 \text{S\scriptsize YM.} & & & & & & & l_1(l_2+l_3)
\end{bmatrix}
\begin{Bmatrix} u_{y1} \\ u_{z1} \\ \theta_{y1} \\ \theta_{z1} \\ u_{y2} \\ u_{z2} \\ \theta_{y2} \\ \theta_{z2} \end{Bmatrix}
\quad (2.2\text{-}9)
$$

where

$$
l_1 = \frac{6\hat{D}_{11}\, I_z}{a^3\left[1+\beta_{xy}\right]}
$$

$$
l_2 = \frac{a^2}{2}
$$

$$
l_3 = \frac{a^2}{6}\left(1+\beta_{xy}\right)
$$

$$
\beta_{xy} = \frac{\hat{D}_{11}\, I_z}{\hat{D}_{66}\, A_{xy}\, a^2}
$$

$$
\hat{D}_{66} = D_{66} - \frac{D_{45}^2}{D_{55}}
$$

2.2.1.5 Shear Beam Stiffness Coefficients

The shear beam[1,3] stiffness coefficients are based on the assumed deformation shape for bending about the y axis,

$$u_x = \frac{3}{2}(\theta_{y1} + \theta_{y2}) + \zeta\left(\theta_{y1} + \frac{x}{a}[\theta_{y2} - \theta_{y1}]\right)$$

$$u_\zeta = -\frac{x}{a}(u_{\zeta 1} - u_{\zeta 2}) + u_{\zeta 1} - \left(\theta_{y1}x + \frac{x^2}{2a}[\theta_{y2} - \theta_{y1}]\right) \tag{2.2-10}$$

where a is the beam length.

Comparing (10) and (2.1-1) and (2.1-2) it can be seen that deformations of both the beam and the facet vary linearly. Writing the total energy as the sum of the bending and shear energies, integrating over the uniform crossection and along the length of the line and using Castigliano's theorem gives the load deflection relation,

$$
\begin{Bmatrix} F_{\zeta 1} \\ M_{y1} \\ F_{\zeta 2} \\ M_{y2} \end{Bmatrix}
=
\begin{bmatrix}
\frac{D_{55}A_{x\zeta}}{a} & -\frac{D_{55}A_{x\zeta}}{2} & -\frac{D_{55}A_{x\zeta}}{a} & -\frac{D_{55}A_{x\zeta}}{2} \\
 & \frac{D_{55}A_{x\zeta}a}{4} + \frac{2\hat{D}_{11}I_y}{a} & \frac{D_{55}A_{x\zeta}}{2} & \frac{D_{55}A_{x\zeta}a}{4} - \frac{2\hat{D}_{11}I_y}{a} \\
 & & \frac{D_{55}A_{x\zeta}}{a} & \frac{D_{55}A_{x\zeta}}{2} \\
 \text{SYM.} & & & \frac{D_{55}A_{x\zeta}a}{4} + \frac{2\hat{D}_{11}I_y}{a}
\end{bmatrix}
\begin{Bmatrix} u_{\zeta 1} \\ \theta_{y1} \\ u_{\zeta 2} \\ \theta_{y2} \end{Bmatrix}
\tag{2.2-11}
$$

A similar result can be written for bending about the ζ axis. Combining this with (11) and rearranging terms gives, (2.2-12),

$$
\begin{Bmatrix} F_{y1} \\ F_{\zeta 1} \\ M_{y1} \\ M_{\zeta 1} \end{Bmatrix}
= D_{55}
\begin{bmatrix}
\frac{A_{xy}}{a} & 0 & 0 & \frac{A_{xy}}{2} & -\frac{A_{xy}}{a} & 0 & 0 & \frac{A_{xy}}{2} \\
0 & \frac{A_{x\zeta}}{a} & -\frac{A_{x\zeta}}{2} & 0 & 0 & -\frac{A_{x\zeta}}{a} & -\frac{A_{x\zeta}}{2} & 0 \\
0 & -\frac{A_{x\zeta}}{2} & \frac{A_{x\zeta}a}{4} + \frac{2\hat{D}_{11}I_y}{aD_{55}} & 0 & 0 & \frac{A_{x\zeta}}{2} & \frac{A_{x\zeta}a}{4} - \frac{2\hat{D}_{11}I_y}{aD_{55}} & 0 \\
\frac{A_{xy}}{2} & 0 & 0 & \frac{A_{xy}a}{4} + \frac{2\hat{D}_{11}I_\zeta}{aD_{55}} & -\frac{A_{xy}}{2} & 0 & 0 & \frac{A_{xy}a}{4} - \frac{2\hat{D}_{11}I_\zeta}{a}
\end{bmatrix}
\begin{Bmatrix} u_{y1} \\ u_{\zeta 1} \\ \theta_{y1} \\ \theta_{\zeta 1} \\ u_{y2} \\ u_{\zeta 2} \\ \theta_{y2} \\ \theta_{\zeta 2} \end{Bmatrix}
$$

$$\begin{Bmatrix} F_{y2} \\ F_{32} \\ M_{y2} \\ M_{32} \end{Bmatrix} = D_{55} \begin{bmatrix} -\frac{A_{xy}}{a} & 0 & 0 & -\frac{A_{xy}}{2} & \frac{A_{xy}}{a} & 0 & 0 & -\frac{A_{xy}}{2} \\ 0 & -\frac{A_{x3}}{a} & \frac{A_{x3}}{2} & 0 & 0 & \frac{A_{x3}}{a} & \frac{A_{x3}}{2} & 0 \\ 0 & -\frac{A_{x3}}{2} & \frac{A_{x3}a}{4} - \frac{2\hat{D}_{11}I_y}{D_{55}a} & 0 & 0 & \frac{A_{x3}}{2} & \frac{A_{x3}a}{4} + \frac{2\hat{D}_{11}I_y}{a} & 0 \\ \frac{A_{xy}}{2} & 0 & 0 & \frac{A_{xy}a}{4} - \frac{2\hat{D}_{11}I_2}{D_{55}a} & -\frac{A_{xy}}{2} & 0 & 0 & \frac{A_{xy}a}{4} + \frac{2\hat{D}_{11}I_4}{a} \end{bmatrix} \begin{Bmatrix} u_{y1} \\ u_{31} \\ \theta_{y1} \\ \theta_{31} \\ u_{y2} \\ u_{32} \\ \theta_{y2} \\ \theta_{32} \end{Bmatrix}$$

2.2.1.6 Total Element Stiffnesses

The total element stiffness consists cf a summation of matrices. In the case of the classical beam, the summation includes eqs. (5), (6), and (9). For the shear-bending beam, the summation includes (5), (6), and (12). The classical beam element should be used in analyses of all frame systems. The shear-bending element should be used for parts of the structures where Facet is used since displacement continuity will then be maintained.

2.2.2 Line Element Loading Vectors

The loading vectors corresponding to distributed loads can be obtained from the loading conditions. In this section loading vectors are developed for thermal, acceleration and pressure environments. Potential energy mass matrices are obtained. The mass and pressure are assumed uniformly distributed along the length. Temperature is assumed to be constant over the length and vary through the depth and width of the element.

2.2.2.1 Thermal Loading Vector

If the ends of the element are clamped, temperature changes from the fabrication temperature induce reactive forces and moments at the restraints. These generalized forces constitute the components of the loading vector to be imposed on the structure. For the temperature distribution assumed, the reactions can be written.

$$
\begin{Bmatrix} F_{x1} \\ M_{y1} \\ M_{z1} \\ F_{x2} \\ M_{y2} \\ M_{z2} \end{Bmatrix} = \alpha \hat{D}_{11} \begin{Bmatrix} A T_o \\ I_y \frac{T_z}{d} \\ I_z \frac{T_y}{d} \\ -A T_o \\ -I_y \frac{T_z}{d} \\ -I_z \frac{T_y}{d} \end{Bmatrix}
$$

(2.2-13)

where A is the crossectional area in the x-y plane, T_o, the constant temperature change along the length, $\frac{T_z}{d}$ the effective temperature gradient through the depth and $\frac{T_y}{d}$ the effective gradient over the width

of the element. Note that these forces do not imply that the temperature necessarily varies linearly over the width or depth. The generalized forces are expressed in terms of the microscopic values by the relations

$$F_{x_j} = \pm \int_A \hat{D}_{11} \alpha T_o \, dA$$

$$M_{y_j} = \pm \int_A \hat{D}_{11} \alpha T_{\bar{3}} \bar{3} \, dA$$

(2.2-14)

$$M_{3j} = \pm \int_A \hat{D}_{11} \alpha T_{\bar{y}} \bar{y} \, dA$$

It is also noted that the thermal loading vector is applicable to both the classical and shear-bending beams.

2.2.2.2 Acceleration and Pressure Loading Vectors

For uniformly distributed mass, the displacement functions (4) and (7) or (10) and equation (A-8) lead to the following gridpoint forces,

$$\begin{Bmatrix} F_{x_1} \\ F_{y_1} \\ F_{3_1} \\ F_{x_2} \\ F_{y_2} \\ F_{3_2} \end{Bmatrix} = \frac{M_B}{2} \begin{bmatrix} 1 & 0 & 0 \\ 0 & 1 & 0 \\ 0 & 0 & 1 \\ 1 & 0 & 0 \\ 0 & 1 & 0 \\ 0 & 0 & 1 \end{bmatrix} \begin{Bmatrix} q_x \\ q_y \\ q_3 \end{Bmatrix}$$

(2.2-15)

where M_B is the total mass of the beam and,

q_i are acceleration components in the local coordinate system.

There are no gridpoint moments for the shear-beam. The classical beam gives the gridpoint moments,

$$\begin{Bmatrix} M_{y1} \\ M_{31} \\ M_{y2} \\ M_{32} \end{Bmatrix} = \frac{M_\beta}{12} \begin{bmatrix} 0 & 0 & 1 \\ 0 & 1 & 0 \\ 0 & 0 & -1 \\ 0 & -1 & 0 \end{bmatrix} \begin{Bmatrix} g_x \\ g_y \\ g_z \end{Bmatrix}$$

(2.2-16)

The pressure loading vectors for the two beams can be obtained from (108) and (16) by selecting $M_\beta = \rho$, $g_3 = 1$, and $g_x = g_y = 0$.

2.2.2.3 Inertia Matrix

The inertia matrix consists of contributions from the rod, tube, and beam elements. The mass is assumed to lie on a line along the neutral axis of the element. Using the rod displacement function, substitution of the kinetic energy in Lagrange's equation leads to the rod inertia loading matrix

$$\begin{Bmatrix} F_{x1} \\ F_{x2} \end{Bmatrix} = \frac{M}{6} \begin{bmatrix} 2 & 1 \\ 1 & 2 \end{bmatrix} \begin{Bmatrix} \ddot{u}_{x1} \\ \ddot{u}_{x2} \end{Bmatrix}$$

(2.2-17)

Similarly, using the displacement function for the classical beam, the inertia loading matrix is

$$\begin{Bmatrix} F_{y1} \\ F_{31} \\ M_{y1} \\ M_{31} \\ F_{y2} \\ F_{32} \\ M_{y2} \\ M_{32} \end{Bmatrix} = \begin{bmatrix} \bar{M} \end{bmatrix} \begin{Bmatrix} \ddot{u}_{y1} \\ \ddot{u}_{31} \\ \ddot{\theta}_{y1} \\ \ddot{\theta}_{31} \\ \ddot{u}_{y2} \\ \ddot{u}_{32} \\ \ddot{\theta}_{y2} \\ \ddot{\theta}_{32} \end{Bmatrix}$$

(2.2-18)

$$\bar{M}_{k\ell} = \bar{M}_{\ell k}; \quad \delta_{x_3} = (1+12\beta_{x_3})^{-2}; \quad \delta_{xy} = (1+12\beta_{xy})^{-2}$$

$$\bar{M}_{11} = \bar{M}_{55} = (48\beta_{x_3}^2 + \frac{42}{5}\beta_{x_3} + \frac{13}{35})\delta_{x_3} = \hat{M}_{22} = \hat{M}_{66}$$

$$\bar{M}_{44} = \bar{M}_{88} = (\frac{6}{5}\beta_{x_3}^2 + \frac{1}{5}\beta_{x_3} + \frac{1}{105})a^2\delta_{x_3} = \hat{M}_{33} = \hat{M}_{77}$$

$$\bar{M}_{41} = \bar{M}_{14} = (-6\beta_{x_3}^2 - \frac{11}{10}\beta_{x_3} + \frac{13}{35})a\delta_{x_3} = \hat{M}_{32} = \hat{M}_{23}$$

$$\bar{M}_{51} = \bar{M}_{15} = (24\beta_{x_3}^2 + \frac{18}{5}\beta_{x_3} + \frac{9}{70})\delta_{x_3} = \hat{M}_{67} = \hat{M}_{26}$$

$$\bar{M}_{81} = \bar{M}_{18} = (6\beta_{x_3}^2 + \frac{9}{10}\beta_{x_3} + \frac{13}{420})a\delta_{x_3} = \hat{M}_{72} = \hat{M}_{27}$$ (2.2-19)

$$\bar{M}_{54} = \bar{M}_{45} = (-6\beta_{x_3}^2 - \frac{9}{10}\beta_{x_3} - \frac{13}{420})a\delta_{x_3} = \hat{M}_{63} = \hat{M}_{36}$$

$$\bar{M}_{84} = \bar{M}_{48} = (-\frac{6}{5}\beta_{x_3}^2 - \frac{1}{5}\beta_{x_3} - \frac{1}{140})a^2\delta_{x_3} = \hat{M}_{73} = \hat{M}_{37}$$

$$\bar{M}_{85} = \bar{M}_{58} = (6\beta_{x_3}^2 + \frac{11}{10}\beta_{x_3} + \frac{11}{210})a\delta_{x_3} = \hat{M}_{76} = \hat{M}_{67}$$

where $\hat{M}_{k\ell} = \bar{M}_{x_2}$ with x_3 subscripts replaced by xy

Using the displacement function for the shear-bending beam, its inertia loading matrix is found to be

$$[\bar{M}] = \frac{M}{6}\begin{bmatrix} 2 & 0 & 0 & 0 & 1 & 0 & 0 & 0 \\ & 2 & 0 & 0 & 0 & 1 & 0 & 0 \\ & & 0 & 0 & 0 & 0 & 0 & 0 \\ & & & 0 & 0 & 0 & 0 & 0 \\ & & & & 2 & 0 & 0 & 0 \\ & & & & & 2 & 0 & 0 \\ & & & & & & 0 & 0 \\ \text{SYM.} & & & & & & & 0 \end{bmatrix}$$ (2.2-20)

There is no inertia matrix due to mass for the torque tube because the mass is assumed to lie on the twist axis. Therefore, the total mass matrix consists of (17) and either (18) and (19) or (20).

2.2.3 Line Element Stress Displacement Equations

Stress resultants for the ends of the line element are obtained directly

from the product of the element stiffness matrices and the displacements,

$$
\begin{Bmatrix} N_{11} \\ M_{11} \\ M_{22_1} \\ V_2 \\ V_3 \\ M_{33} \\ M_{22}' \\ M_{33}' \end{Bmatrix} = \begin{bmatrix} 1 & 0 & 0 & 0 & 0 & 0 & 0 & 0 & 0 & 0 & 0 & 0 \\ 0 & 0 & 0 & 1 & 0 & 0 & 0 & 0 & 0 & 0 & 0 & 0 \\ 0 & 0 & 0 & 0 & 1 & 0 & 0 & 0 & 0 & 0 & 0 & 0 \\ 0 & 0 & 1 & 0 & 0 & 0 & 0 & 0 & 0 & 0 & 0 & 0 \\ 0 & 1 & 0 & 0 & 0 & 0 & 0 & 0 & 0 & 0 & 0 & 0 \\ 0 & 0 & 0 & 0 & 0 & 1 & 0 & 0 & 0 & 0 & 0 & 0 \\ 0 & 0 & 0 & 0 & 0 & 0 & 0 & 0 & 0 & 0 & 1 & 0 \\ 0 & 0 & 0 & 0 & 0 & 0 & 0 & 0 & 0 & 0 & 0 & 1 \end{bmatrix} \begin{Bmatrix} F_{x_1} \\ F_{y_1} \\ F_{z_1} \\ M_{x_1} \\ M_{y_1} \\ M_{z_1} \\ F_{x_2} \\ F_{y_2} \\ F_{z_2} \\ M_{x_2} \\ M_{y_2} \\ M_{z_2} \end{Bmatrix} \quad (2.2\text{-}21)
$$

where the stiffness matrix is the total stiffness matrix, and

N_{11}	Normal force in x direction, ends 1 and 2
M_{11}	Twisting moment, x vector, ends 1 and 2
M_{22}	Bending moment y vector, end 1
V_2	Shear force in x-z plane
V_3	Shear force in x-y plane
M_{33}	Bending moment, z vector, end 1
M_{22}'	Bending moment, y vector, end 2
M_{33}'	Bending moment, z vector, end 2

Note that N_{11}, M_{11}, V_2, and V_3 are defined only at end one of the line.

At the other end, values of these quantities are of the same magnitude

and opposite sign.

2.2.4 Line Element Transformations

Two types of transformations are necessary for the line element. Trans-

formations are required of line element gridpoint coordinates and of

forces and deflections.

Coordinates of the line element may be given in an overall or local rec-
tangular cartesian system. The local system has its x-y plane coincident
with a principal plane of the element. Matrices of coefficients are
developed in the natural rectangular cartesian coordinate system which
in addition to having its x-y plane coincident with a principal plane has
the x axis lying along the line. The transformations required between
the overall and local axes and the natural axis are a degenerate form of
those for the Facet given in 2.1.4.1.

Forces and displacements may be represented in the local or overall system
at each gridpoint. To provide for this option, the transformation from
the natural to the appropriate final coordinate system is required.
These transformations and transformations to impose boundary conditions
which represent joint eccentricities are degenerate forms of the trans-
formations for the Facet given in 2.1.4.2.

Elastic coefficients for the line element are referenced to the natural
coordinate system. Thus, no stress and strain transformation is required.

SECTION 3

SAMIS LINK THEORY AND USE
IN STRUCTURAL ANALYSIS

SAMIS contains program links for performing all the steps in predicting
static structural response and undamped resonances. The principal
steps are listed in the first column of Table 3-1. The first step in-
volves generating stiffness, stress, and loading coefficients for each
element of the structure. The element stiffness coefficients are added
to form the stiffness coefficients for the entire structure. For the
same reason, loading coefficients are added.

In general, boundary conditions are imposed on the unrestrained struc-
tural representation by defining conditions on the displacements. These
restraints require a congruent transformation of the stiffness and mass
matrices and a premultiplication of other loading vectors.

If the analyst desires, he may introduce changes to the matrices to re-
flect experimental or theoretical data. These changes are read in and
additions and/or subtractions used to change matrix coefficients. Dis-
placements are found by solving the load-deflection relations. This is
a set of linear, homogeneous, simultaneous equations involving the square,
symmetric and positive definite restrained stiffness matrix and the re-
strained loading vectors. Element stresses are obtained by premultiply-
ing the displacements by the elemer stress matrices.

A symetric dynamic matrix is developed by defining a transformation
based on either the restrained stiffness or mass matrix. The change of

TABLE 3-1

LINK USE IN STRUCTURAL ANALYSIS

STRUCTURAL ANALYSIS STEP	IMPLEMENTATION WRITEUP SITE	PRINCIPAL PARTICIPANTS
Generate coefficients in the equations of motion	TECH:* 2.0-2.2, 3.6	BILD, READ, ADDS
Impose holonomic force and/or displacement boundary conditions	TECH: 3.1	BILD, WASH, MULT, FLIP
Modify matrices in equations of motion using analyst's data	TECH: 3.6	READ, ADDS, SUBS
Calculate displacements for static loads	TECH: 3.2, 3.4	CHOL, ITER
Calculate element stresses from displacements	TECH: 2.1, 2.2, 3.6	BILD, MULT
Define dynamic matrix in symmetric form	TECH: 3.3	IN, MULT, FLIP
Determine resonant modes and frequencies	TECH: 3.5	ROOT, MULT, FLIP

* "TECH" refers to the SAMIS Technical Document.

coordinates requires performing a congruent transformation of the stiff-ness matrix. After obtaining modes and frequencies in the transformed coordinate system, modal displacements are converted back to the original basis by a matrix multiplication.

The second column of Table 3-1 indicates where further explanation of SAMIS implementation can be found for each analysis step. The third column defines the principal links used performing the analysis steps. In each step, the ADDS, SUBS, WASH, FLIP, MULT, and CHOL links may also be required if matrices are partitioned.

The basis for calculations for most of the complicated operations can be found in mathematical reference books such as references 1 and 2. There-fore, descriptions in the paragraphs that follow are oriented toward the application of the techniques to structural analysis.

3.1 WASH MULTIPLICATION (WASH)

Wash multiplication is a special multiplication provided to simplify de-leting or extracting partitions from a matrix or scaling elements of a partition. It yields a matrix C as the result of A operating on B, i.e.,

$$[C] = [A]_{op.}[B]$$

(3-1)

The operation is designed to partition and perform the congruent multiplication

$$[C] = [A^T][B][A]$$

(3-2)

when A is a diagonal matrix.

To reduce input, there are five modes of operation. To explain these, consider the matrix

$$[B] = \begin{bmatrix} B_{1,1} & B_{1,2} \\ B_{2,1} & B_{2,2} \end{bmatrix}$$

The results of the Wash operation for several A matrix inputs and modes are given below:

	A Output			C Output	
Row	Column	Value	Mode	Values	Operation
1	1	2.0	0	$4B_{11}$, $2B_{12}$, $2B_{21}$, B_{22}	Scaling
1	1	0.0	0	B_{22}	Deletion
1	4*	2.0	1	$2B_{11}$, $2B_{12}$, B_{21}, B_{22}	Scaling
1	1	2.0	2	$4B_{11}$, $2B_{12}$, $2B_{21}$	Extraction
1	3*	1.0	2	B_{11}, B_{12}	Extraction
3*	1	1.0	2	B_{11}, B_{21}	Extraction
1	2	2.0	2	$2B_{11}$, $4B_{12}$, $2B_{22}$	Extraction
1	1	3.0	3	$9B_{11}$, B_{12}, B_{21}, B_{22}	Scaling
1	2	2.0	3	B_{11}, $4B_{12}$, B_{21}, B_{22}	Scaling
1	1	5.0	4	$25B_{11}$	Extraction
1	2	2.0	4	$4B_{12}$	Extraction

* Note that these column numbers match none of the column numbers of the B matrix.

The congruent transformation (2) arises whenever a change of coordinates is made. Consider the strain energy expression (A-6).

$$U = \frac{1}{2} \lfloor v \rfloor [K] \{v\}$$

(3-3)

If the old displacements are linear functions of the new they can be written

$$\{v\} = [A]\{\bar{v}\}$$

(3-4)

where the Aij are constants and A is a rectangular matrix. Substituting (4) in (3) gives

$$U = \frac{1}{2} \lfloor v \rfloor [A]^T [K][A]\{\bar{v}\}$$

(3-5)

Thus, the stiffness matrix is changed to a new basis by a congruent transformation. Similarly, initial stress, damping, and mass matrices involve congruent transformations. The loading transformation to the new coordinate system involves a single matrix multiplication,

$$\{\bar{P}(t)\} = [A]^T \{P(t)\}$$

(3-6)

The primary use of a coordinate change is in imposing boundary conditions. An holonomic set in forces and/or displacements can be reduced to the form (4). In the special but frequently occurring case when displacement components are fixed at the gridpoints (including the idealized end conditions of simple supports and fixity), the matrix A is a diagonal matrix.

3.2 CHOLESKI'S METHOD (CHOL)

Choleski's method is a procedure for solving a set of simultaneous equations. The process consists of a triangular decomposition and

solution of two sets of simultaneous equations for which the square matrix is ir'tially of triangular form.

Consider the equations

$$\{P\} = [K]\{v\}$$

(3-7)

where K is a square, symmetric matrix, the P matrix coefficients are known and   unknown. Then, if K is positive definite it can always be decomposed in the form

$$[K] = [U]^T[U]$$

(3-8)

Where U is an upper triangular matrix, i.e., U takes the form

$$\begin{bmatrix} u_{11} & u_{12} & u_{13} & \cdots & u_{1N} \\ 0 & u_{22} & u_{23} & \cdots & u_{2N} \\ 0 & 0 & u_{33} & \cdots & u_{3N} \\ \vdots & \vdots & & \ddots & \vdots \\ 0 & 0 & 0 & \cdots & u_{NN} \end{bmatrix}$$

(3-9)

The u_{ij} can be found directly by solving the equations (8). Substituting (8) in (7) gives

$$\{P\} = [U]^T[U]\{v\} = [U]^T\{\bar{v}\}$$

(3-10)

where $\{\bar{v}\} = [U]\{v\}$

(3-11)

Then (10) can be solved for $\bar{V}$ and (11) subsequently solved for the unknown V since U and U^T must be non-singular.

This algorithm conserves storage space. Since K is symmetric, only the upper (or lower) half of K needs to be stored. U is upper triangular and can replace K as it is generated. With U available, the unknown can replace the P components. Similarly, the unknown V can replace the $\bar{V}$.

This method also is economical of machine time because it takes advantage of matrix symmetry and sparcity. The number of calculations for a large full matrix equals $\dfrac{n^3}{6}$ where n is the matrix order. The usual Gauss-Jordan elimination disregarding symmetry would require $n^3/3$ operations.

The method is well suited for structural analysis. Stiffness matrices are generally sparse matrices. The algorithm is easily modified so that variable bandwidth operations are performed and additional storage space thereby saved. In this form, all the non-zero elements are contained in a band near the diagonal. The bandwidth is defined as either the number of columns to the right of the diagonal or number of rows below the diagonal or number of rows below the diagonal within which all the non-zero elements are contained. The bandwidth of any row in the K matrix is the same as that of the corresponding row in the U^T matrix, as long as the bandwidth does not decrease more than one element for each successive row.

In the process of forming the diagonal elements of the decomposed matrix, square roots are taken. If any of these arguments are negative, the matrix cannot be positive definite. On the other hand, the stiffness matrix

must be positive definite, if the system is conservative. Therefore, if a Choleski decomposition can be performed in solving the simultaneous equations, then the mathematical model being analyzed represents a conservative system.

The Choleski process can also be used to solve simultaneous equations even when the square matrix is not symmetric or positive definite. Consider the equation

$$[P] = [A]\{v\} \tag{3-12}$$

where the v_i are unknown. Multiplying both sides of the equation by the transpose of the A matrix and solving for the v_i, it is found that

$$[A]^T\{P\} = [A]^T[A]\{v\}$$

$$\{v\} = [A^TA]^{-1}[A]^T\{P\} \tag{3-13}$$

$$= [A]^{-1}[A^T]^{-1}[A]^T\{P\}$$

$$\therefore \quad \{v\} = [A]^{-1}\{P\} \tag{3-14}$$

If the matrix A is nonsingular, A^TA will be positive definite and symmetric. Thus, the matrix arithmetic routines can be used to put (12) in the form (13) and the Choleski process used to obtain the v_i of equation (14). Though this approach looks inefficient, it is competitive with direct Gauss–Jordan elimination solution of (12) because advantage is taken of the symmetry (and sparcity) of A^TA .

To illustrate decomposition, consider the stiffness matrix of a straight uniform segment string with three gridpoints between the pinned ends; the stiffness matrix is given by

$$[K] = \frac{AE}{L} \begin{bmatrix} 2 & -1 & 0 \\ -1 & 2 & -1 \\ 0 & -1 & 2 \end{bmatrix}$$

(3-15)

Equation (8) gives for U

$$[U] = \sqrt{\frac{AE}{L}} \begin{bmatrix} \sqrt{2} & -\frac{1}{\sqrt{2}} & 0 \\ 0 & \sqrt{\frac{3}{2}} & -\sqrt{\frac{2}{3}} \\ 0 & 0 & \sqrt{\frac{4}{3}} \end{bmatrix}$$

(3-16)

Comparing (15) and (16) it can be seen that the form of the band has been preserved in the decomposition.

The ordering of the equations affects the number of equations that can be handled in a given space. Thus , if the first two rows and columns of (15) are interchanged, K becomes

$$[K] = \frac{AE}{L} \begin{bmatrix} 2 & -1 & -1 \\ -1 & 2 & 0 \\ -1 & 0 & 2 \end{bmatrix}$$
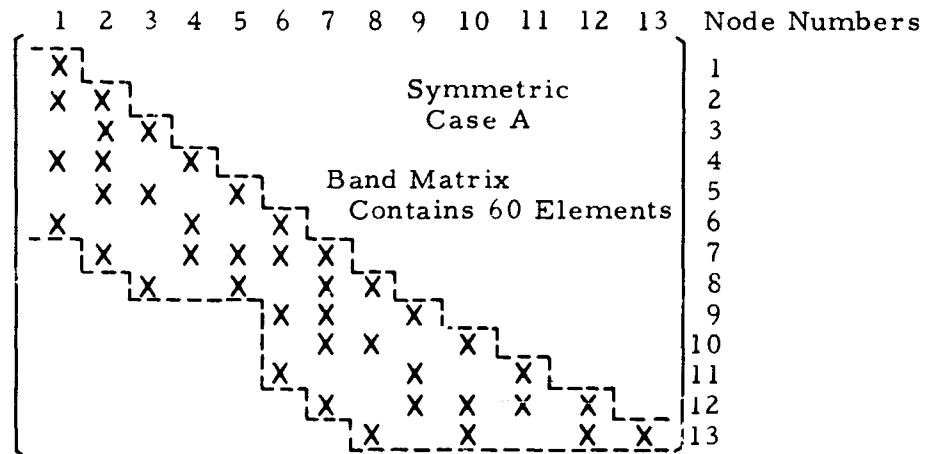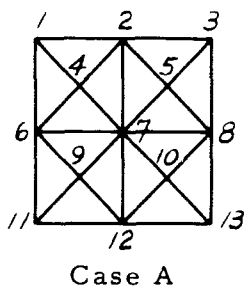
(3-17)

and in this case, all elements on and to the right of the diagonal must be stored. To maximize the number of equations to be handled in core (and hence reduce machine time), it is desirable to have small bandwidth and few zero elements in the band.

The bandwidth growth is controlled by the numbering sequence chosen for the gridpoints and the topology of the problem. The stiffness matrix for a Facet provides non-zero terms at and between all gridpoints bounding the Facet. With this knowledge it is easy to determine how the bandwidth will vary for a given problem.
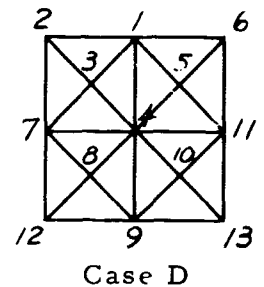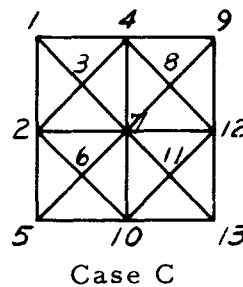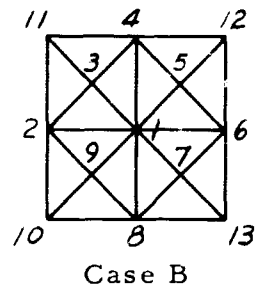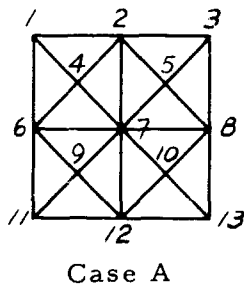
The plot in Figure 3-1 provides an illustration of how the gridpoint numbering affects the band. The variable band matrix lies between the dotted lines. A quick way to determine the number of elements within the band is the tabular method shown in the figure. In the first column are listed the gridpoint numbers, in the second column, the largest difference between each gridpoint number and its adjacent higher gridpoint number in the system. In the third column is the number of elements in the row. This number is one greater than the element in the second column or one less than the number in the third column which precedes it, whichever is greater. Thus, the bandwidth at point 9 for case A is the greater of 4 or 5, i.e., 5. Summing the elements in the third column gives the number of elements in the band matrix.

The figure shows four gridwork numbering schemes and the number of elements for each. It can be seen that three schemes require about the

GRAPHICAL SOLUTION

Case A

Node Numbers 1 2 3 4 5 6 7 8 9 10 11 12 13

Symmetric
Case A

Band Matrix
Contains 60 Elements

TABULAR SOLUTIONS

Case A   Case B   Case C   Case D

Node	Δ	Band	Δ	Band	Δ	Band	Δ	Band
1	5	6	8	9	3	4	5	6
2	5	6	9	10	5	6	5	6
3	5	6	8	9	4	5	4	5
4	3	5	8	9	5	6	7	8
5	3	4	7	8	5	6	6	7
6	5	6	7	8	4	5	5	6
7	5	6	6	7	5	6	5	6
8	5	6	5	6	4	5	4	5
9	3	5	1	5	3	4	4	5
10	3	4	0	4	3	4	3	4
11	1	3	0	3	2	3	2	3
12	1	2	0	2	1	2	0	2
13	0	1	0	1	0	1	0	1
Elements		60		81		57		64

JOINT NUMBERING EFFECT ON BAND

Fig. 3-1

same space while the second is much less efficient. This is typical of the numbering problem. It suggests that only a little thought needs to be devoted to choosing the numbering scheme to arrive at a reasonable numbering. Though the numbering problem could be handled by the computer, it does not appear to be a justifiable procedure.

3.3 CHOLESKI DECOMPOSITION AND INVERSION (CHIN)

The Chin subprogram includes a Choleski decomposition and inversion of the decomposed triangular matrix. A discussion of the decomposition is given in 3.2. The calculation of the inverse can also be done in variable bandwidth form but, in general, requires additional space. The inverse matrix U^{-1} is found directly by solving the equations

$$[U][U]^{-1} = [I] \tag{3-18}$$

where I is the identity matrix and U the triangular decomposition of K.

There are two applications for this operation in structural analyses. One is for static problems, the other for dynamic. In the static case, the CHIN link provides an economical way of obtaining an influence matrix. Since

$$[U]^{T}[U] = [K]$$

then $[U]^{-1}[U^{T}]^{-1} = [K]^{-1}$ $\tag{3-19}$

and noting that

$$[U^{T}]^{-1} = [U^{-1}]^{T}$$

The transpose of U^{-1} can be taken and a multiplication performed to find the inverse of K.

In the dynamics problem, CHIN provides the transformation required to generate a symmetric dynamic matrix. The dynamic equations are

$$[K]\{v\} = [M]\{\ddot{v}\}$$ (3-20)

where M is the square positive definite mass matrix and the dots denote time derivatives. Assuming sinusoidal motion (20) becomes

$$[K]\{v\} = \omega^2 [M]\{v\}$$ (3-21)

where ω is the resonant frequency. Now let

$$\{v\} = [U]^{-1}\{\bar{v}\}$$ (3-22)

where $U^{t}U = K$ and $UU^{-1} = I$ (3-23)

then (21) can be written

$$[K][U]^{-1}\{\bar{v}\} = \omega^2 [M][U]^{-1}\{\bar{v}\}$$ (3-24)

Multiplying (24) by (U^{-1T}) gives

$$[U^{-1}]^{T}[K][U]^{-1}\{\bar{v}\} = \omega^2 [U^{-1}]^{T}[M][U]^{-1}\{\bar{v}\}$$ (3-25)

But, from (23), the left hand side of (25) is the identity matrix. Since M is symmetric, the right hand side is symmetric. This is the required symmetric dynamic matrix. Note that (22) must be used to transform displacements to the original system. Note also that K must be positive definite in order to decompose and invert the matrix as indicated in (23).

If M is a diagonal matrix and non-singular, the roles of M and K can be reversed. In this case, WASH multiplication can be used to generate the left hand side of (25).

3.4 SEIDEL ITERATION (ITER)

Seidel iteration is an iterative method for solving simultaneous equations. If it is required to solve the equations

$$[K]\{V\} = \{P\}$$

(3-26)

for V, then to state the Seidel algorithm concisely, it is convenient to reformulate (26) as

$$[I - \bar{L} - \bar{U}]\{V\} = \{\bar{P}\}$$

(3-27)

where I is the identity matrix, $\bar{L}$ a lower triangular matrix with a null diagonal, $\bar{U}$ a similar upper triangular matrix, and $\bar{P}$ the P after normalization indicated. Then, Seidel iteration can be stated in the form of a recursion relating successive values i and $i + 1$ of the unknown V vector.

$$\{V\}_{\dot{\iota}+1} = \{V\}_{\dot{\iota}} + \beta\left[\{\bar{P}\} + [L]\{V\}_{\dot{\iota}+1} - [I - U]\{V\}_{\dot{\iota}}\right] \qquad (3\text{-}28)$$

where β is the overrelaxation factor and the subscript denotes the iteration number. β is one in the iteration process originally defined by Seidel[3]. It can be proved that a necessary and sufficient condition for convergence of the iteration is that the matrix K shall be positive definite.

When β is greater than one, Seidel iteration is termed extrapolated Seidel iteration or successive overrelaxation. The improved economy of this approach is well known.[4, 5, 6] An understanding of the role of β is obtained by writing the recursion in the form of an eigenvalue problem. This is done by defining an error vector equal to the difference between the final vector and the most recent one, i.e. $\epsilon_i = V_f - V_i$ where the subscript denotes the iteration number (f = final). Then the iteration (28) can be written,

$$\lambda\{\epsilon\}_{\dot{\iota}+1} = [I - \beta L]^{-1}[\beta U - (\beta - 1)I]\{\epsilon\}_{\dot{\iota}} = [E]\{\epsilon\}_{\dot{\iota}} \qquad (3\text{-}29)$$

where E is the iteration matrix and ϵ the error vector.

The optimum value β_0 is defined as that which minimizes the largest latent root of the iteration matrix. Young[5] has proven if the matrices possess

property A and are in their consistent ordering* that the iteration con-
verges for $0 \leqslant \beta \leqslant 2$. The optimum relaxation factor is then re-
lated to the maximum latent root by

$$\beta_o = 2 \left(1 + \sqrt{1 - \frac{(\lambda_\beta + \beta - 1)^2}{\lambda_\beta \beta^2}} \right)^{-1}$$

(3-30)

where β is the value of the overrelaxation factor associated with λ_β .
Though most structural problems involve matrices that do not possess prop-
erty A, eq. (30) has been successfully used to determine the optimum over-
relaxation factor and is the basis used in the ITER link for determining β_o .

The basic algorithm used is a modification of the one proposed by Carré[2].
It consists of the following steps:

1. Let the overrelaxation factor equal one and perform one cycle
   of iteration to establish an initial vector[7].

2. Determine the optimum relaxation factor by performing λ
   iterations with $\beta = 1.4$. After each cycle of iteration an
   estimate of the maximum latent root is obtained by

$$\lambda \approx \eta_{k-1} / \eta_k$$

(3-31)

---

* A matrix has property A if there exists two disjoint sets S and T of W
  the first N integers such that the union of S and T is W and if $a_{ij} \neq 0$
  and $j \neq i$ either i is an element of S and j of T or i an element of T and
  j of S. The ordering is consistent if for an ordering vector bq, , when-
  ever $a_{ij} \neq 0$ and q_i q_j the ith row follows the jth row in the ordering,
  and whenever $a_{ij} \neq 0$ and q_i q_j the jth row follows the ith.

where n_k is a measure of the norm of the kth error vector. This is defined as the arithmetic sum of the residuals $\{P\} - [K]\{v\}$. $\curlywedge$ is taken as the number of iterations required until (31) differs by less than one part in one thousand for each successive iteration. The optimum relaxation factor is then determined from (30). Step 2 is omitted for the second and succeeding vectors in $\{P\}$ and the factor from the first vector used.

3. Perform $\mathcal{L}$ iterations using the optimum relaxation factor. is either the iteration limit or the number of cycles to obtain a stated number of figures of accuracy. The accuracy obtained is defined by

$$\text{Accuracy} = \frac{\text{Current Residual Norm}}{\text{Maximum Residual Norm}} \qquad (3\text{-}32)$$

The maximum residual is selected by comparing the norm of the residual at the end of each cycle with the previous maximum.

Seidel iteration has some advantages for structural analyses. It is easily programmed, and takes advantage of matrix sparcity, and is efficient when few loading cases are of interest. Therefore, it economically provides the capability to solve large sets of simultaneous equations. The process must converge since the stiffness and flexibility matrices must be positive definite. When it fails to converge, analysis of the iteration vectors will usually define the nature of the error in formulation of the problem.

The economy of the process compared with Choleski's method is problematical, but the method can lead to smaller manipulation errors. The number

of cycles of iteration depends on the maximum latent root of the iteration matrix as shown in Fig. 3-2. This curve can be used to determine whether additional iteration cycles are economically reasonable. These curves are based on the theoretical convergence rate and are confirmed by the numerical results shown. The number of cycles of iteration required is defined by

$$C = -2.3D/\ln \lambda_m \tag{3-33}$$

where C is the number of cycles; D, the number of significant digits required, and λ_m the maximum latent root of the iteration matrix. It is noted that starting iteration with a good guess has little effect on the number of cycles required.

The value of the latent root is not known a priori, unfortunately. However, experience indicates that iteration is more attractive than direct methods for large order matrices of high density and large order wide band matrices of low density within the band. The density of the matrix is measured by the number of none zero elements divided by the maximum number of elements. Figure 3-2 includes information showing experience in solving typical structures. The accuracy of the iteration is limited by the accuracy retained in calculating the residuals, $\{P\} = [K]\{v\}$

3.5 CHARACTERISTIC ROOTS (ROOT)

Jacobi's method[2, 8] is incorporated in the ROOT link. It is the purpose of this link to obtain the characteristic roots and vectors of a symmetrical matrix.
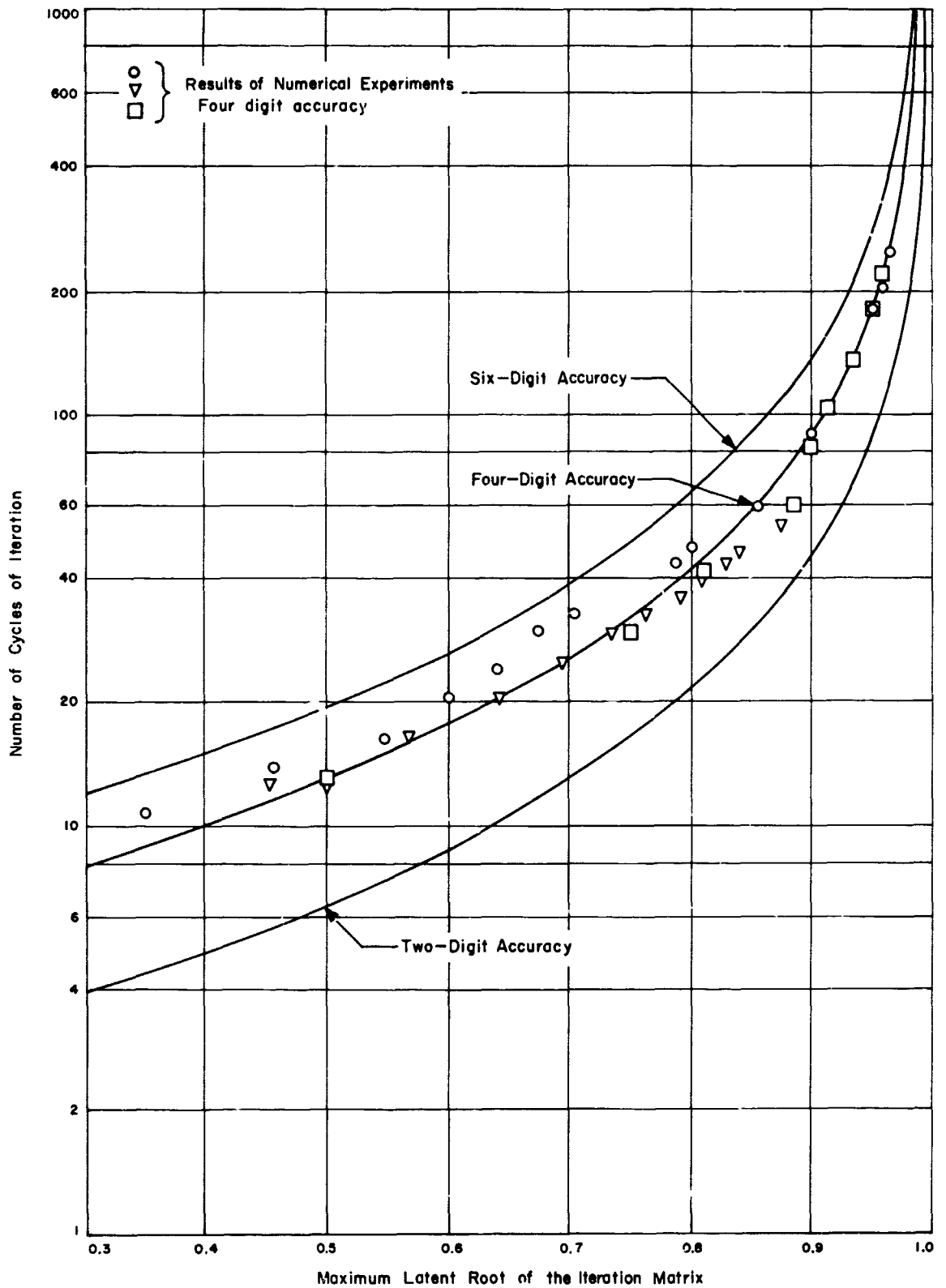
NUMBER OF ITERATION CYCLES REQUIRED

Fig. 3-2

The method hinges on the fact that a similarity transformation does not change the characteristic roots of a matrix, i.e., given a matrix K of order n and with n roots, the characteristic roots are defined by the zeros of

$$\left| \lambda [I] - [K] \right| = 0 \qquad (3\text{-}34)$$

Applying a similarity transformation

$$\left| \lambda [S][S]^{-1} - [S][K][S]^{-1} \right| = \left| \lambda [I] - [S][K][S]^{-1} \right| = 0 \quad (3\text{-}35)$$

since S is an orthogonal matrix ($S^T = S^{-1}$). Then the roots of K are the same as those of $S K S^{-1}$.

Jacobi's method[2] consists of imposing successive similarity transformations until $S K S^{-1}$ is reduced to a diagonal matrix. The vectors of S are then the modal v ctors of the matrix. A principal advantage of the approach is that modal vectors are orthogonal even when multiple roots occur. The theoretical disadvantage in efficiency compared with Given's method[2] (a factor of 20) is not realized in practice due to added complexity of logic for Given's method (the factor is about 2 in practice). The method is described and compared with others in reference 8.

Roots obtained by this process are subject to error due to overflow or underflow during calculations. Overflow occurs when a number is greater than the largest number the computer can handle. Underflow occurs when the number is smaller than the smallest number the machine can handle.

Smaller roots obtained may be invalid due to underflow or the inability to carry enough significant figures. This should be suspected when the spread between exponents of the roots exceeds eight, the number of significant figures carried on the IBM 7094. When this occurs, the lower roots can be obtained by using CHIN to invert the matrix and obtaining the reciprocal roots.

Several techniques are available for obtaining the characteristic roots and vectors for a matrix that is too large for the ROOT link. The techniques considered here consist of ways of approximating the lower roots. Repeated application of these processes can yield as many accurate modes for the system as the maximum number of roots that can be obtained from the ROOT link.

One technique consists of taking advantage of gridpoints with no mass loading. Repeating the dynamic equation (15),

$$[K]\{v\} = \omega^2 [M]\{v\} \tag{3-36}$$

If a number of rows and columns of M are null, then (36) can always be visualized in the partitioned form

$$\begin{bmatrix} K_{11} & K_{12} \\ K_{21} & K_{22} \end{bmatrix} \begin{Bmatrix} v_1 \\ v_2 \end{Bmatrix} = \omega^2 \begin{bmatrix} M_{11} & 0 \\ 0 & 0 \end{bmatrix} \begin{Bmatrix} v_1 \\ v_2 \end{Bmatrix} \tag{3-37}$$

where M_{11} is square, symmetric, and positive definite. From this point there are two ways to obtain a dynamic matrix of the same order as M_{11}.

First, the second set of equations of (37) can be solved for V_2 and the result substituted in the first set of equations giving

$$[K_{11} - K_{12} K_{22}^{-1} K_{21}]\{V_1\} = \omega^2 [M_{11}]\{V_1\} \tag{3-38}$$

Then the equations can be treated as described in Section 3.3 to obtain a symmetric dynamic matrix. Secondly, the equations (37) can be solved directly for the displacements for the non-null vectors on the right hand side (using CHOL or ITER) giving

$$\begin{Bmatrix} V_1 \\ V_2 \end{Bmatrix} = \omega^2 \begin{bmatrix} [K_{11} - K_{12} K_{22}^{-1} K_{21}]^{-1} M_{11} \\ -[K_{22}^{-1} K_{12}][K_{11} - K_{12} K_{22}^{-1} K_{21}]^{-1} M_{11} \end{bmatrix} \{V_1\} \tag{3-39}$$

Then, the first set of equations can be separated and the transformation (22) used. In this case, the equation becomes

$$\{\bar{V}_1\} = \omega^2 [U^T][K_{11} - K_{12} K_{22}^{-1} K_{21}]^{-1} [M_{11}][U^{-1}]\{\bar{V}_1\} \tag{3-40}$$

or, $\{\bar{V}_1\} = \omega^2 [U][K_{11} - K_{12} K_{22}^{-1} K_{21}]^{-1}$

since as before, $U^T U = M_{11}$ and therefore $M_{11} U^{-1} = U^T$.

Another procedure for extracting roots is based on partitioning the matrix. Consider the equations (37), with $M_{22} \neq 0$, as two separate systems:

$$[K_{11}]\{\bar{V}_1\} = \omega^2 [M_{11}]\{\bar{V}_1\} \tag{3-41}$$

$$[K_{22}]\{\bar{V}_2\} = \omega^2 [M_{22}]\{\bar{V}_2\}$$

Then the characteristic roots of each system can be established independently. Selecting the lower roots and vectors from each system, two transformations are defined.

$$\{\bar{V}_1\} = [A_1]\{\bar{\bar{V}}_1\}$$
$$\{\bar{V}_2\} = [A_2]\{\bar{\bar{V}}_2\} \tag{3-42}$$

Where A_1 and A_2 have more columns than rows. Imposing (42) on the original set of equations gives the constrained set

$$\begin{bmatrix} A_1^T K_{11} A_1 & A_1^T K_{12} A_2 \\ A_2^T K_{21} A_1 & A_2^T K_{22} A_2 \end{bmatrix} \begin{Bmatrix} \bar{\bar{V}}_1 \\ \bar{\bar{V}}_2 \end{Bmatrix} = \omega^2 \begin{bmatrix} A_1^T M_{11} A_1 & 0 \\ 0 & A^T M_{22} A^T \end{bmatrix} \begin{Bmatrix} V_1 \\ V_2 \end{Bmatrix} \tag{3-43}$$

Note that because A_1 and A_2 are rectangular, the order of (43) is less than that of (37).

The roots of (43) provide estimates of the lower resonances of the system (37). It can be proven that the estimates cannot be lower than those of the original system.

On the basis of the characteristic vectors of the constrained system, a new transformation (42) can be written and the process repeated until the lower roots are as close as desired to the lower roots of the complete system.

Partitioning of the equations into the two systems can be arbitrary or based on the geometry of the structure. A description of the use of the method using partitioning based on the geometry is given in Ref. 9 and 10.

3.6 MATRIX ARITHMETIC LINKS

The operations performed by ADDS, SUBS, AND MULT result in addition, subtraction, or multiplication of two matrices. Because operations a.'e performed with coded elements, the routines can be used for other purposes.

The ADDS links forms a list consisting of all the elements in both input matrices. This list is then ordered in the sequence of increasing code. If two or more elements have a common code, these elements are added. The SUBS routine multiplies all the elements of the second matrix by -1.0 and performs the ADDS operations.

In addition to matrix addition, ADDS and SUBS can be used to augment a matrix with additional rows and/or columns or to increase or decrease specific elements of a matrix.

The MULT routine takes all the elements with any given row code from the multiplier matrix and all the elements with any given column code from the multiplicand. Products of the vector components are taken whenever the column code of the multiplier corresponds with the row code of the multiplicand. These products are coded with the row code of the multiplier and column code of the multiplicand. Elements with the same final codes are added.

In addition to matrix multiplication, this routine can be used to extract from a matrix any rows or columns times scalars, or to reassign matrix row or column numbers in a matrix.

SECTION 4

ERRORS IN FINITE ELEMENT ANALYSES

Because the computations in finite element analyses are deceptively simple, it is easy to fall into the trap of committing errors and then becoming disillusioned with the method. This section of the document will present a discussion of the errors that can be encountered. Having been warned of the difficulties, the analyst will be prepared to avoid the pitfalls and better evaluate the meaningfulness of his results.

The five basic steps in the finite element analysis are illustrated in Fig. 4-1. In the first step a mesh is defined for the given structure. Definition of the mesh here consists of placing gridpoints on the structure between which the strings of the mesh which are imagined to be stretched. For the Facet representation, flat triangular sheets are imagined to stretch between gridpoints.

The second step of the analysis is to make fictitious cuts in the structure and to map the structure onto the mesh. In the mapping process the structural geometry is deformed to comply with the mesh shape and geometry. For the beam shown, the curved beam is cut into segments and mapped onto the folded, straight line geometry.

The third step in the analysis consists of defining mathematical models for each of the structure's components. These models express the load-deflection relationships for each element. The models can be derived using finite differences, variational approaches, analogs or from experimental data. The generality of the model is limited by the endurance of the theoretician and the programmer.
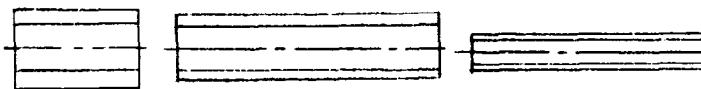
1. Define a mesh for the given structure.

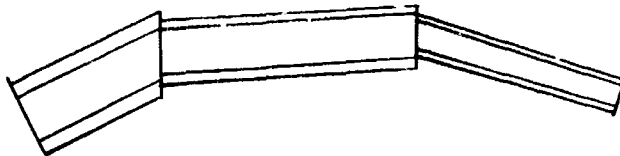2. Make fictitious cuts and map the structure onto the mesh.
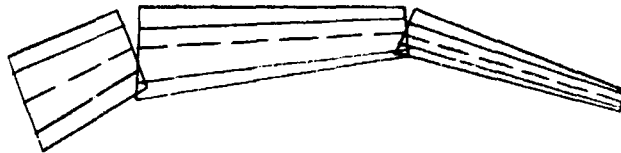
3. Define a mathematical model for each component.

$$[k]\{v\} = \{p\} \quad OR, \quad \{v\} = [k]^{-1}\{p\}$$

4. "Fasten" components together.

$$[K]\{\Delta\} = \{P\} \quad OR, \quad \{\Delta\} = [S]\{P\}$$

5. Solve simultaneous equations, obtain determinate, evaluate eigenvalues.

FINITE ELEMENT ANALYSIS STEPS

Fig. 4-1

The fourth step in the analysis consists of fastening the components of the structure together to form the mathematical model of the complete structure. In this step the representation of each of the components are used. The results of combining the components are the load-deflection relationships for the complete structure.

The final step in the finite element analysis involves the calculations required for predicting structure behavior. Included in this step are the solution of simultaneous equations to predict displacement of stresses, evaluation of the determinate to predict buckling loads, and evaluation of eigenvalues and eigenvectors to represent the buckling or resonance response of the structure. Other calculations may involve the integration of simultaneous differential equations to predict the dynamic response of the structure or evaluation of roots of polynomials to define the dynamic stability of a structural system.

There are three types of errors that are encountered in the analysis. These are the idealization, discretization and manipulation errors. Idealization errors are involved in forming the mathematical model of the structure. The discretization error is induced by replacing the continuous structure by a number of finite elements. The manipulation errors are encountered only in the numerical calculations.

In the next paragraphs are presented the causes, nature, types and methods of reducing errors of the idealization, discretization, and manipulation classifications.

4.1 IDEALIZATION ERRORS

Idealization errors may be classified by how they are induced. Geometric errors, lumped para...eter errors, anisotropy errors and errors in approximating the boundary conditions define the classes of idealization errors. All of these errors are induced by limitations of the idealized model. Hence, in principle, the idealization error can be entirely eliminated by broadening the generalization of the mathematical model. In practice, the absolute magnitude of the idealization error is difficult to evaluate. Independent caluclations based on different limited models can be used, however, to estimate the relative importance of the error. This phenomenological approach was used by Archer and Samson.[1] Model test data or independent theory provide a suitable means for obtaining an estimate of the absolute error.

For a given number of gridpoints, the magnitude of the geometric error is dependent upon the choice of the gridpoint locations. Errors are induced in representing the surface area of the structure, the length of the distance between gridpoints and the volume included within the gridwork envelope. The envelope of the structural representation may inscribe or circumscribe the geometry. The magnitude and sign of the error will depend upon which choice or compromise is made.

In addition, errors are involved in representing the orientation of one structural element to another. This error influences the stresses acting in each element and will be shown to be the most significant geometric error. The size of the error depends on the distribution of stiffness.

Moments, for example, become transferred from bending to stretching stresses across any given folded boundary and, depending upon the relative bending and stretching stiffness of each component, the error introduced may be large or small.

For any fixed number of gridpoints an adequate idealization of the structure is often unattainable for an "exact" representation of the structure. This is evident if one considers that the number of independent components in the matrix exceeds the number of geometric parameters describing the element. Consider the Facet representation. The stiffness matrix for the Facet is a singular matrix until a sufficient number of boundary conditions are imposed. For the displacements assumed, the number of boundary conditions required to make the system stable is five. There are then ten independent equations represented by the stiffness matrix. Because of symmetry, the number of coefficients that can be independent is 55. On the other hand, the geometry and orientation of the triangular Facet is defined by the x-, y- and z-coordinates at the three gridpoints of the structure and the thickness of the panel. In addition, a maximum of 13 additional parameters, introduced as material coefficients for an aelotropic material (one plane of symmetry), are available to eliminate the geometric error. Therefore, there exist but 23 parameters which the analyst can select in order to simulate the 55 coefficients required for a perfect idealization. Even if 55 parameters did exist for the modeling of the structure it is reasonable to expect that the work involved in determing the proper model would be unjustified in view of the fact that an approximate solution is being obtained in any event.)

The geometric error also depends upon the number of gridpoints used to describe the structural envelope. As the number of points is increased the geometric error can usually be made as small as the analyst desires. (An exception is shown by Stong for the cylinder.) It is important to recognize, however, that when networks with different number of gridpoints are compared the structures being analyzed may also differ. This situation arises when a new structural idealization is made for the refined network. Since manufacturing costs usually limit the structure to simple geometries it is generally more economical to improve the mathematical generality of the model rather than to depend upon the refinement of the network to represent geometry. To illustrate these concepts and to obtain some estimation of the magnitude of the errors induced by geometric approximations consider the problem depicted in Figure 4-2. The structure consists of a string of constant cross sectional area stretched over a rigid frictionless cylinder. The string is fastened at one end and loaded at the other end in the direction of the cylinder tangent. The angle defining the sector of the cylinder will be treated as a variable. The true deflection, V_{so} along the tangent and the true length L_{so} of the string are given by

$$V_{So} = \frac{PR\theta}{AE} ; \qquad L_{So} = R\theta \tag{4-1}$$

where P is the load; R, the radius of the cylinder; θ, the sector angle; A, the string cross sectional area; and E, Young's Modulus. The deflection, V_{si}, and length, L_{si} of the chord model of the string is given by

$$V_{Si} = \frac{2PR \sin \theta/2}{AE \cos^2 \theta/2} ; \qquad L_{Si} = 2R \sin \theta/2 \tag{4-2}$$

The geometric error appears in two ways: the chord length of the string is less than the arc length and the chord string has a smaller load. Let the error in the deflection be defined as

$$e = 1 - \frac{V_{si}}{V_{so}} \tag{4-3}$$

Using (1) and (2) in (3) the error induced by the length approximation can be considered to be a function of the factor $\frac{2}{\theta} \sin \theta/2$. That part induced by the orientations of the structure is induced by the factor $(\cos^2\theta/2)^{-1}$, i.e.

$$e = \left(\frac{2 \sin \theta/2}{\theta}\right)\left(\cos^2 \theta/2\right)^{-1} \tag{4-4}$$

$$\underset{\text{Length Factor}}{} \quad \underset{\text{Orientation Factor}}{}$$

The length factor is less than one for all angles of θ less than 180°. The orientation error factor, on the other hand, increases from one up to a maximum value of infinity when the cylindrical sector has an angle of 180°. Since the total error involves the product of these two errors, the effect of the length error tends to compensate for the orientation error for small angle sectors, if the structure is an inscribed one. As the angle increases the error induced by the misorientation of the load dominates. Figure 4-2 shows a plot of the magnitude of the error given by Eq. (4-4) as a function of the angle of the sector. This figure shows that the error becomes greater than five per cent when the angle gets above 26°. Note that the structure represented is too flexible.
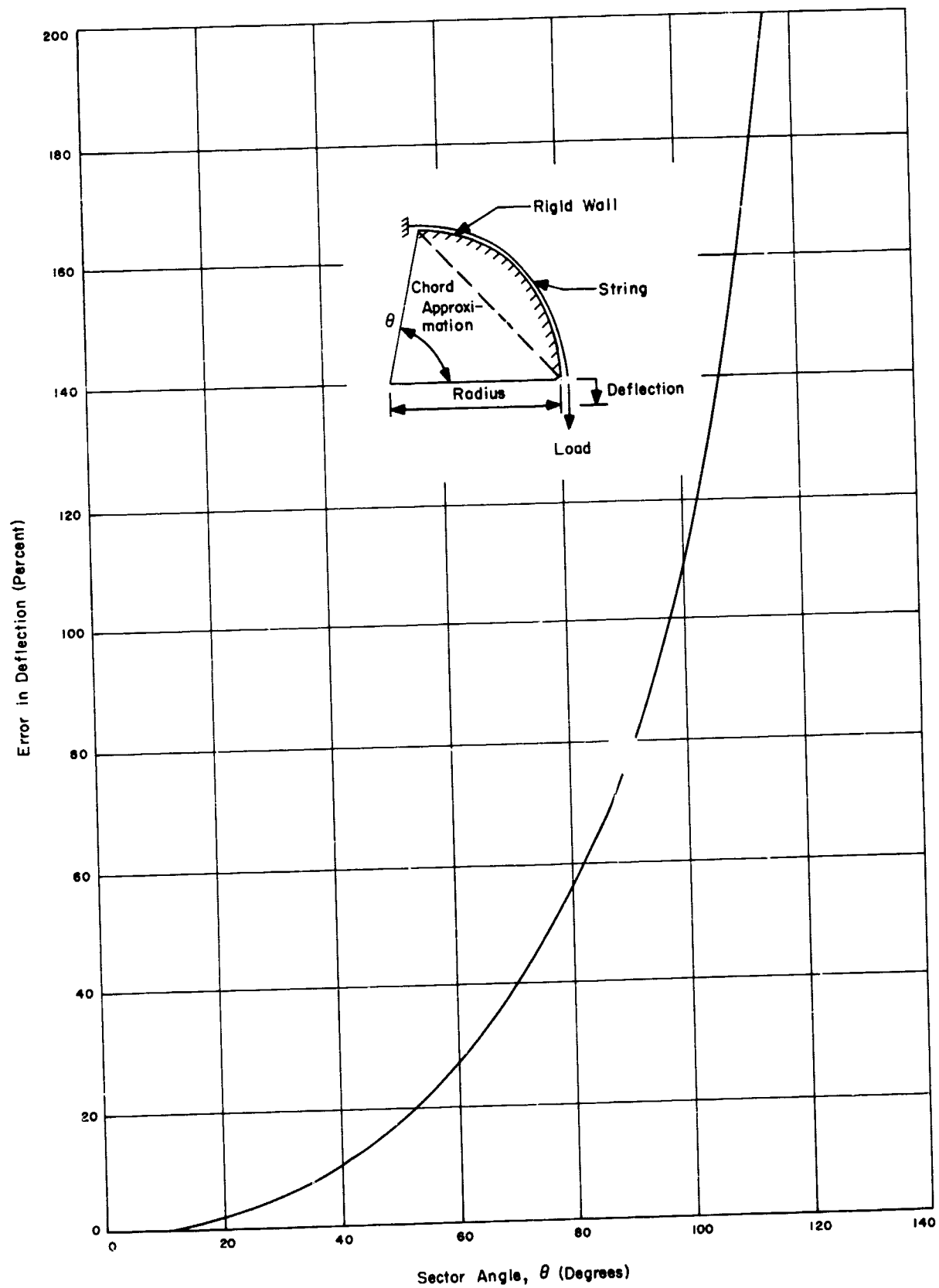
DEFLECTION ERROR FOR A CURVED STRING

Fig. 4-2

As a second problem consider the curved beam in Fig. 4-3. Neglecting shear deformations and axial elongations, the true deflection normal to the beam and true length of the beam are given by

$$V_{BO} = \frac{PR^3}{2EI}\left(\theta - \frac{1}{2}\sin 2\theta\right); \qquad L_{BO} = R\theta \qquad (4\text{-}5)$$

where I is the moment of inertia of the beam about its effective neutral axis. The deflection and length of an inscribed chord beam subtending the arc of the beam elastic axis are given by

$$V_{BI} = \frac{8PR^3}{3EI}\sin^3\frac{\theta}{2}\cos^2\frac{\theta}{2}; \qquad L_{BI} = 2R\sin\frac{\theta}{2} \qquad (4\text{-}6)$$

Defining the error as before, the error in using the chord beam can be determined and is shown in Fig. 4-3. If the deflection error is to be less than five per cent, the sector angle must be less than 30°. Note that the error in the beam problem is less than the error in the string problem (Fig. 4-2) for angles greater than zero.

In the beam problem, it is not easy to separate the orientation and the length error. The relative error can be determined by writing the deflection in terms of a beam which is scaled to the actual length of the curved beam. Then the deflection is given by the formula,

$$V = \frac{PR^3}{EI}\frac{\theta^3}{3}\cos^2\frac{\theta}{2} \qquad (4\text{-}7)$$

In this case, the orientation error is in the numerator whereas in the string problem it is in the denominator. The dashed curve of
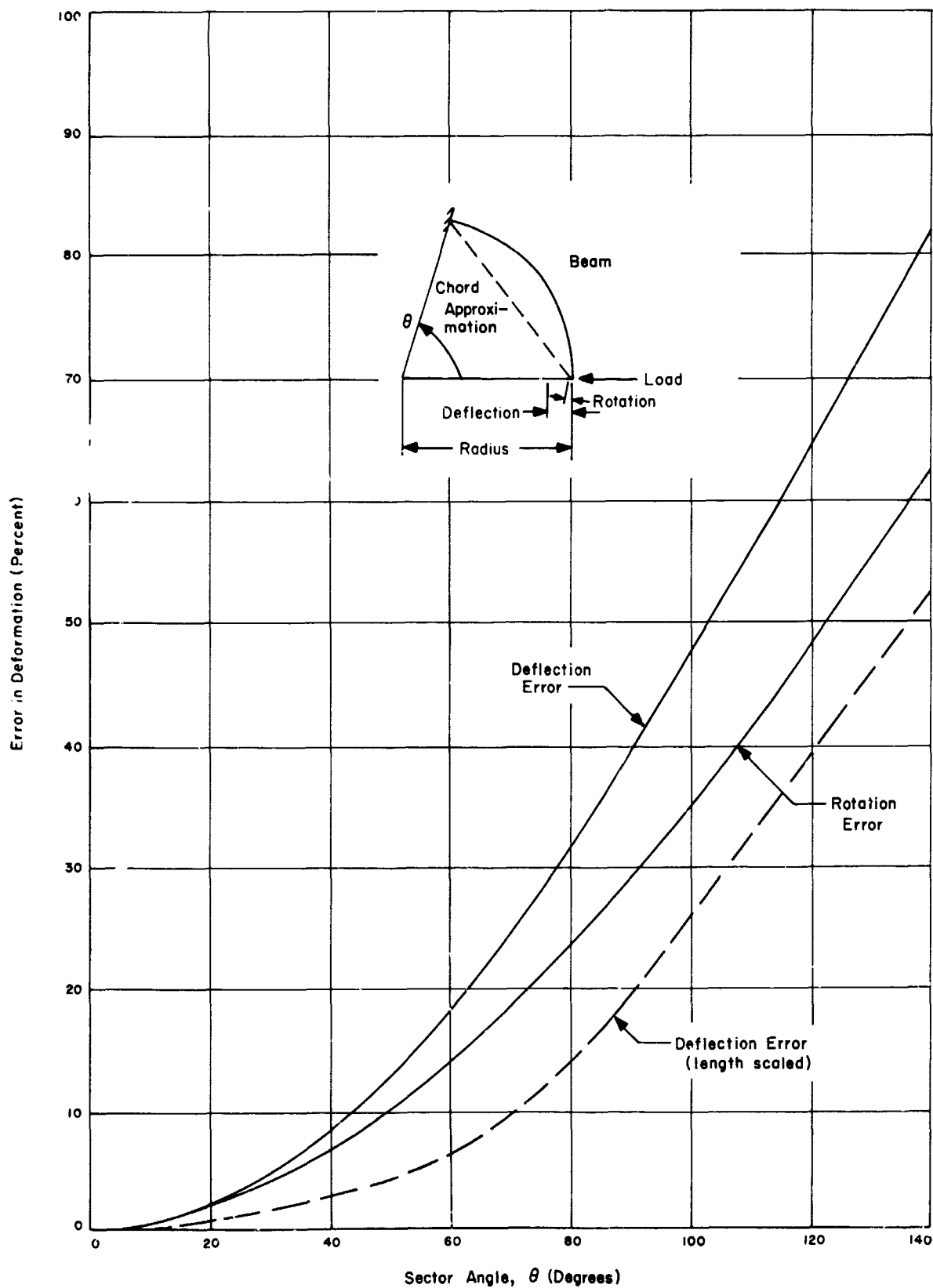
DEFORMATION ERRORS FOR A CURVED BEAM

Fig. 4-3

Fig. 4-3 shows the error, using this approximation, as a function of the size of the angle. This figure suggests that the best approximation is to choose the gridwork points so that the true length of the structure is represented. Scaling the beam length reduces the deflection error by less than half as shown in Fig. 4-3. Thus it can be concluded that the misorientation error is more significant than the length error for the beam as well as the string. The inscribed structure always results in a structure which is too stiff.

In the problem selected for the beam, the gridpoint locations could have been chosen so that the deflection at the tip would have been exact. However, suppose that the beam is to be represented so that the rotation at the tip due to the tip load is to be exactly modeled. The exact solution for the rotation of the tip due to the side load is given by

$$\theta_P = \frac{PR^2}{EI} \left(1 - \cos \theta \right) \tag{4-8}$$

The tip rotation of the chord beam, however, is given by

$$\theta_C = \frac{PR^2}{EI} \left(2 \sin^2 \tfrac{\theta}{2} \right) \left(\cos \tfrac{\theta}{2} \right) \tag{4-9}$$

The error caused by approximating the beam by its chord is shown in Fig. 4-3. The rotation error is somewhat less than the deflection error for a given angle. Therefore, if the rotation is the critical item the angle subtending the chord can be slightly larger. In other words, a coarser gridwork can be used. This application illustrates that the best

location of the gridpoints depends upon what is being modeled. The
choice of gridpoint locations will be different depending on whether the
deflection or the rotation is required to be accurate. If both must be
accurate, the length alone will not suffice to scale the structure so
that the simulation is correct. (Detailed study of the problem will show
that if both aspects are to be well modeled, a very good model nearly
coincides with the rotation model).

There is a simple way to eliminate the geometric error. That means is
to choose to represent the structural geometry as it actually exists.
Rather than use flat or straight elements, curved elements can be selec-
ted and the stiffness relationships derived from these. In the analysis
of spherical shells, for example, the representation of the elements of
the shells as Facets is replaced by a representation as triangular spheri-
cal shell components. This increase in the generalization of the geometry
of the subelement will permit the use of fewer gridpoints to represent
the structure to a given accuracy.

These problems illustrate some of the previous ideas mentioned with respect
to geometric idealization errors. They show that the best placement of
gridpoints depends upon the particular problem being solved. The place-
ment depends on the problem boundary conditions, the true geometry of the
structure, and whether the type of approximation desired is to be too
stiff or too flexible. The problems suggest that the error diminishes
as the network is refined. They show that correcting for length errors
may or may not lead to an improved answer. They also indicate that the

chord approximation involves little error for arcs less than about 25°. Finally, they demonstrate that selection of the model is sensitive to what elastic characteristic is to be modeled.

Another type of idealization error may be termed the lumped parameter error. This error is induced by limitations of the model in describing the disposition of structural material within element boundaries. If the elastic energy of the structure is considered, the lumped parameter error is an error in defining the limits over which the integration is taken. The geometric error, on the other hand, involves errors in defining the path of the integration and the orientation of that path with respect to neighboring elements.

Though both geometric and lumping errors are induced by limitations of the mathematical model available to represent the structure, the geometric error is usually larger than the lumped parameter error. For example, in the prediction of the deflection of a beam clamped at one end and loaded at the other the deflection is given by

$$V = \frac{PL^2 \ell}{3EI} \tag{4-10}$$

where ℓ is the projected length and L the true length.

The geometric error is one affecting L, the length of the beam, and this error is much more significant in affecting the deflection than the same percentage in the lumped parameter I, the moment of inertia of the beam.

The lumped parameter error is not only smaller than the geometric error but can often be corrected by adjustment of input parameters. For a

straight stringer, selection of the area of the stringer as the mean area provides an exact representation of the elastic energy of the structure. For a beam, selection of the mean shear area provides an exact representation of the shear rigidity of the structure. In the case of the triangular facet it is possible to integrate the energy independently of the analysis for any variation of thickness and enter an effective thickness into the computer program as input to provide exact simulation of the element geometry for midplane stretching deformations.

To illustrate the importance of the lumped parameter error in comparison with the geometric error consider again the problem of the string on the frictionless rigid cylinder. In this case assume that the cross sectional area of the string varies linearly along the length of the string from a value of A_1 at the point of loading to A_2 at the upper end where the string is fixed. Then the exact solution for the deflection in the direction in the load is given by

$$V_{SO} = \frac{PR}{(A_2 - A_1)} \cdot \ln \frac{A_2}{A_1} \tag{4-11}$$

The comparable solution for the chord is given by

$$V_{SI} = \frac{4PR \sin \theta/2}{(A_1 + A_2)E \cos^2 \theta/2} \tag{4-12}$$

Using the definition of the error, Eq. (3), then the interaction of the length, orientation, and lumped parameter errors can be determined. The total error is given by

$$e = 1 - \left(\frac{2\sin \theta/2}{\theta}\right)\left(\frac{1}{\cos^2 \theta/2}\right)\left(\frac{2\left[\frac{A_2}{A_1} - 1\right]}{\left[\frac{A_2}{A_1} + 1\right]\ln \frac{A_2}{A_1}}\right)$$

| Length | Orientation | Lumping |
| Factor | Factor | Factor |

(4-13)

The three factors on the right hand side of the equation define the con-
tribution of the length, orientation, and lumping errors respectively.
The maximum lumping factor is one and the minimum zero.

Figure 4-4 shows how the lumping error is affected by the ratio of the
cross sectional areas of the ends of the string. The lumping error here
is predicated on the assumption that the constant area of the stringer is
the average area. The maximum value that the length factor can assume
is $2/\pi$ and is assumed when the angle θ is equal to 180°. At the same
angle the orientation error assumes its maximum value, infinity. Thus,
the lumping error is bounded whereas the geometric error is unbounded.

Another idealization error is that induced by the structural aniso-
tropy. The Facet model admits definition of the material aeolotrophy and
requires that geometric anisotropy be simulated by material. The material
aeolotropy is represented directly by the elast° constants in the stress-
strain relationship. Geometric anisotropy, on the other hand, is that
induced by the arrangement or form that the material takes in the structure.
For example, if a sheet is manufactured with integral stringers, geometric
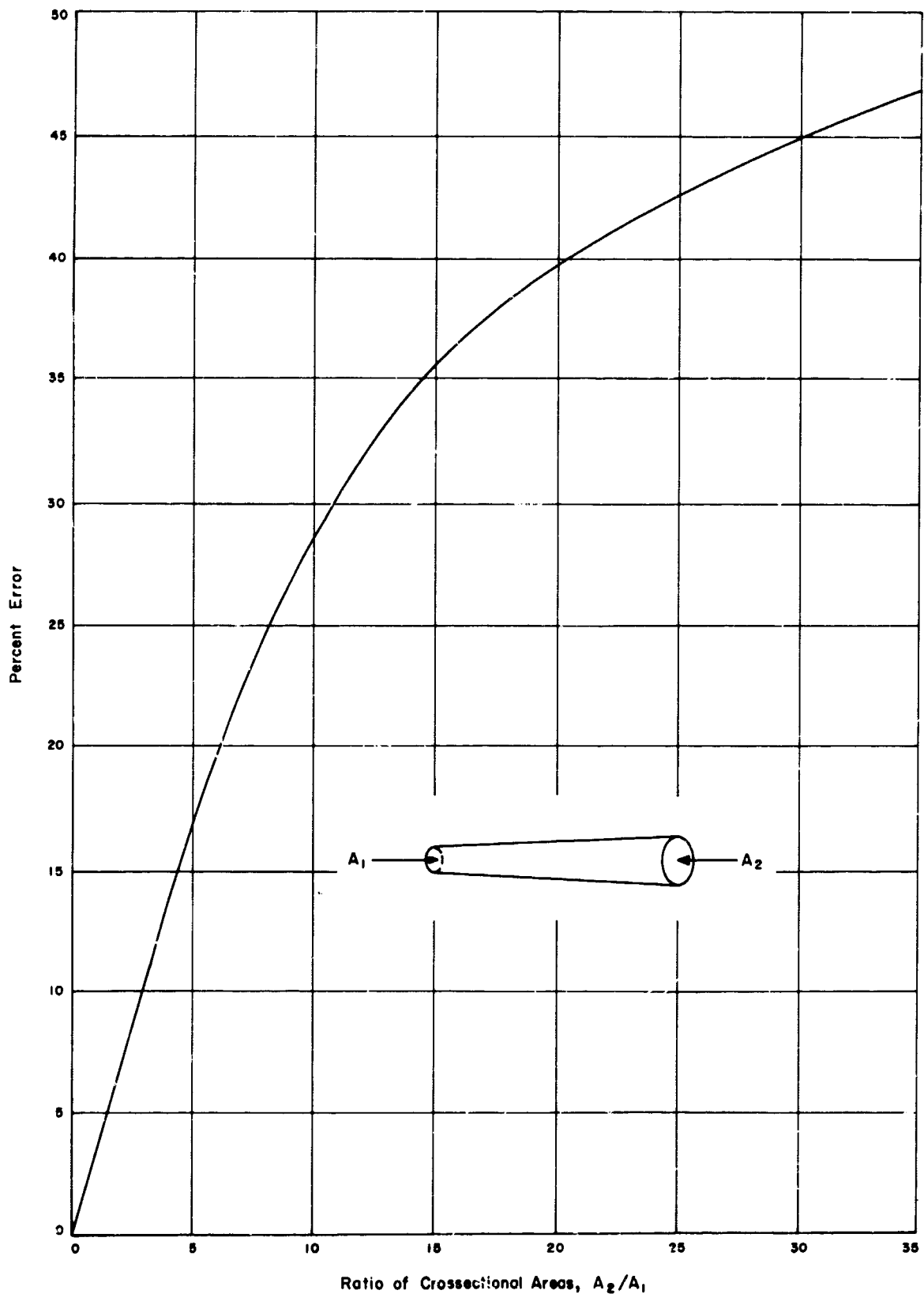
Fig. 4-4

DEFLECTION ERROR DUE TO LUMPING

Fig. 4-4

anisotropy is induced. Sandwich construction, glass laminates, wire wound shells, and other composite structural components can be considered as having geometric anisotropy. Geometric anisotropy does not depend upon material characteristics. It can occur even when the material is iso-tropic.

"hen the assumed strains are constant over the element the geometric anisotropy can be exactly represented by an equivalent material anisotropy. This can be shown by considering the matrix formulation of the stiffnesses in accordance with Appendix A. The strain energy is given by the expression (A-5).

$$U = \frac{1}{2} \int_{V_o} \lfloor u \rfloor [B]^T [D] [B] \{u\} \, dV_o \qquad (4\text{-}14)$$

Here V_o designates the volume over which the integration is to be per-formed. If the strains are constant, all of the matrices are independent of the coordinates and the integration can be applied directly to the co-efficients of the D matrix, the matrix of material constants. The con-stant strain case arises in the rod, shear moment beam, triangular slice, three-dimensional solid tetrahedron, and the torque tube structures. Matrices for these elements have been previously developed and described in the literature.[2.1, 2.2, 2.3, 2.13] When the strains are not constant it is necessary to approximate the geometric anisotropy with a material anisotropy. The approximation can be accomplished by comparing the inte-grals representing the energy terms.

In assuming material constants for the anisotropic material, it is necessary that the coefficients satisfy certain requirements in order that the problem idealize a realizable structure. One criterion is that the matrix of material coefficients be symmetric. Another criterion is that the matrix of material coefficients must be a positive semi-definite matrix. In finding an equivalent anisotropy care should be used to insure that these conditions are met. If material constants are based on accurate test data, the matrix of coefficients will inherently satisfy the positive semi-definite requirement.

Another contribution to the idealization error is evoked in approximating the boundary conditions. If either the complementary or potential energy approaches are used, the force or the displacement boundary conditions must be approximate depending upon the solution being attempted. In the case of the minimum potential energy approach, as used for the Facet, the approximations are made with respect to the displacement boundary conditions. Concentrated gridpoint forces corresponding to stress are defined uniquely by the minimum potential energy formulation. The definition of these forces is reviewed in Appendix A.

The gridpoint forces are not usually obtained from the integral formulation, however. The justification for avoiding this approach is the complexity of integration involved and the fact that the problem is only being approximated in any case. Therefore, the stress boundary conditions are idealized as a set of gridpoint forces. However, if a problem is being solved for which an exact solution is known, a consistent variational approach is obtained only by using the integral formulation to define gridpoint forces.

The degree of approximation involved in simulating the displacement boundary conditions (or alternately the force boundary conditions when the assumed functions are stress functions) depends upon the nature of the assumed functions. In the case of Facet, the displacements along the edge are assumed to be linear. If the imposed displacements are actually a higher order function of the coordinate along an edge than a first order, an approximation is involved. It is difficult to evaluate the magnitude of the approximation using the analysis except by refining the network in the region of the boundary involved.

In summary, the idealization error magnitude depends upon the generality of the mathematical model. The magnitude of the error can be determined by analyzing different structures or by using independent analysis procedures such as experimental or analytical approaches. The idealization error can be made to vanish as the number of gridpoints increased indefinitely. In order that this vanishing occur, it is usually necessary that with each refinement of network, a new mathematical model be formulated. From a mathematical point of view this means that each gridwork represents the analysis of a different structure. It is more attractive to eliminate the geometric error by simulating the geometry exactly.

4.2 THE DISCRETIZATION ERROR

The discretization error is caused by replacing the structural continuum by a model consisting of a finite number of structural elements. The error is a function of the assumed stress or displacement functions used, the network grid size, and the subelement topology.

Of paramount importance in fixing the magnitude of the discretization error is the selection of the assumed functions. If these functions are carefully chosen the accuracy of the analysis is maximized for a given network refinement. In addition as the network is refined, a monotonic decrease in the error can be guaranteed. Moreover with refinement of network and proper selection of function, elimination of discretization error for the structure can be insured.

If these functions are chosen so that the analysis is consistent with either a minimum complementary energy or a minimum potential energy formulation, something can be said about the relation between the approximate answer and the exact answer to the problem. If both solutions are used it is possible to bound the strain energy and the stresses, strains and displacements at any point of the structure.

It has been proven that the strain energy of the solution containing no discretization error must be greater than that of the minimum potential energy solution and less than that of any minimum complementary solution. (See Synge[2.28] 1957, page 98-117). Based on Prager's method[2.27], Benthem[2.29] has given a basis for bounding displacements at a point. Development and use of bounding a displacement, mean stress, and mean strain are reviewed in Appendix B.

Requirements on displacement functions to be consistent with the minimum potential approach are reviewed in Ref. 2.26. Ref. 2.26 also gives a requirement to insure monotonic convergence for the solution. The Facet displacement function conforms with the requirements delineated there.

Requirements for suitable assumed stress functions are implied in Ref.
2.26. Because the complementary energy approach is the dual to the
minimum potential energy approach, requirements a > almost parallel.

Since the discretization error vanishes as the grid interval is de-
creased to zero, the mesh size is a direct means of controlling the mag-
nitude of the error. If the error is to diminish in a regular way it is
reasonable to require that the mesh refinement proceed in a regular
fashion. Reducing the mesh size in one direction only in a problem of
a plane, for example, will lead to convergence to an approximate solution.
Because of the distortion of the gridwork shape, the approximation ob-
tained will not be the elasticity solution. This is shown by the data
in Table 4-1. A consistent refinement of mesh should involve fictitious
cuts in all directions. The efficacy of this approach is demonstrated
by the data of Table 4-2.

To illustrate the effect of refinement of mesh on the discretization
error consider the box beam problem of Ref. 2.3. Figure 4-5 shows the
beam with the loading. The error, compared with the theoretical solution,
as a function of the number of cuts along the length of the beam is por-
trayed by the curves. In the analysis, refinement of mesh was performed
in both directions simultaneously.

There are two solutions. The difference in the solutions is caused by
the use of a different beam representation for the ribs of the box. The
effect on the answers can be seen by the two curves in the figure. A
regular reduction of error occurs. The upper curve relates to an analysis

TABLE 4-1

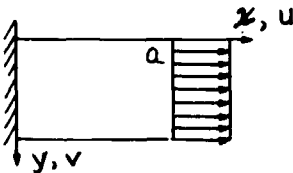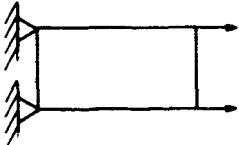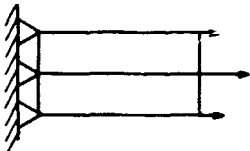EFFECT OF ONE DIRECTIONAL MESH REFINEMENT
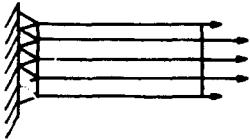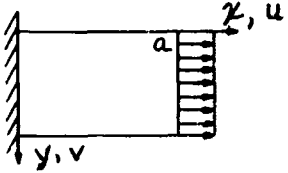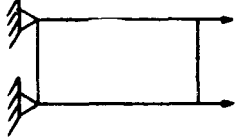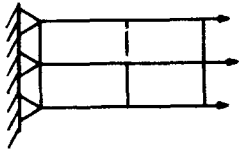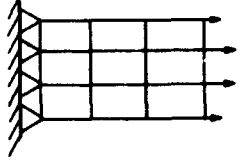
Problem	Results	Analysis Method	No. of Nodes
	$u_a = 2.703$ $v_a = 0.686$	Finite Differences	48
	$u_a = 2.605$ $v_a = 0.784$	Stiffness Method	4
	$u_a = 2.778$ $v_a = 0.836$	Stiffness Method	6
	$u_a = 2.821$ $v_a = 0.850$	Stiffness Method	8
	$u_a = 2.839$ $v_a = 0.857$	Stiffness Method	10

TABLE 4-2

EFFECT OF UNIFORM MESH REFINEMENT

Problem	Results	Analysis Method	No. of Nodes
	$u_a = 2.703$ $v_a = 0.686$	Finite Differences	48
	$u_a = 2.605$ $v_a = 0.784$	Stiffness Method	4
	$u_a = 2.695$ $v_a = 0.689$	Stiffness Method	9
	$u_a = 2.719$ $v_a = 0.692$	Stiffness Method	16
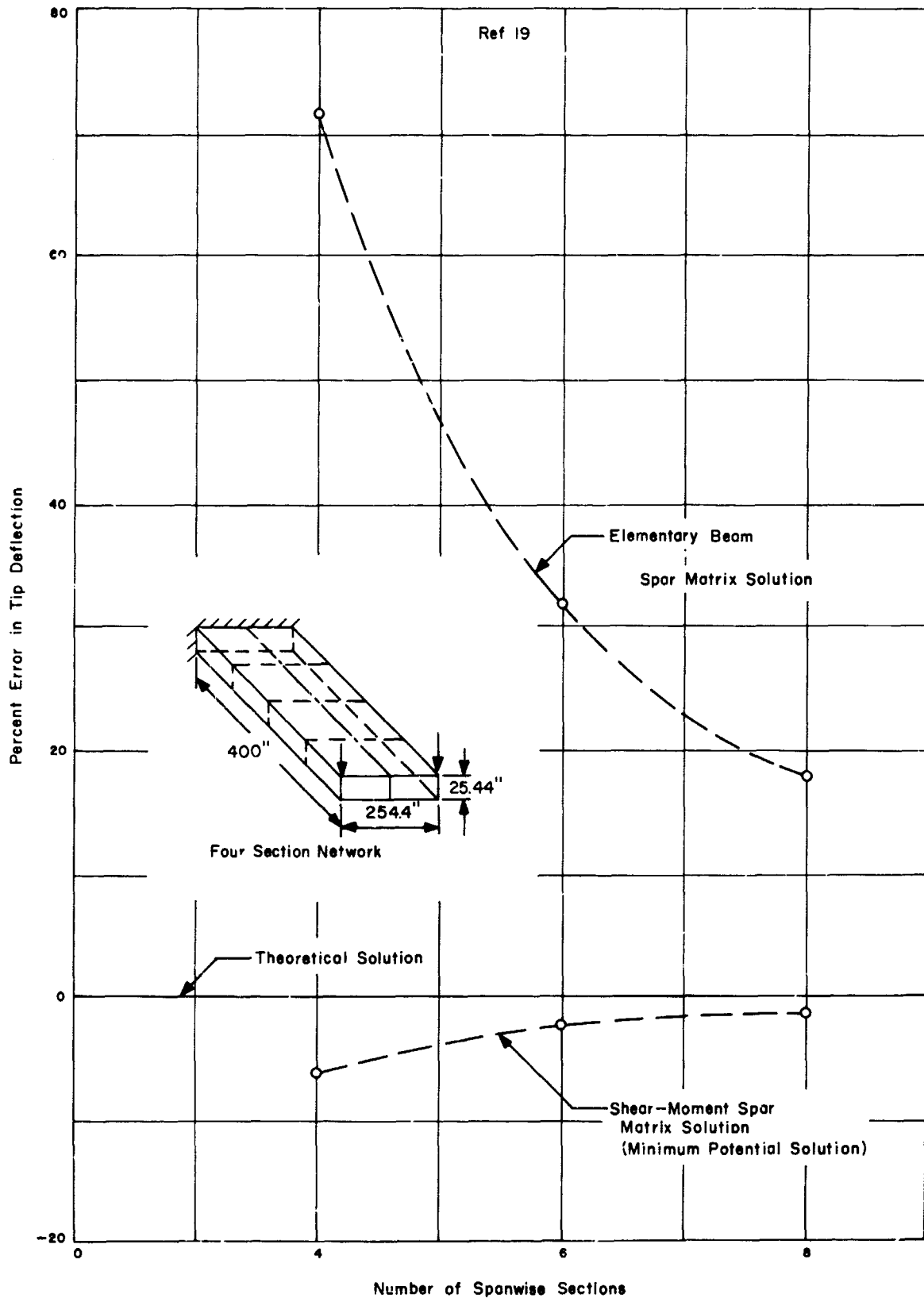
SOLUTION CONVERGENCE FOR A BOX BEAM

Fig. 4-5

in which the components do not conform with a minimum potential formulation or the monotonic convergence criterion. The basis for the solutions of the lower curve conforms with both these requirements.

The regularity of the convergence for the minimum potential approach suggest that the number of calculations can be reduced by using extrapolation. Richardson's technique[3,4] has been used with some success to extrapolate the answers. The extrapolated answer for the box beam problem on this basis using the three soluti ns indicated in Figure 4-5 for the elementary beam was within one percent of the exact solution obtained analytically[2.26].

In an actual structure, it is not necessarily true that extrapolation will provide a better answer than the answer obtained in the analysis itself due to round-off errors in the calculations. However, by obtaining both minimum potential and minimum complementary energy solutions, the response characteristics can be bounded. An answer lying between the bound can be taken to reduce the statistical magnitude of the discretization error.

The brute force means of reducing the discretization error is to perform an analysis with a finer gridwork. The cost of refinement includes the computer time and time required for the preparation of input data. Time required for the preparation of the input data varies directly with the number of elements being analyzed. The computer time is proportional to the number of gridpoints of the system for a fixed bandwidth stiffness matrix. Since the number of elements is increased by a factor of about

four if the network grid size is cut in half the cost of the new analysis will be about four times the cost of the original solution. The beam problem suggests that the discretization error varies inversely as the square of the number of gridpoints. Then the error for the reduced grid will be one-fourth of the original error. Thur the discretization error varies approximately inversely with the cost of the analysis.

From a practical viewpoint, the error in the analysis depends upon the rate of change of the strain or stress over the structure. Since the strains in an element are approximately constant for the assumed displacement function of the rod, torque tube and Facet, more elements should be used in areas in which the strain varies at a rapid rate. The engineer should use judgment in putting more elements in regions in which he expects a higher strain rate to improve his analytical accuracy.

The magnitude of the discretization error is influenced by the geometry of the elements of the structure. From a mathematical point of view, the error can be stated as a function of the largest angle of the triangle. Figure 4-6 shows the maximum error as a function of the maximum angle. This figure shows the error increases rapidly when the maximum angle of the triangle exceeds 120°

This figure also shows that the optimum triangular topology is an equilateral triangle. The data upon which this figure is based was obtained by Synge[2.28] and applies to the triangular slice and the in-plane stresses of Facet.

The discretization error can also be reduced for a given network by choosing more favorable topologies. Numerical experiments have shown that
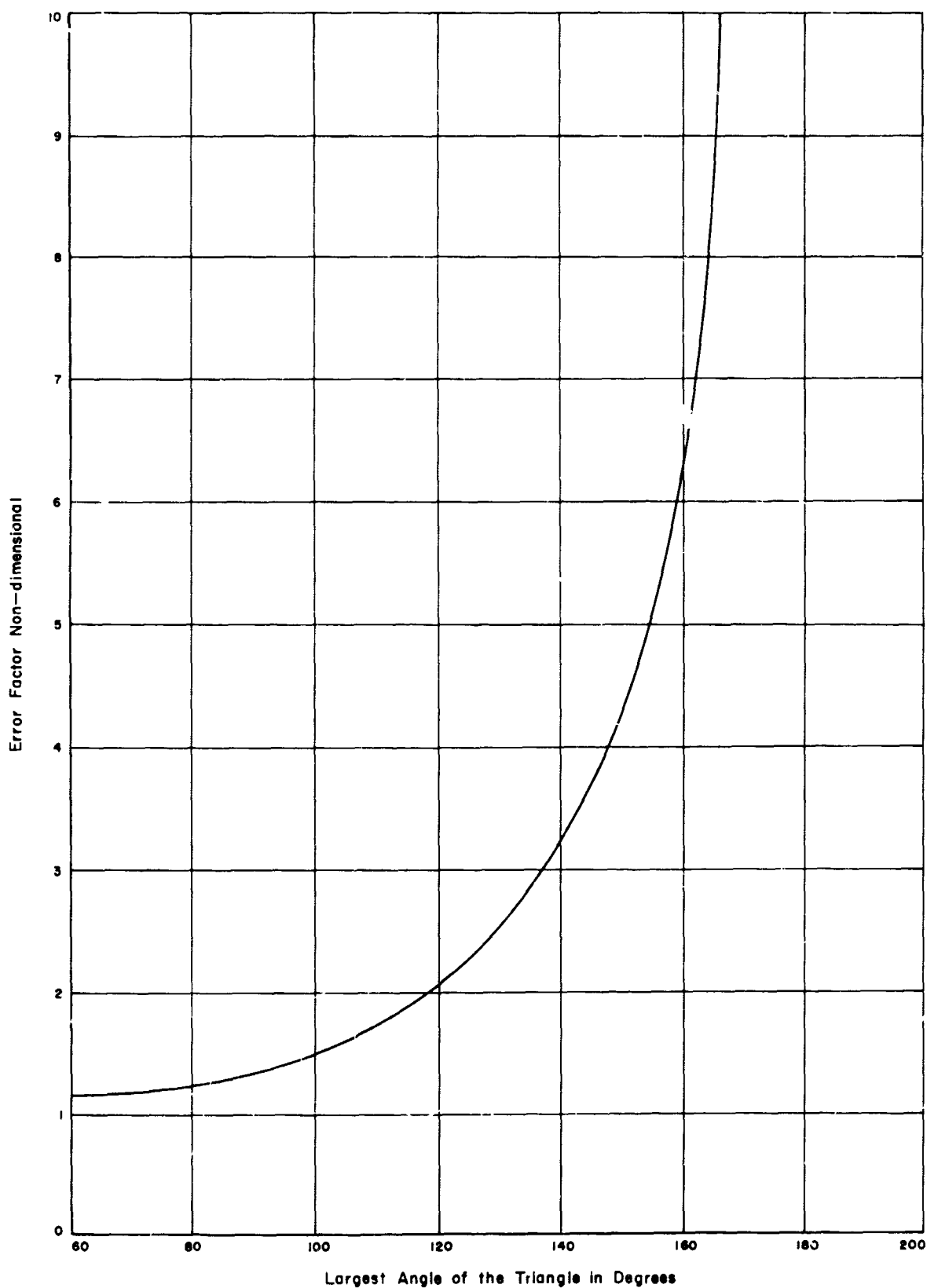
EFFECT OF TRIANGULAR SLICE SHAPE ON MAXIMUM ERROR

Fig. 4-6

the triangular topology usually involves more error than the rectangular. Collatz[5] has made an analogous statement with respect to finite-difference gridworks.

In review, the magnitude of the discretization error depends on the choice of assumed functions. If functions are chosen to comply with the minimum potential formulation (the choice used in Section 2 for the Facet rod, beam and tube) and, alternately, with the minimum complementary formulation, bounds on stress, strain, and displacement at a point can be defined. If functions are properly chosen, reduction in the discretization error can be guaranteed for each network refinement. If refinement is made simultaneously in both directions extrapolation may prove useful in reducing the error. Some reduction in the error can also be effected by choosing favorable geometries for the elements, such as an equilateral triangle, and more favorable topologies, such as the rectangle and prism[2,13] for a surface element.

4.3 MANIPULATION ERRORS

Manipulation errors are encountered only in the numerical calculations. The two types of these errors are process and step errors. Process errors are caused by failure to perform the proper mathematical manipulations or by failure of an iterative process to yield the solution. Examples of process errors would be the multiplication of two matrices when the addition was desired, or failure of an iterative process for eigenvalues to yield the correct estimate of the eigenvalues.

These errors can be controlled by providing calculation checks. The structural analyst has available direct checks such as the calculation of

equilibrium and orthogonality conditions as well as indirect checks on
process errors. Indirect checks include evaluation of the symmetry of
stiffness and flexibility matrices, or determination of the positive-
definiteness of these matrices. It is important that the analyst
include checks to insure that no process errors are committed.

The other type of manipulation errors are step errors. These are classi-
fied as truncation or round-off errors. The truncation error is caused
by carrying a limited number of significant figures in the calculations
and dropping less significant figures. On the IBM 7094 approximately
eight significant figures are carried (12 on Philco S-2000). Round-off
errors are induced by the rounding off of the last character of the
product after each multiplication and each dividend after each division.

Whether round-off or truncation errors occur depends on the program being
used. FORTRAN II programs incur truncation errors during calculations.
On printout, round-off errors are encountered. On the Philco 2000, on
the other hand, ALTAC programs result in rounding errors in both the
calculations and printout. From a statistical point of view, the latter
approach is better.

Step errors are affected by the sequence of the calculations, the numbers
used, and the number of calculations involved. To see how the sequence
of operations affect the error, consider the simple operation of adding
a set of numbers. In this operation the number of calculations is inde-
pendent of the method chosen. The answer may be formed in many ways, but
consider these two:

1. Accumulate the numbers, taking them in the order in
   which they are defined.

2. Accumulate the result by adding addends in the order
   of increasing absolute value starting with the smallest.

Though the average error is the same for both methods, the variance will
be greater for the first case. To illustrate the error consider the set
a, b_i where $i = 1,2,....n$. Assume that three significant figures are
carried. Let $b_i = -1.00 \times 10^{-3}$, $a = +1.00$, and $n = 100$. Method 1.
gives 1.00 as an answer, whereas method 2. gives 0.90, the correct answer.

The magnitude of the numbers involved affects the number of figures
effectively carried. Since floating decimal arithmetic is used, a limited
range is defined for the exponent. On the IBM 7094 for example, the expo-
nent of 2 cannot exceed ± 128 and of 10, ± 38. Numbers smaller than 2^{-128} are
assumed to be zero. Numbers greater than 2^{128} are taken to be the max-
imum number possible. (Limits on the Philco 2000 are $2^{\pm 2048}$ $10^{\pm 620}$).
Since these errors are normally not signalled in FORTRAN programs, their
existence may be unknown. These errors can be detected by changing the
program or scaling problem numbers and rerunning the problem.

Significant figures can also be lost by not using normalized numbers. This
would mean that the number would be preceded by zeros. This difficulty is
surmounted in FORTRAN by normalizing all numbers operated on. The only un-
normalized numbers possible are those read as input.

Because the accumulation of step error is so dependent on the sequence and
method of calculation and because these methods are often modified to facili-
tate data handling or programming, indirect measurements of the error are

often desirable. These methods include symmetry, equilibrium, orthogonality, conditioning, and recalculation checks. Any of these checks can be performed with existing SAMIS links.

Since the stiffness matrices, mass matrices, and dynamic matrices are used in symmetric form, congruent transformations and inversions can be checked by rechecking symmetry. (The ROOT program provides a direct symmetry check). Since the stiffness matrix includes rigid body states, macroscopic equilibrium can be used to check the solution for the whole or any part of the structure. One special case, for the whole structure, is equivalent to multiplying the displacements found by the total stiffness matrix and comparing the result with the originally imposed loads.

Orthogonality checks can be used to validate the eigenvectors. If desired, similarity transformations can be used to generate a dynamic matrix which can be compared with the original.

Conditioning checks include calculating matrix condition numbers [6,2.5] or scaling input to measure conditioning. The condition number is defined as the ratio of the maximum to minimum eigenvalue of the matrix. The larger the number, the greater the tendency to accumulate round-off errors.

The conditioning can be greatly influenced by the coordinate systems selected to solve a problem as well as by structural form. Use of coordinate systems coincident with principal actions of behavior improves conditioning. Choice of axes lying in the surface of and normal to a shell is an example of choosing coordinates related to principal behavior. If the structure is well designed, its form will not dominate the condition number. Badly designed structures are those with subsystems which are

nearly mechanisms

When linear operations are performed, scaling and recalculation can be used to measure error. For example, the effect of multiplying matrices by a scalar are predictable on the final result since only linear equations are involved. The difference between actual and predicted results can be used as a measure of error.

Several approaches are available to minimize or reduce the manipulation errors. These are to precondition the equations, use double-precision arithmetic, select low-error algorithms or improve an approximate solution.

Various special techniques have been used for improving the conditioning of the matrices before operations[7,8,9]. These generally are ways of transforming the equations depending on the algorithm being used and the sizes of the numbers. For example, if the matrix equation

$$[A]\{x\} = \{C\} \tag{4-15}$$

is to be solved the equation can be transformed to the forms

$$[B][A]\{x\} = [B]\{c\} \quad \text{or} \quad [A][E]\{y\} = \{c\}$$

$$\text{where} \quad \{x\} = [E]\{y\} \tag{4-16}$$

$$\text{and} \quad \{x\} = [BA]^{-1}[B]\{c\} \quad \text{or} \quad \{x\} = [E][AE]^{-1}\{c\}$$

The coefficients of B or E or both B and E are then selected to reduce the manipulation errors. Though such an approach may be useful on occasion, its economy is questionable.

Use of double precision arithmetic is the brute force approach to reducing the manipulation errors. In this process, each piece of data consists of two words in the computer: a greater and a lesser part. Twice as many significant figures are retained in each arithmetic operation.

The IBM 7094 has been especially wired to perform all double precision arithmetic in only slightly more time than required for single precision. This machine feature is not available on the IBM 7090 or Philco 2000. Because more space is required for each piece of data, penalties are involved in programming time over and above arithmetic time. It is reasonable to expect that the total cost of double precision arithmetic is to increase the time about fifty per cent over single precision calculation time.

Difficulties with round-off experienced to date have not been those which double precision could help. These difficulties are generally introduced by the analyst's desire to make a member infinitely stiff with respect to another or by using elements with degenerate elasticities (e.g., a beam with no axial stiffness) thus creating a nearly singular stiffness matrix. If single-precision arithmetic is used a ratio of panel thicknesses of ten to one may describe an infinitely thick panel whereas a ratio of 100 to 1 might be admissible for double precision. If degeneracy is caused by omitted resistance, higher precision will not remove the singularity. To avoid the numerical difficulties, holonomic constraints are introduced.

Introduction of these constraints is described in Section 3.1.

Since single precision arithmetic has proven adequate for all but special problems, a more efficient program will be based on this limitation. If round-off or truncation error becomes excessive, techniques for reducing the error may be employed before resorting to double precision arithmetic.

Selection of low error algorithms is an attractive means of reducing round-off and truncation errors. The question of which is the least error algorithm is the area designated as error analysis in mathematical literature.

One approach to error analysis is to determine how each calculation affects the manipulation error. This is a difficult and tedious process. Von Neuman and Goldstine took this approach in their monumental thesis on round-off errors in matrix processes[10]. Their approach predicted maximum error rather than the statistical error. (The statistical error is more meaningful and as shown by Turing[5], much smaller).

Recently Wilkinson[11] took an alternate approach to error analysis which has proven more fruitful. His approach is to assume that the answer obtained is correct and determine the magnitude of the change to be made in the original problem. His analyses have shown that triangular decomposition involves less round-off error than other processes for solving the simultaneous equations.

From a statistical point of view the average error in analysis is independent of the number of calculations However, the standard deviation of the error (and the maximum error) increases with the number of calculations

performed. Therefore, the algorithm that involves the lowest number of calculations will tend to result in the least step errors. It is interesting to note that the triangular decomposition is a direct method which involves the least number of calculations compared with other direct methods, which do not take advantage of matrix symmetry and sparcity.

Direct improvement of an approximate but unsatisfactory solution is the usual approach to reducing solution error. An example of a direct method can be shown for the solution of the simultaneous equations,

$$[A]\{x\} = \{C\}$$

(4-17)

Suppose an approximate solution $\bar{x}$ has been found. Then the equation

$$[A]\{\bar{x}\} = \{\bar{C}\}$$

(4-18)

can be formed by performing a matrix multiplication. Subtracting equations (17) and (18) and using the distributive property, it is found that

$$[A]\{x - \bar{x}\} = \{P - \bar{P}\}$$
$$\text{or} \quad [A]\{\bar{\bar{x}}\} = \{\bar{\bar{P}}\}$$

(4-19)

Equation (19) can then be solved for $x - \bar{x}$. The improved solution for x is given by $x = \bar{x} + \bar{\bar{x}}$. The maximum number of significant figures that can be obtained by this technique is dependent on the maximum number of figures obtained in forming C at each step. Some significant figures must also be retained in forming γ in order that solution im-

Iterative methods can also be used to improve a solution. If a characteristic vector is unsatisfactory, for example, the approximate vector may be used in an iterative procedure (power method, whose accuracy is limited only by the ability to retain significance in the matrix multiplications and vector normalizing. Similarly, a solution of a set of simultaneous equations can be used as the starting vector in a Gauss-Seidel iterative solution (see Section 3.4) or Morris' escalator method[3.1]. These methods may be used to reduce the error in a solution or to estimate the accuracy of an approximate solution.

It is characteristic of the step error that it increases as the number of the gridpoints are increased. As the number of points is increased the number of equations being solved increases. This increases the number of calculations required to solve the problem. As a consequence, the round-off error tends to increase.

4.4 ERROR CONTROL

Table 4-3 summarizes error causes, nature, types and control methods. Control of discretization error can be provided a priori. Care exercised in selecting analysis functions and element shapes can lead to measurable and boundable discretization errors which can be reduced by extrapolation techniques.

Though manipulation errors cannot be directly controlled, several methods are available for measuring the magnitude of step errors and checking that process errors are eliminated. Satisfactory techniques are also available for reducing errors once they are known to exist. Among these are iterative improvement and use of higher precision arithmetic.

The errors remaining, the idealization errors, are induced by the necessity of using a limited mathematical model of the structure. These errors can be reduced by including additional element geometries such as curved surface components of shells of revolution. Analysis limitations will, however, always exist. Thus, for continuous structures, selection of a satisfactory idealization will be the most demanding consideration for the analyst.

TABLE 4-3

ERROR	IDEALIZATION	DISCRETIZATION	MANIPULATION
Causes	Mesh mapping, model limitations	Model limitations, "fastening" incompleteness	Solution methods, significant figure limits
Nature	Dependent on gridpoint location and spacing Does not necessarily diminish with grid refinement Not easily measurable and may be unbounded	Dependent on mesh size May be made to vanish with grid refinement Usually measurable and can be bounded	Dependent on number of gridpoints and coordinate systems used. Generally increases with grid refinement Usually indirectly measurable and can be bounded
Types	Mapping - envelope and orientation Lumping - local geometry, materials, boundary condition	Continuity - stress and displacement Boundary - loads and deformations	Process - direct and iterative Step - truncation and round-o.
Methods of Reducing and Controlling Errors	Remapping - circumscribed vs. inscribed Scaling - length vs. orientation Remodeling - limitations, lumping vs. length and orientation Extending model	Using orderly mesh refinement Selecting good element topologies Requiring higher order continuity Selecting consistent generalized coordinates Using bounding technique Selecting functions leading to monotonic convergence Extrapolating Error estimating Reidealizing Remodeling	Checking calculations - symmetry, equilibrium, positive definiteness orthogonality Measuring convergence - criterion, resubstitution Performing algorithm error analyses Performing independent analyses Condition checking Carrying additional figures

REFERENCES

SECTION 1 REFERENCES:

1. Levy, Samuel, "Structural Analysis and Influence Coefficients for Delta Wings," *Jour. Aero. Science*, Vol. 20, No. 7, July 1953, pp. 449-454.

2. Turner, M. J., Clough, R. W., Martin, H. C., and Topp, L. J., "Stiffness and Deflection Analysis of Complex Structures," *Jour. Aero. Science.*, Vol. 23, No. 9, Sept. 1956, pp. 805-823.

3. Melosh, R. J., and Merritt, R. G., "Evaluation of Spar Matrices for Stiffness Analysis," *Jour. of Aero./Space Science*, Vol. 25, No. 9, Sept. 1958, pp. 537-543.

4. Dill, E. H., and Ortega, M. A., "Derivation of a Stiffness Matrix for a Rectangular Plate Element in Bending," Boeing Company Structural Analysis Research Memorandum No. 13, Seattle, June 1960.

5. Melosh, R. J., "A Stiffness Matrix for the Analysis of Thin Plates in Bending," *Jour. of the Aero. Sciences*, Vol. 28, No. 1, Jan. 1961, pp. 34-42.

6. Papenfuss, B. W., "Lateral Plat Deflection by Stiffness Matrix Methods," Unpublished Master's Thesis, University of Washington, Seattle, June 1961.

7. Meyer, R. R., and Harmon, M. B., "Conical Segment method for Analyzing Shells of Revolution for Edge Loading," *AIAA Jour.*, Vol. 1, No. 4, April 1963, pp. 886-891.

8. Grafton, P. E. and Strome, D. R., "Analysis of Axisymmetric Shells by the Direct Stiffness Method," *AIAA Jour.*, Vol. 1, No. 5, Oct. 1963.

9. Popov, E., Penzien, J., and Lu, Z., "Finite Element Solution for Axisymmetric Shells," *Jour. EM Div. ASCE*, Vol. 90, No. EM5, Oct. 1964.

10. Percy, J., Pian, T., Klein, S., and Navaratne, D. R., "Application of the Matrix Displacement Method to Linear Elastic Analysis of Shells of Revolution," AIAA Paper 65-142, presented at 2nd Aero. Sciences Annual Meeting, New York City, Jan. 1965.

11. Martin, H. C., "Plane Elasticity Problems and the Direct Stiffness Method, "The Trend in Engineering," Vol. 13, Jan. 1961.

12. Gallagher, R. H., Padlog, J., and Bitluard, P. P., "Stress Analysis of Heated Complex Shapes," ARS Jour., May 1962.

13. Melosh, R. J., "Structural Analysis of Solids," Third Computer Conference on Electronic Computation, Jour. Struct. Div., ASCE, August 1963.

14. Argyris, J. H., "Matrix Analysis of Three Dimensional Elastic Media - Small and Large Deflection," AIAA Jour., Vol. 3, No. 1, Jan. 1965, pp. 45-51.

15. Wilson, E., "Structural Analysis of Axisymmetric Solids," AIAA Paper 65-143, presented at 2nd Aero. Sciences Annual Meeting, New York City, Jan. 1965.

16. Clough, R. W., and Rashid, Y., "Finite Element Analysis of Axisymmetric Solids," Jour. EM Div. ASCE, Vol. 91, No. EM 1 Feb. 1965, pp. 71-86.

17. Turner, M. J., The Direct Stiffness Method of Structural Analysis, Reprint of a paper presented at a meeting of the AGARD Structures and Materials Panel, at the Technische Hochschule, Aachen, Germany, on Sept. 17, 1959.

18. Melosh, R. J., and Merritt, R. G., "Prediction of Flexibility and Natural Modes of Low Aspect Ratio Wings Using Stiffness Matrices," Aero/Space Engineering, Vol. 19, July 1960, pp. 25-31.

19. Greene, B. E., Strome, D. R., and Weikel, R. C., "Application of the Stiffness Method to the Analysis of Shell Structures," Paper presented at the Aviation Conference of the American Society of Mechanical Engineers, Los Angeles, March 15, 1961.

20. Turner, M. J., Martin, H. C., and Weikel, R. D., "Further Development and Applications of the Stiffness Method," paper presented at a meeting of the AGARD Structures and Materials Panel in Paris, July 6, 1962.

21. Renton, S. D., "Stability of Space Frames by Computer Analysis," Jour. Struct. Div., Proc. ASCE, Vol. 88, No. ST4, Aug. 1962, pp. 81-103.

22. Gallagher, R. H., and Padlog, J., "Discrete Element Approach to Structural Instability Analysis," AIAA Jour., Vol. 1, No. 6, June 1963.

23. Wilson, E. L., "Matrix Analysis of Nonlinear Structures," Proc. Second ASCE Conference on Electronic Computation, Pittsburgh, Pa. Sept. 1960.

24. Turner, M. J., Dill, E. H., Martin, H. C., and Melosh, R. J., "Large Deflections of Structures Subjected to Heating and External Loads," Jour. of the Aero/Space Sciences, Vol. 27, Feb. 1960, pp. 97-107.

25. Weikel, R. C., Jones, R. E., Seiler, J. A., Martin, H. C., Greene, B. E., "Nonlinear and Thermal Effects on Elastic Vibrations," Aeronautical System Division Report ASD-TDR-62-156.

26. Melosh, R. J., "Basis for Derivation of Matrices for the Direct Stiffness Method," AIAA Jour., Vol. 1, No. 7, July 1963, pp. 1631-1637.

27. Prager, W., "Tn. Extremum Principles of the Mathematical Theory of Elasticity a. their Use in Stress Analysis," University of Washington Eng. Exp. Station Bull. No. 119, Seattle, 1951.

28. Synge, J. L., The Hypercircle in Mathematical Physics, Cambridge University Press, Cambridge, 1957.

29. Benthem, J. P., "On the Analysis of Swept Wing Structures," National Aero and Astronautical Research Institute Report S 578, Amsterdam, June 1961.

REFERENCES

SECTION 2 REFERENCES:

1. Melosh, R. J., "A Flat Triangular Shell Element Stiffness Matrix," presented at WPAFB Conference on Matrix Methods in Structural Mechanics, Wright-Patterson AFB, Ohio, October 26-28, 1965.

2. Utku, Senol, "Stiffness Matrices for Thin Triangular Elements of Nonzero Gaussian Curvature," AIAA Paper No. 66-530, Fourth Aerospace Sciences Meeting, Los Angeles, California, 1966.

3. Sokolnikoff, I. S., Mathematical Theory of Elasticity, McGraw-Hill Book Co., New York, 1956, p. 87.

4. Koiter, W. T., "A Consistent First Approximation in the General Theory of Thin Elastic Shells," Proceedings of the Symposium on the Theory of Thin Elastic Shells, New York: Interscience Publishers, Inc., 1960, pp. 12-33.

5. Melosh, R. J., and Lang, T. E., "Modified Potential Energy Mass Representations for Frequency Prediction," presented at WPAFB Conference on Matrix Methods in Structural Mechanics, Wright-Patterson AFB, Ohio, October 26-28, 1965.

6. McCalley, R. B., "Mass Lumping for Beams," Report DIG/SA 63-68, General Electric Company, Knolls Atomic Power Laboratory, Schenectady, New York, July 1, 1963.

7. Utku, Senol, "Computation of Stresses in Triangular Finite Elements," Technical Report No. 32-948, Jet Propulsion Laboratory, June 15, 1966.

8. Utku, Senol, "On the Behavior of Triangular Shell Element Stiffness Matrices associated with Polyhedral Deflection Distributions," Submitted to AIAA 5th Annual Meeting, New York, January 1967.

REFERENCES

SECTION 3 REFERENCES:

1. Frazer, R. A., Duncan, W. J., and Collar, A. R., Elementary Matrices,
    London: Cambridge University Press, 1957, pp. 132-133.

2. Modern Computing Methods, Philosophical Library, New York, 1961.
    Chaps. 3, 4, and 5.

3. Seidel, L. "Oben ein Verfahren die Gleichungen, auf Welche die
    Methode der kleinstein Zuadrate fuhrt, sowie lineare Gleichugen
    uberkaupt, durch (successive) Annaherung aufzulosen." Abhandl bayer,
    Akad, Wiss., Math-Physik, Kl., 11:81, 1847

4. Carre, B. A., "The Determination of the Optimum Accelerating Factor
    by Successive Over-Relaxation," J. Computing, 1961, pp. 73-78.

5. Young, D. M., "Iterative Methods for Solving Partial Difference
    Equations of the Elliptic Type," Trans. Am. Math. Soc., V76,
    1954, pp. 92-111.

6. Engeli, M., "Over-relaxation and Related Methods," (Chap. IV of
    Refined Iterative Methods for Computation and Solution of the
    Eigenvalues of Self-Adjoint Boundary Value Problems.) Engeli, M.;
    Ginsberg, T. H.; Rutihauser, H.; Stiefel, Birkhauser Verlag, Basel,
    Stuttgart, 1959.

7. Sheldon, J. W., "On the Spectral Norms of Several Iterative
    Processes," J. Assoc. Computing Machines, Vol. 6, 1959, p. 494.

8. White, P. A., "The Computation of Eigenvalues and Eigenvectors of a
    Matrix," Jour. Soc. Indust. and Appl. Math., Vol. 6, No. 4,
    Dec. 1958, pp. 393-437.

9. Hurty, W. C., "Vibrations of Structural Systems by Component Mode
    Synthesis," J. Eng. Mech. Div. ASCE, Vol. 86, n. EMA, Aug. 1960,
    pp. 51-69.

10. Przemieniecki, J. S., "Matrix Structural Analysis of Substructures,"
    AIAA Jour., Vol. 1, No. 1, Jan. 1963, pp. 138-147.

REFERENCES

SECTION 4 REFERENCES:

1. Archer, J. S., and Samson, C. H., *Structural Idealization for Digital Computer Analysis*, 2nd Conf. on Electronic Computation ASCE, Pittsburgh, Sept. 1960, pp. 283-325.

2. Strng, C. L., *The Amateur Scientist*, Simon and Schuster, New York, 1960, pp. 409-410.

3. Richardson, L. F., and Gaunt, J. A., "The Deferred Approach to the Limit," *Phil. Trans. A.*, Vol. 229, 1926, pp. 299-361.

4. Forsythe, G. E., and Wasow, W. R., *Finite-Difference Methods for Partial Differential Equations*, New York: John Wiley & Sons, Inc., 1961.

5. Collatz, L., "The Numerical Treatment of Differential Equations," Berlin, Springer, 1960, p. 370.

6. Turing, A. M., "Rounding-Off Errors in Matrix Processes," *Quart. J. Mech. and Physics.*, September 1948.

7. Fox, L., "Notes on Solution of Algebraic Linear Simultaneous Equations," *Quart. J. Mechanics and Applied Math*, June 1948, p. 149.

8. Head, J. W., Oulton, G. M., "Solution of Ill-Conditioned Linear Simultaneous Equations," *Aircraft Engineering*, Oct. 1958, pp. 309-312.

9. Riley, J., "Solution of Linear Equations with Positive Definite Symmetric, But Possible Ill-Conditioned Matrix," *Math. Tables and Aids to Computation*, Vol. IX, July 1955, No. 51.

10. von Neumann, J., and Goldstine, H. H., "Numerical Inverting of Matrices of High Order, II," *Amer. Math. Soc. Proc.*, V.2, 1951, pp. 188-202.

11. Wilkinson, J. H., "Rounding Errors in Algebraic Processes," *Information Processing*, 1960, pp. 44-53.

APPENDIX A

FINITE ELEMENT FORM OF THE METHOD
OF MINIMUM POTENTIAL ENERGY

Assume a set of displacements as linear function of some arbitrary parameters; the generalized coordinates. Displacements must be continuous over the element, preserve displacement continuity across element boundaries, and match displacement boundary conditions, but need not satisfy the Cauchy equilibrium equations. Then, the displacements can be written in the form,

$$\{q\} = [A(x, y, z)]\{d\} \tag{A-1}$$

where q_i, i = 1, 2, 3, are the displacements and d_j; j = 1, 2, ...m, the generalized deformations, usually gridpoint displacements.

Using (1), the strain-deformation, stress-strain, and strain-energy relation, the strain energy can be written in terms of the deformations. Let the linear operator transforming displacements to strains be the matrix B, then

$$\{\epsilon\} = [B]\{q\} \tag{A-2}$$

where ϵ_k are strains, the B_{ki} are differential operators and k = 1, 2, 3 ...6, in general. Furthermore, let the stress-strain relation be taken as

$$\{\sigma\} = [D]\{\epsilon\} \tag{A-3}$$

where σ_ℓ $\ell = 1, 2, 3 \ldots 6$ are stresses and $D_{\ell K}$ material constants. Then, since the strain-energy expression is,

$$U = \frac{1}{2} \int_{V_0} \{\epsilon\}^T \{\sigma\} \, dV_0 \qquad (A\text{-}4)$$

where V_0 indicates integration over the volume of the structure and the superscript T denotes matrix transpose, (2) and (3), change (4) to,

$$U = \frac{1}{2} \int_{V_0} \lfloor q \rfloor [B]^T [D] [B] \{q\} \qquad (A\text{-}5)$$

Substituting (1) in (5), the strain energy can be written in more useful form,

$$U = \frac{1}{2} \int_{V_0} \lfloor d \rfloor [A]^T [B]^T [D] [B] [A] \{d\} \, dV_0 \qquad (A\text{-}6)$$

or, $\quad U = \frac{1}{2} \lfloor d \rfloor [K] \{d\}$

$$[K] = \int_{V_0} [A]^T [B]^T [D] [B] [A] \, dV_0 \qquad (A\text{-}7)$$

The matrix K is called the stiffness matrix. Since D is a positive semi-definite matrix for any real material, so is the stiffness matrix.

Now, the potential energy functional is written in terms of the displacements and prescribed quantities. The functional is defined by

$$V = U - \int_{S_t} \lfloor T \rfloor \{d\} \, dS_t - \int_{V_0} \lfloor G \rfloor \{d\} \, dV_0 \qquad (A\text{-}8)$$

where the T_i are surface tractions; G_i, body forces, and S_t deontes that part of the surface over which tractions are prescribed. The T_i are

defined in terms of stresses on the surface by the operator N whose terms are components of the surface normal, i.e.,

$$\{T\} = [N]\{\sigma_t\} \tag{A-9}$$

The subscript t designates prescribed quantities, i.e., stresses in this case. Using (9) and (1), (8) becomes,

$$V = U - \int_{S_t} \lfloor d \rfloor [A]^T [N] \{\sigma_t\} dS_t - \int_{V_o} \lfloor d \rfloor [A]^T \{G\} dV_o \tag{A-10}$$

The generalized force-deformation equations are found by minimizing the potential permitting only the deformations to vary. From (7) and (10) this operation gives,

$$\{P\} = [K]\{d\}$$
$$\{P\} = \left\{ \frac{\partial}{\partial d} \left\langle \int_{S_t} \lfloor d \rfloor [A]^T [N] \{\sigma_t\} dS_t + \int_{V_o} \lfloor d \rfloor [A]^T \{G\} dV_o \right\rangle \right\} \tag{A-11}$$

Since K relates generalized forces and deformations, it is justified in being called a stiffness matrix. The generalized forces are seen to consist of weighted integrals of the prescribed stresses and body forces. Thus, the theory defines the forces corresponding to a prescribed set of stresses; no new approximation is necessary.

Displacement boundary conditions are satisfied by specifying some of the d_j. Assuming those specified are the first "n" d_j $(n < m)$, then (11) takes the form, omitting body forces,

$$\{\bar{p}\} = [K_{22}]\{d_{m-n}\}$$

$$\{\bar{p}\} = \{\frac{\partial}{\partial d_{m-n}} \int_{S_t} [d_{m-n}][A_{m-n}]^T [N_{m-n}]\{\sigma_t\} dS_t\} - [K_{21}]\{d_n\} \qquad \text{(A-12)}$$

$$[K] = \begin{bmatrix} K_{11} & K_{12} \\ K_{21} & K_{22} \end{bmatrix}; \quad [N] = [N_n, N_{m-n}]; \quad [A] = [A_n, A_{m-n}]$$

where the subscripts indicate the number of components.

Equations similar to (12) are also obtained if the v_{n-m} are any linear function of v_n. Thus, if

$$\{d\} = [L]\{d_n\}$$

$$\{\dot{p}\} = [L]^T [K][L]\{d_n\}$$

$$\{\dot{p}\} = \{\frac{\partial}{\partial d_n} \int_{S_t} [d_n][L]^T [A]^T [N]\{\sigma_t\} dS_t\} \qquad \text{(A-13)}$$

Having found d_i from (11), (12) ~ 13), the assumed displacements are found from (1). Alternate assum, ...ons of the form (1) can lead to the same generalized force-displacement equations for a given problem, however. Therefore, use of (1), (2), and (3) in an approximate solution determines only one of an infinity of possible stress states that are meaningful. Moreover, stresses so determined in general will not satisfy the microscopic equations of equilibrium.

APPENDIX B

BOUNDING ELASTIC BEHAVIOR

Bounds on displacement at a gridpoint and mean values of strain and stress along a line between gridpoints can be obtained conveniently using the developments of Prager[2.27], Synge[2.28], and Benthem[2.29]. Development of equations here will follow Benthem (1961, pp 28-42).

A loading consisting of a superposition of the real loads and an influence loading is considered. From (A-6), (A-7), (A-10), and (A-11). The total potential energy is given by

$$V_{R+F} = \frac{1}{2} \lfloor d_R + d_F \rfloor [K] \{ d_R + d_F \} - \int_{S_t} \lfloor T_R + T_F \rfloor [A] \{ d_R + d_F \} dS_t \quad \text{(B-1)}$$

where the subscripts R and F refer to the real and influence loads respectively. As before S_t denotes the part of the surface over which tractions are prescribed. The summed subscript indicates the combined loading.

The strain energy of the exact solution is half the work of the surface forces integrated over the entire surface of the body[2.30]. Moreover, the stiffness matrix is symmetric. Therefore, (1) can be rewritten in the form,

$$V_{R+F} = \bar{V}_R + \bar{V}_F + \frac{1}{2} \int_S \left\langle \lfloor T_R \rfloor [A] \{ d_F \} + \lfloor T_F \rfloor [A] \{ d_R \} \right\rangle dS$$
$$- \int_{S_t} \left\langle \lfloor T_R \rfloor [A] \{ d_F \} + \lfloor T_F \rfloor [A] \{ d_R \} \right\rangle dS_t \quad \text{(B-2)}$$

where

$$\bar{V}_R = \frac{1}{2} \lfloor d_R \rfloor [K] \{ d_R \} - \int_{S_t} \lfloor T_R \rfloor [A] \{ d_R \} dS_t$$

$$\bar{V}_F = \frac{1}{2} \lfloor d_F \rfloor [K] \{ d_F \} - \int_{S_t} \lfloor T_F \rfloor [A] \{ d_F \} dS_t$$

S denotes integration over the entire surface. Using Betti's theorem (2) can be expressed in a more usable form. Then, since

$$\int_S \lfloor T_F \rfloor [A] \{d_R\} = \int_{S_u} \lfloor T_R \rfloor [A] \{d_F\} dS_u + \int_{S_t} \lfloor T_R \rfloor [A] \{d_F\} dS_t ; \quad \text{(B-3)}$$

$$V_{R+F} = V_R' + V_F' + \int_{S_t} \lfloor T_F \rfloor [A] \{d_R\} dS_t + \int_{S_u} \lfloor T_R \rfloor [A] \{d_F\} dS_u \quad \text{(B-4)}$$

If displacements are set zero for the influence loading, wherever displacements are prescribed for the real loads, the last integral in (4) vanishes. The remaining integral, denoted $V_{R\alpha}$, involves a linear function of the real load gridpoint displacements. If the energy of (4) is subtracted from that of the solution energy for the same loading,

$$\tilde{V}_{R+F} - V_{R+F} = \tilde{V}_R - V_R' + \tilde{V}_F - V_F' - \tilde{V}_{R\alpha} - V_{R\alpha}'$$

where the tilde indicates that the quantity is for the elasticity solution.

If all the loads and displacements for the real loading are multiplied by a scaler β_1, and for the influence loading by β_2 from (1) and (5),

$$\tilde{V}_{(R+F)\beta} - V_{(R+F)\beta} = (\tilde{V}_R - V_R')\beta_1^2 + (\tilde{V}_F - V_F')\beta_2^2 - (\tilde{d}_{R\alpha} - d_{R\alpha})\beta_1\beta_2 \quad \text{(B-6)}$$

with subscripts modified to indicate the loading change. The potential for a structure with loads specified over some part of the body must be negative. See (A-10) and (A-11). Moreover, according to the theorem of minimum potential energy, the energy of the solution must be less than

that of any approximation. Thus, (6) must be negative for all β_1 and β_2, i.e., (6) must be a negative definite quadratic form. Therefore, it is required that,

$$
(\tilde{V}_R - V_R) < 0; \qquad (V_F - V_F) < 0;
$$
$$
(V_R - V_R)(V_F - V_F) - \frac{1}{4}(d_{R\alpha} - \tilde{d}_{R\alpha})^2 < 0 \tag{B-7}
$$

By an analogous argument, inequalities can be written for the complementary energy case. The result corresponding to (7) is

$$
(V_R^* - \tilde{V}_R^*) > 0; \qquad (V_F^* - \tilde{V}_F^*) > 0;
$$
$$
(V_R^* - \tilde{V}_R^*)(V_F^* - V_F^*) - \frac{1}{4}(d_{R\alpha}^* - d_{R\alpha})^2 > 0 \tag{B-8}
$$

The final inequalities in (7) and (8) can be rewritten using the first two inequalities in both these equations and noting that $V^* = -\tilde{V}$ for the solution. The resulting inequalities are:

$$
(V_R^* + V_R)(V_F^* + V_F)(-1)^2 < \frac{1}{4}(d_{R\alpha} - \tilde{d}_{R\alpha})^2 \tag{B-9}
$$

$$
(V_R^* + V_R)(V_F^* + V_F) > \frac{1}{4}(d_{R\alpha}^* - \tilde{d}_{R\alpha})^2 \tag{B-10}
$$

Taking the square root of (9) and (10) and considering the possible relations between V_{RL} and V_{RL}^* gives,

$$
\text{IF } d_{R\alpha}^* > d_{R\alpha}: \quad -2R + d_{R\alpha} < \tilde{d}_{R\alpha} < 2R + d_{R\alpha} \tag{B-11}
$$
$$
\text{IF } d_{R\alpha}^* < d_{R\alpha}: \quad -2R + d_{R\alpha}^* < \tilde{d}_{R\alpha} < 2R + d_{R\alpha}^* \tag{B-12}
$$
$$
D = \sqrt{(V_R^* + V_R)(V_F^* + V_F)} \tag{B-13}
$$

The physical interpretation of the quantity bounded in (11), (12), and (13) depends on the influence loading selected. Two choices and the corresponding interpretation of $\tilde{d}_{R\alpha}$ are as follows:

1. Let the influence loading be a single unit load at point α . Then $d_{R\alpha}$ is the deflection at gridpoint α due to the real loads and is in the direction of the influence load.

2. Let the influence loading be two unit self-equilibrating loads applied at two gridpoints in the direction of the line joining the points. Then $\tilde{d}_{R\alpha}$ is a known scalar multiple of the mean strain along the line between the points and in the direction of that line. Thus, coosing a positive unit load in the x direction at gridpoint α_1 and a negative unit load at α_2 , with α_1 and α_2 lying on a line parallel to the x axis, the integral in (4) gives,

$$\tilde{d}_{R\alpha} = u_{\alpha_1} - u_{\alpha_2} = \int_{x_{\alpha_2}}^{x_{\alpha_1}} \left(\frac{\partial u}{\partial x}\right) dx = \bar{\epsilon}_{xx} \left(x_{\alpha_1} - x_{\alpha_2}\right) \qquad \text{(B-14)}$$

The bar denotes the mean value. The mean is defined in the usual way.

When the stress-strain coefficients are constants between nodes α_1 and α_2, $\tilde{d}_{R\alpha}$ can also be interpreted as a known scalar multiple of mean stress. For an isotropic material in the example chosen,

$$\tilde{d}_{R\alpha} = \frac{1}{E} \int_{x_{\alpha_2}}^{x_{\alpha_1}} E \left(\frac{\partial u}{\partial x}\right) dx = \frac{\bar{\sigma}_{xx}}{E} \left(x_{\alpha_1} - x_{\alpha_2}\right) \qquad \text{(B-15)}$$

In principle, gridpoints can be placed as close together as desired. Then, bounds for stress and strain at a point can be found.

The procedure for bounding elastic behavior by the stiffness method of bounds is summarized as follows:

1. Obtain solutions for the real and influence loadings using stiffness matrices based on deformation-consistent displacement functions. Establish the values of V_R, V_F and $V_{R\alpha}$.

2. Obtain solutions for the real and influence loadings using stiffness matrices based on stress-consistent displacements. Establish the values of V_R^*, V_F^*, and V_R^* .

3. Use (11) or (12) and (13) and appropriate geometry and material constants to bound desired quantities.